Universidad de Investigación de Tecnología Experimental Yachay

ESCUELA DE CIENCIAS DE LA TIERRA ENERGÍA Y AMBIENTE

Characterization of the Silante Fm. Along the Salinas-Lita Transect in Northern Ecuador

Trabajo de integración curricular presentado como requisito para la obtención del título de Geólogo

Autor:
Luis Bryan Sarmiento López

Tutor:
PhD. Rafael Almeida

Urcuquí, September 2020

Urcuquí, 13 de noviembre de 2020

SECRETARÍA GENERAL
(Vicerrectorado Académico/Cancillería)
ESCUELA DE CIENCIAS DE LA TIERRA, ENERGÍA Y AMBIENTE
CARRERA DE GEOLOGÍA
ACTA DE DEFENSA No. UITEY-GEO-2020-00015-AD

A los 13 días del mes de noviembre de 2020, a las 16:30 horas, de manera virtual mediante videoconferencia, y ante el Tribunal Calificador, integrado por los docentes:

Presidente Tribunal de Defensa	Dr. CARRILLO ALVAREZ, EMILIO , Ph.D.
Miembro No Tutor	Dr. VAZQUEZ TASET, YANIEL MISAEL , Ph.D.
Tutor	Dr. ALMEIDA GONZALEZ, RAFAEL VLADIMIR , Ph.D.

El(la) señor(ita) estudiante **SARMIENTO LOPEZ, LUIS BRYAN**, con cédula de identidad No. **1724886385**, de la **ESCUELA DE CIENCIAS DE LA TIERRA, ENERGÍA Y AMBIENTE**, de la Carrera de **GEOLOGÍA**, aprobada por el Consejo de Educación Superior (CES), mediante Resolución **RPC-SE-10-No.031-2016**, realiza a través de videoconferencia, la sustentación de su trabajo de titulación denominado: **CHARACTERIZATION OF THE SILANTE FM, ALONG THE SALINAS LITA TRANSECT IN NORTHERN ECUADOR**, previa a la obtención del título de **GEÓLOGO/A**.

El citado trabajo de titulación, fue debidamente aprobado por el(los) docente(s):

Tutor	Dr. ALMEIDA GONZALEZ, RAFAEL VLADIMIR , Ph.D.

Y recibió las observaciones de los otros miembros del Tribunal Calificador, las mismas que han sido incorporadas por el(la) estudiante.

Previamente cumplidos los requisitos legales y reglamentarios, el trabajo de titulación fue sustentado por el(la) estudiante y examinado por los miembros del Tribunal Calificador. Escuchada la sustentación del trabajo de titulación a través de videoconferencia, que integró la exposición de el(la) estudiante sobre el contenido de la misma y las preguntas formuladas por los miembros del Tribunal, se califica la sustentación del trabajo de titulación con las siguientes calificaciones:

Tipo	Docente	Calificación
Presidente Tribunal De Defensa	Dr. CARRILLO ALVAREZ, EMILIO , Ph.D.	9,5
Miembro Tribunal De Defensa	Dr. VAZQUEZ TASET, YANIEL MISAEL , Ph.D.	9,5
Tutor	Dr. ALMEIDA GONZALEZ, RAFAEL VLADIMIR , Ph.D.	9,3

Lo que da un promedio de: **9.4 (Nueve punto Cuatro)**, sobre 10 (diez), equivalente a: **APROBADO**

Para constancia de lo actuado, firman los miembros del Tribunal Calificador, el/la estudiante y el/la secretario ad-hoc.

Certifico que *en cumplimiento del Decreto Ejecutivo 1017 de 16 de marzo de 2020, la defensa de trabajo de titulación (o examen de grado modalidad teórico práctica) se realizó vía virtual, por lo que las firmas de los miembros del Tribunal de Defensa de Grado, constan en forma digital.*

SARMIENTO LOPEZ, LUIS BRYAN
Estudiante

Dr. CARRILLO ALVAREZ, EMILIO , Ph.D.
Presidente Tribunal de Defensa

EMILIO CARRILLO ALVAREZ

Firmado digitalmente por EMILIO CARRILLO ALVAREZ
Nombre de reconocimiento (DN): c=EC, o=BANCO CENTRAL DEL ECUADOR, ou=ENTIDAD DE CERTIFICACION DE INFORMACION-ECIBCE, l=QUITO, serialNumber=0000230933, cn=EMILIO CARRILLO ALVAREZ
Fecha: 2020.12.03 09:54:15 -05'00'

Dr. ALMEIDA GONZALEZ, RAFAEL VLADIMIR , Ph.D.
Tutor

YANIEL MISAEL VAZQUEZ TASET

Firmado digitalmente por YANIEL MISAEL VAZQUEZ TASET
Nombre de reconocimiento (DN): cn=YANIEL MISAEL VAZQUEZ TASET, serialNumber=161120172257, ou=ENTIDAD DE CERTIFICACION DE INFORMACION, o=SECURITY DATA S.A. 2, c=EC
Fecha: 2020.12.03 07:59:03 -05'00'

Dr. VAZQUEZ TASET, YANIEL MISAEL , Ph.D.
Miembro No Tutor

ANDREA YOLANDA TERAN ROSALES

Firmado digitalmente por ANDREA YOLANDA TERAN ROSALES
Fecha: 2020.11.13 19:02:54 -05'00'

TERÁN ROSALES, ANDREA YOLANDA
Secretario Ad-hoc

AUTORÍA

Yo, **LUIS BRYAN SARMIENTO LÓPEZ**, con cédula de identidad **1724886385**, declaro que las ideas, juicios, valoraciones, interpretaciones, consultas bibliográficas, definiciones y conceptualizaciones expuestas en el presente trabajo; así cómo, los procedimientos y herramientas utilizadas en la investigación, son de absoluta responsabilidad de el/la autora (a) del trabajo de integración curricular. Así mismo, me acojo a los reglamentos internos de la Universidad de Investigación de Tecnología Experimental Yachay.

Urcuquí, noviembre 2020.

____

Luis Bryan Sarmiento López
CI:1724886385

AUTORIZACIÓN DE PUBLICACIÓN

Yo, **LUIS BRYAN SARMIENTO LÓPEZ,** con cédula de identidad **1724886385**, cedo a la Universidad de Tecnología Experimental Yachay, los derechos de publicación de la presente obra, sin que deba haber un reconocimiento económico por este concepto. Declaro además que el texto del presente trabajo de titulación no podrá ser cedido a ninguna empresa editorial para su publicación u otros fines, sin contar previamente con la autorización escrita de la Universidad.

Asimismo, autorizo a la Universidad que realice la digitalización y publicación de este trabajo de integración curricular en el repositorio virtual, de conformidad a lo dispuesto en el Art. 144 de la Ley Orgánica de Educación Superior

Urcuquí, noviembre 2020.

Luis Bryan Sarmiento López
CI: 1724886385

DEDICATORY

I want to dedicate this work to my parents Lucia López and Luis Abelardo Sarmiento because this achievement is theirs, and to my grandfather Eladio López for being the voice of wisdom that helps me make my way to my goals.

Luis Bryan Sarmiento López

ACKNOWLEDGEMENT

I want to thank my parents, Eng. Lucia López and J.D Luis Sarmiento, who with their effort, sacrifice and work made it possible for me to continue with my academic studies.

My sincere thanks to all the professors who instructed me throughout my academic career, teaching me about ethics, truth and the importance of teamwork. Thanks to them I always have the desire to keep trying without giving up.

I would like to thank in a very special way my tutor, Dr. Rafael Almeida, for his support, teachings, and unconditional patience that he gave me during my degree process.

I want to thank my jury, Dr. Yaniel Vazquez, and Dr German Martin, for their assistance in the development of my degree project.

I would like to thank the Instituto de Investigación Geológico y Energético of Ecuador for the collaboration in the development of thin sections of rocks.

I want to thank my Monos, Bryan Aldaz, Cristhian Preciado, Carlos Placios, Isaac Bravo, Hector Mejia, who were there in good and bad times, that without them I would not have passed this process as a champion. Also, a deep thanks to my friends Mafer Molina, Fernanda Romero, Anderson Rivadeneira, Sebastian Alcivar, Carlos Veloz, Kleber Sanmartin, Andres Chalampuente, Bryan Chamba, Joseph Cobo, Dario Castro, Milena León, María Reinoso, Karen Ortiz, Erika Fonseca who offered their sincere friendship and I know I can count on them.

I want to give special thanks to Chem. Dayanna Vera for her unconditional support and long hours of work together.

I want to thank my career mates who showed me that when you work as a team you can achieve wonderful things.

RESUMEN

La formación de Silante es una secuencia de estratos depositados en un ambiente continental que abarca alrededor de 100 km que se extiende en un cinturón desde las Ilinizas en el sur hasta el transecto Salinas-Lita en el norte. Está compuesto por breccias, conglomerados matriz soportados, lutitas, areniscas y toba. La formación Silante ha sido descrita muy bien al oeste de Quito, en el transecto Aloag-Santo Domingo y en el transecto Calacali-Nanegalito. Sin embargo, no se ha estudiado en detalle en el extremo norte del cinturón de Silante, a lo largo del transecto Salinas-Lita. Por esta razón, nos centramos en esta ubicación. Este estudio consistió principalmente en estudios de campo que fueron: Mapeo geológico del área de trabajo, descripción sedimentológica y petrofísica de los estratos, y la medición de características de deformación. Como resultado, dividimos Silante Fm en dos miembros, describimos los cambios en los entornos de deposición, e identificamos una fase importante de deformación de la Cordillera Occidental.

Palabras Clave:

Geología, Formación Silante, Salinas-Lita, Cordillera Occidental

ABSTRACT

The Silante formation is a sequence of strata deposited in a continental environment that spans around 100 km which extends in a belt from the Ilinizas in the south to the Salinas-Lita transect in the north. It is composed of breccias, matrix supported conglomerates, red mudstone, siltstone and tuff. The Silante Formation has been described very well at west of Quito, in the Aloag-Santo Domingo transect and the Calacali-Nanegalito transect. However, it has not been studied in detail at the northern end of the Silante belt, along the Salinas-Lita transect. For this reason, we focused on this location. This study consisted mostly of field surveys which were: geological mapping of the work area, sedimentological and petrographic description of the strata, and the measurement of deformation features. As a result, we divided Silante Fm into two members, we describe changes in deposition environments, and we identify an important phase of deformation of the WC.

.

Key Words:

Geology, Silante Formation, Salinas-Lita, Western Cordillera.

INDEX

AUTORÍA IV

AUTORIZACIÓN DE PUBLICACIÓN V

DEDICATORY VI

ACKNOWLEDGEMENT VII

RESUMEN VIII

ABSTRACT IX

LIST OF FIGURES XII

I. INTRODUCTION 1

II. GEOLOGICAL FRAMEWORK 3

2.1. Stratigraphy of the Western Cordillera 5
2.1.1 Basement of the WC 5
2.1.1.1 Pallatanga Formation 5
2.1.1.2 San Juan Unit 6
2.1.1.3 Totoras Amphibolite 6
2.1.1.4 The Pujilí Melange 6
2.1.2 The Rio Cala Group 7
2.1.2.1. La Portada Formation 7
2.1.2.2. Mulaute Formation. 7
2.1.2.3. Pilatón Formation. 8
2.1.2.4. Natividad Formation. 8
2.1.2.5. Rio Cala Formation. 8
2.1.2.6. Yunguilla Formation. 9
2.1.3 Angamarca Group 9
2.1.3.1. Pilaló Formation 9
2.1.3.2. Saguangal Formation 10
2.1.3.3. Saquisilí Formation. 10
2.1.3.4. Unacota Formation. 10
2.1.3.5. Apagua Formation 11
2.1.3.6. Laurel Formation 11
2.1.3.7. Rumi Cruz Formation 11
2.1.4 Zambagua Group 12
2.1.4.1. San Juan de Lachas Formation 12
2.1.5 Macuchi Block 12

2.1.5.1. Macuchi Unit 12
2.1.6 Silante Formation 13

2.2. Silante Formation Previous Works 13

III. METHODS 18

IV. GEOLOGICAL FEATURES OF THE STUDY AREA 22

4.1. Stratigraphy 22
4.1.1. Stratigraphic Column 22
4.1.2. Lithofacies 24
4.1.2.1. Pallatanga Formation 24
4.1.2.2. Yunguilla Formation 24
1.1.2.1. Silante Formation 26
4.1.2.4. Quaternary Volcanic Deposits 36

4.2. Structural Features 37
4.2.1. Faults 37
4.2.2. Folds 41
4.2.3. Fractures 41
4.2.4. Structural Cross Section 41

V. DISCUSSION 45

5.1. Stratigraphy of the Silante Fm in the intramontane basin of Salina-Lita transect 45

5.2. Structural geology of the Silante strata 46

5.3. Basin Evolution 47

5.4. Comparison with previous studies 49

5.5. Correlation with Chota Basin 50

VI. CONCLUSIONS 52

VII. BIBLIOGRAPHY 53

ANNEXES 56

List of Figures

FIGURE 1. 4
FIGURE 2. 4
FIGURE 3. 16
FIGURE 4. 17
FIGURE 5 24
FIGURE 6.. 25
FIGURE 7.. 27
FIGURE 8... 29
FIGURE 9. 30
FIGURE 10... 33
FIGURE 11. 34
FIGURE 12. 35
FIGURE 13. 38
FIGURE 14.. 39
FIGURE 15. 40
FIGURE 16.. 42
FIGURE 17.. 43
FIGURE 18.. 44
FIGURE 19.. 44
FIGURE 20. 48
FIGURE 21.. 51
FIGURE 22. 67
FIGURE 23.. 71
FIGURE 24. 78

I. INTRODUCTION

A sedimentary basin is a depression in the crust of the Earth where we can expect to find sediment accumulation (Colombo, 1992). The stratigraphic succession within a sedimentary basin may provide records of the geological history that occurred in a specific area over a specific period (Kerr et al., 2003; Mccann et al., 2003). Intramontane basins are basins surrounded by mountains, which can form in different tectonic contexts such as strike-slip settings, extensional settings, intra-arc settings, or on top of fold-and-thrust belts (Mccann et al., 2003; Rodríguez et al., 2012). The evolution of mountain ranges is complex, but intramontane basins are excellent sources of information that have recorded the tectonic evolution, uplift, and environmental conditions of for the surrounding mountain ranges (Streit et al., 2017).

Ecuador, located at the northwestern part of South America, is traversed by the Andean mountain range in an approximate north-south direction. Ecuador is segmented into the following tectonic provinces from east to west: The Oriente Basin, Subandean Zone, Cordillera Real, Inter-Andean Valley, Cordillera Occidental, and Coastal forearc basin (Jaillard et al., 2004; Toro & Jaillard, 2005; Vallejo, 2007; Vallejo et al., 2009). The Cordillera Occidental, or Western Cordillera (WC), was formed by the accretion of an allochthonous oceanic block to the South American plate margin in the Late Cretaceous (Jaillard et al., 2004; Toro & Jaillard, 2005; Vallejo, 2007; Vallejo et al., 2009). This oceanic block has been defined as the Caribbean Plateau due to similarities with rocks found throughout northwestern South American in Venezuela, and Colombia (Kerr et al., 2003). Overlying this oceanic basement there is a sequence of marine sedimentary rocks, younger volcanic rocks, and continental red beds (Jaillard et al., 2004; Vallejo, 2007; Vallejo et al., 2009).

The WC has recorded the tectonic evolution of the northwestern Andes which has included the development of strike-slip faults, fold and thrust belts, and intramontane basins. The Silante Fm is a continental sequence deposited in an intramontane basin, that has been described in the central part of the WC (Figure 2). It is composed of breccias, matrix-supported conglomerates, red mudstones, shales, siltstones, and violaceous tuffs deposited in continental environments (Hughes & Pilatasig, 2002; Vallejo, 2007; Vallejo et al., 2009). However, the age and stratigraphic context of the

Silante Fm are still controversial, as different authors have proposed different scenarios. For example, Egüez (1986) proposed that the Silante Fm was deposited in the Late Cretaceous between marine deposits; on the other hand, Vallejo (2007) proposes that Silante Fm was deposited during the Paleocene unconformably over marine deposits; and more recently, Almagor (2019) proposed that the Silante Fm was deposited in Oligocene-Miocene times and overlies the San Juan de Lachas Fm. The Silante Fm has been mapped over an area of approximately 162 km long by 12 km wide, which extends from Naranjal in Imbabura, to South of the Illinizas, and intermittently it is covered by younger volcanic deposits along the belt (Figure 2) (Boland et al., 1998). In addition, it has not been possible to determine the stratigraphic margins of the top and the base of the Silante Fm (Boland et al., 1998; Hughes & Pilatasig, 2002; Vallejo, 2007; Vallejo et al., 2009). For this reason, the characterization of Silante Fm is important and it will help to understand the evolution of the WC and the northwestern part of the Andes.

There have been few studies of the Silante Fm in northern Ecuador (Boland et al., 1998; Vallejo, 2007). The Salinas-Lita road, which follows the Mira River valley in northern Ecuador, provides a series of road and river cuts across the WC, where the Silante Fm and underlying Cretaceous bedrock are well exposed (Figure 1). In this study, we focused on the Silante Fm and carried out geological mapping along the Salinas–Lita transect, as well as measured stratigraphic sections and structural features. We used these observations to characterize the depositional setting and deformation of the Silante Fm, and we compare our results with those from the central WC. We reinterpret all the continental strata exposed along the Salinas-Lita transect as part of the Silante Fm, and propose a model for basin formation that involves the Silante Fm filling pre-existing topography in the WC. Finally, we interpret its subsequent deformation, and place it in the context of the tectonic evolution of the WC.

II. GEOLOGICAL FRAMEWORK

The Andes of Ecuador is divided into two parallel, more or less north-south ranges, called the Western Cordillera (WC) and the Cordillera Real. These are separated by a prominent valley called the Interandean Depression (Jaillard et al., 2004; Toro & Jaillard, 2005; Vallejo, 2007; Vallejo et al., 2019). From east to west Ecuador is divided into the following tectonic provinces (Figure 2): The Oriente Basin, which constitutes the contemporary retroarc basin, and is composed by Cretaceous marine deposits and Lower Cretaceous fluvial deposits; the Subandean Zone composed by a Jurassic volcanic arc overlayed by a part of the Cretaceous Oriente Basin; the Cordillera Real, that is formed by Paleozoic metamorphic rocks with and Mesozoic granitoids (Litherland et al., 1994; Spikings et al., 2015; Vallejo et al., 2019); the Interandean Depression, which is characterized by Neogene to Quaternary alluvial, colluvial, and volcanic arc sediments; the WC, which is mostly composed of Cretaceous mafic rocks, and Upper Cretaceous marine sedimentary rocks; and finally, the Coastal Plain, which is a forearc basin with Paleogene to Neogene deposit (Jaillard et al., 2004; Toro & Jaillard, 2005; Vallejo, 2007; Vallejo et al., 2019).

The WC was formed by the collision of an oceanic plateau with continental South America in the Late Cretaceous (Hughes & Pilatasig, 2002, Vallejo, 2007; Vallejo et al., 2009, Vallejo et al., 2019). It is limited to the east by an approximate north-south trending ocean-continent suture zone reactivated with transcurrent fault displacement, called the Calalacli-Pujilí-Pallatanga fault (Egüez, 1986; Jaillard et al., 2004; Spikings et al., 2001; Vallejo, 2007; Vallejo et al., 2009). The WC is subdivided into two different sequences with an assemblage of volcano-sedimentary tectonostratigraphic units (Jaillard et al., 2004; Toro & Jaillard, 2005). Fission-track and $^{40}Ar/^{39}Ar$ data show that the WC records cooling at 85 to 60 Ma with a peak from 85 to 80 Ma (Spikings et al., 2005). In the WC we also find a continental sequence called the Silante Fm, which is characterized by fluvial and alluvial lithologies deposited in an intramontane basin.

This chapter presents a brief description of the main lithostratigraphic characteristics of the WC, the main deformation events that have affected it, and previous works on the Silante Fm.

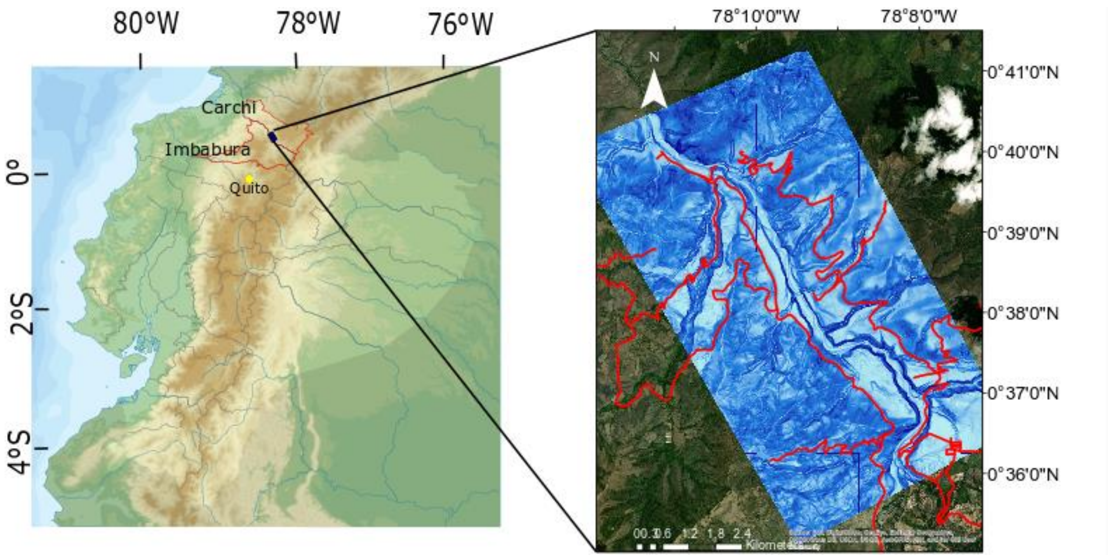

Figure 1. Location map of the work area. Our work area is located north of Ecuador, on the Salinas-Lita road. The red lines are the roads traveled for this work.

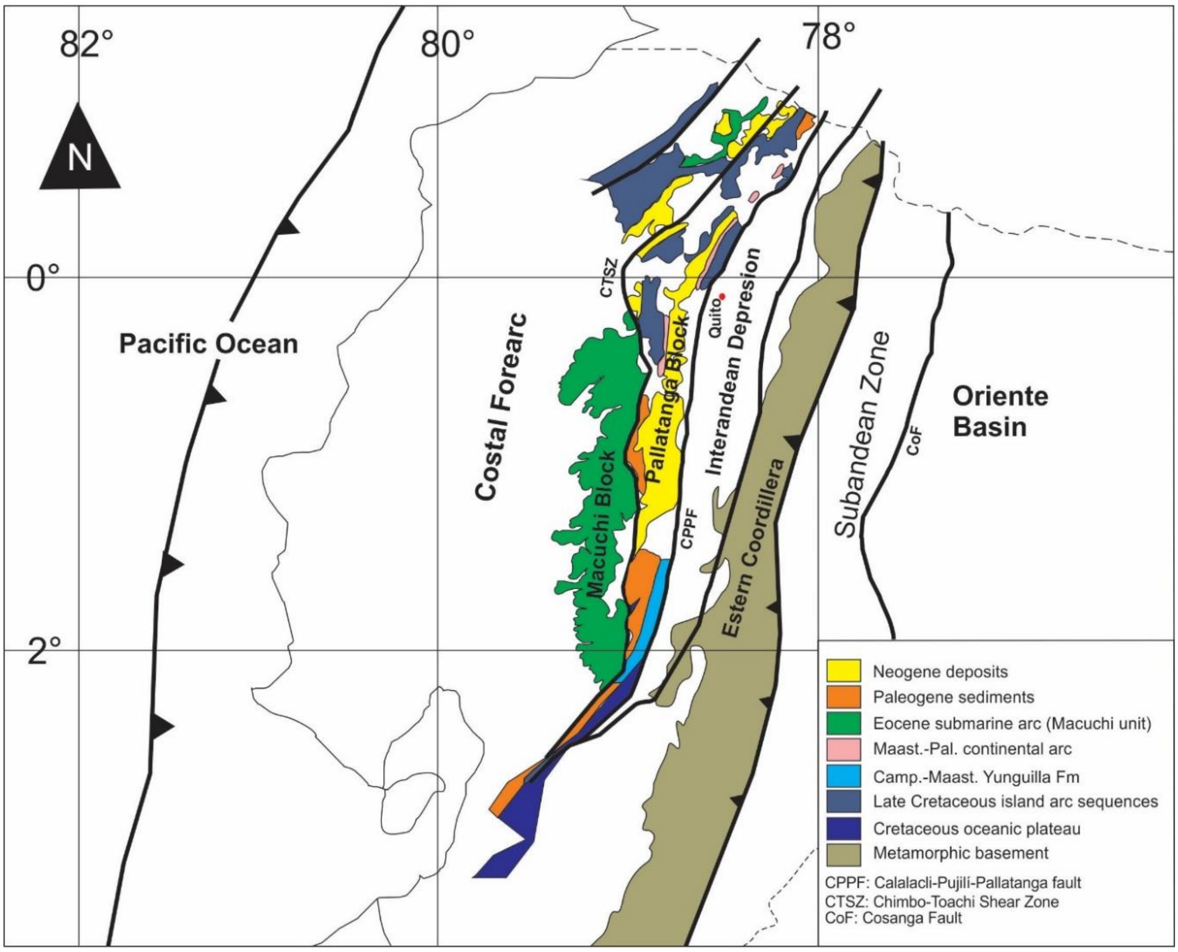

Figure 2. Schematic geological map showing the main tectonic provinces of Ecuador. Silante Fm is represented as the pink color showing Maastrichtian-Paleogene continental arc sequences in the Pallatanga Block. The Macuchi Block and Pallatanga Block make up the WC. Modified image of Vallejo et al. (2019).

2.1. Stratigraphy of the Western Cordillera

The stratigraphy of WC is subdivided into two blocks which are the Pallatanga Block, and the Macuchi Block (Figure 2) (Hughes & Pilatasig, 2002, Vallejo et al., 2019). The Pallatanga Block is composed of parts of the Cretaceous oceanic plateau which forms the WC basement; a Late Cretaceous island arc sequence associated to Campanian-Maastrichtian volcaniclastic and marine deposits; a Paleocene-Eocene post-collisional marine sedimentary sequence with continental crust source from a continental arc; and an Oligocene continental arc possibly associated to an intramontane sedimentary deposit (Hughes & Pilatasig, 2002; Jaillard et al., 2004; Vallejo et al., 2019). The Pallatanga Block is limited to the east by Calalacli-Pujilí-Pallatanga fault (CPPF), which is characterized by a tectonic mélange in Pujilí (Hughes & Pilatasig, 2002). The western limit for Pallatanga Block is defined by Chimbo-Toachi Shear Zone (CTSZ) (Hughes & Pilatasig, 2002). The Macuchi Block is composed of an Eocene submarine volcanic arc and volcaniclastic sediments of the Macuchi Unit (Jaillard et al., 2004; Vallejo et al., 2019). The Macuchi Block is limited to the east by CTSZ and the western limit is buried by alluvial deposits of the coastal plain (Vallejo et al., 2019).

2.1.1 Basement of the WC

The Basement of WC is composed of Pallatanga Formation, San Juan Unit, Totoras Amphibolite, and Pujilí Melange which emerge on the eastern edge of the WC in the form of bands (Figure 2) (Vallejo, 2007; Vallejo et al., 2019). These formations have been interpreted as a part of an oceanic plateau, except for the mélange, which is the product of the collision between the oceanic plateau and the continental margin in the Late Cretaceous (Vallejo, 2007; Vallejo et al., 2019). The formations that constitute Pallatanga Block are described in detail below.

2.1.1.1 Pallatanga Formation

The Pallatanga Fm is composed of basalt, pillow lavas, medium-grained gabbros, some peridotites, and dolerites (Hughes & Pilatasig, 2002; Vallejo, 2007; Vallejo et al., 2009). This formation shows different grades of alterations of plagioclases to albite-clay minerals, and pyroxenes to actinolite-albite (Vallejo, 2007). The Pallatanga Fm. is overlain by Campanian to Maastrichtian radiolarites, and it has a radiometric age of 87.10±1.66 Ma (2 σ), obtained using the U/Pb method (Jaillard et al., 2004; Vallejo, 2007). The Pallatanga Fm has very good outcrops in Pallatanga valley in Chimborazo province, also along the Aloag-Santo Domingo road, Salinas-San Lorenzo road, and the Calacalí-Nanegalito road. Almost all of these outcrops are in the eastern flank of the WC (Hughes y Bermúdez, 1997; Vallejo, 2007).

2.1.1.2 San Juan Unit

The San Juan unit is composed of dunites, layered gabbros, amphibole bearing gabbros, serpentinized peridotites, fine-grained peridotites, and some local anorthosites. These rocks had been defined as an ultramafic intrusive component of the Caribbean Plateau (Vallejo, 2007; Vallejo et al., 2009). Recent radiometric U/Pb data from layered gabbros have an age of 87.10±1.66 Ma (Vallejo, 2007; Vallejo et al., 2009). This formation has an occurrence near the San Juan Village, along the Saloya river, in the Quito-Chiriboga road, and to the east of the Totoras Village (Kerr, Aspden, Tarney, & Pilatasig, 2002; Vallejo, 2007; Vallejo et al., 2009)

2.1.1.3 Totoras Amphibolite

Totora amphibolite is composed of amphibolites (Jaillard et al., 2004; Vallejo, 2007). The amphibolites are characterized by phenocrysts of plagioclase, green hornblende, and quartz-feldspar veins, these veins are younger than rock (Jaillard et al., 2004; Vallejo, 2007; Vallejo et al., 2009). The age of these rocks is 84.69±2.23 Ma, obtained using the $^{40}Ar/^{39}Ar$ method (Vallejo, 2007; Vallejo et al., 2009). This formation has an occurrence near the Totoras Village in the Bolivar province (Vallejo et al., 2009).

2.1.1.4 The Pujilí Melange

The Pujilí Melange is composed of blocks of different compositions (Vallejo, 2007; Vallejo et al., 2009). These blocks are foliated muscovite rich granitoids, amphibolites, and conglomerates with a serpentinite matrix (Vallejo, 2007). The granitoids show indicators of dextral shear movement (Vallejo, 2007; Vallejo et al., 2009). These rocks are interpreted as remnants of the suture zone between the South America continental margin and the allochthonous oceanic blocks during accretion, in the Late Cretaceous (Vallejo, 2007; Hughes & Bermúdez, 1997; Jaillard et al., 2004). This mélange is well exposed along a river in the area between Saquisilí and Pujilí in the Cotopaxi province (Vallejo, 2007; Hughes y Bermúdez, 1997).

2.1.2 The Rio Cala Group

The Rio Cala Group is defined as the Campanian-Maastrichtian volcaniclastic and marine deposits associated to a Late Cretaceous island arc (Vallejo, 2007; Vallejo et al., 2009). This Group is composed of La Portada, Mulaute, Pilatón, Natividad, Rio Cala, Yunguilla formations.

2.1.2.1. La Portada Formation

La Portada Fm is composed of pillow basalts intercalated with mudstones with microfossils (Vallejo, 2007). The basalts are described with aphyric texture and glassy matrix with recrystallization of chlorite and epidote, also the basalts present different grades of oxidation and veins of calcite (Kerr et al., 2002; Vallejo, 2007). The La Portada Fm was interpreted as rocks from a volcanic arc resulting from the subduction of the oceanic crust below an oceanic plateau (Vallejo, 2007; Vallejo et al., 2009). The intercalations of the mudstones in the basalts, taken from outcrops of Otavalo-Selva Alegre road, have recorded microfossils of foraminifera with ages between Santonian to Early Campanian age (Vallejo, 2007). Van Thournout et al. (1992) reported pillow lavas in this formation on the Salinas-Lita road near to the La Concepcion village.

2.1.2.2. Mulaute Formation.

The Mulaute Fm is composed of siltstones, cherts, sandstones with volcanic-source derived clasts, and sandstones with a considerable abundance of plagioclase, epidote, and pyroxene (Vallejo, 2007). The lithologies of this formation are similar to those in the Pilaton Fm (including the majority of mineral alteration) (Vallejo, 2007; Vallejo et al., 2009). According to Vallejo (2009), these rocks are dated around 20.66±2.2 Ma with the $^{40}Ar/^{39}Ar$ method, but the author interpreted that this age was reset, and cannot be used to determine the absolute age of the unit. On the other hand, Hughes and Bermúdez (1997) reported a hornblende K/Ar age of 48.28±0.55 Ma from an intrusion of diorite that is cutting this Formation which provides a minimum age. According to Vallejo et al. (2019), Mulaute Fm is Campanian and it is older than Pilatón Fm. This formation has good outcrops in the Aloag-Santo Domingo road, and the Calacalí-La Independencia road (Vallejo, 2007).

2.1.2.3. *Pilatón Formation.*

The lithologies that we can find in this formation are similar to rocks in Mulaute Fm, siltstones, sandstones with volcanic-source derived clasts, cherts, and sandstones with intercalation of chert (Vallejo, 2007; Van Thournout et al., 1992). The sandstones in Pilaton Fm are mainly composed of epidote, pyroxene, and plagioclase, but the mafic minerals are altered by low grade hydrothermal processes resulting in chlorite and pumpellyite (Vallejo, 2007; Vallejo et al., 2009). The age for the Pilatón Fm is interpreted around Campanian – Maastrichtian period, recorded by foraminifera found in chert intercalations, these microfossils are Globotruncana sp., Guembelina sp., and Globigerina (Vallejo, 2007). This formation has good outcrops in the Aloag-Santo Domingo road, and the Calacalí-La Independencia road (Vallejo, 2007).

2.1.2.4. *Natividad Formation.*

The Natividad Fm is composed of mudstones, basaltic andesite tuffs with crystals of clinopyroxene, and sandstone with a low grade of metamorphism in which mafic minerals can be observed, also the sandstones are silicified and tectonized (Egüez, 1986; Vallejo, 2007; Vallejo et al., 2009). This formation is interpreted as a part of a turbidite fan with volcanic inputs (Vallejo, 2007; Vallejo et al., 2009). The Natividad Fm was deposited during the Campanian to Maastrichtian age based on foraminifera fauna (Vallejo, 2007; Vallejo et al., 2009; Van Thournout et al., 1992). This Formation has very good outcrops in the Otavalo-Selva Alegre road, and Salinas-Lita road. (Boland et al., 2000; Vallejo, 2007).

2.1.2.5. *Rio Cala Formation.*

Rio Cala Formation is mainly composed of massive lavas with basaltic to andesitic composition with phenocrysts, volcanoclastic breccia, and volcaniclastic sandstone (Almagor, 2019; Vallejo, 2007). This formation is interpreted as submarine volcanic arc deposits and has associations of volcaniclastic deposits. The age of the Rio Cala Fm. had been dated to 66.7±7.16 Ma using $^{40}Ar/^{39}Ar$ methods (Almagor, 2019; Vallejo, 2007). Therefore, Vallejo et al. (2019) states that the Rio Cala Fm is Campanian indicating there is a discordance at the beginning of the Maastrichtian. This formation outcrops at the northern part of WC in the Otavalo-Selva Alegre road, and Salinas-Lita road (Boland et al., 2000; Vallejo, 2007).

2.1.2.6. *Yunguilla Formation.*

In general, the Yunguilla Fm is variable along with WC but always is associated with pelagic sediments (Vallejo, 2007). The lithologies that we can find in these formations are pelagic cherts, dark gray massive siltstones, calciturbidites, and well-sorted sandstones (Almagor, 2019; Vallejo, 2007). The Yunguilla Fm is interpreted as the medial to the distal part of a turbidite fan (Almagor, 2019; Vallejo, 2007). Jaillard et al. (2004) propose a Late Campanian to Early Maastrichtian age from foraminifera fauna, and Vallejo (2007) dated five populations of detrital zircons which result in 69 Ma (Almagor, 2019). Vallejo et al. (2019) interpreted this formation as a Campanian-Maastrichtian marine sedimentary sequence with continental crust source. This unit outcrops along the eastern border of WC and has an extension from Cuenca in the Southern Ecuador and Nono village in northern Ecuador (Vallejo, 2007; Vallejo et al, 2009)

2.1.3 Angamarca Group

The rocks of the Angamarca Group form the Paleocene-Eocene post-collisional marine sedimentary sequences with continental crust source from a small continental arc. The Angamarca Group was deposited in a large basin with NNE-SSW trending strike-slip faults (Vallejo, 2007). This Group is subdivided from base to top into the Pilaló, Saguangal, Saquisilí, Unacota, Apagua, El Laurel, and Rumi Cruz formations (Hughes and Bermúdez 1997; Vallejo, 2007; Vallejo et al., 2019).

2.1.3.1. *Pilaló Formation*

The lithologies which make up this formation are black shales, pelagic cherts, siltstones, coarse sandstones, matrix-supported clasts with andesitic composition conglomerate, reworked tuff, and breccia with red oxidized andesites (Almagor, 2019; Vallejo, 2007). The Pilaló Fm was interpreted as rocks from basin plain with inputs from continental volcanic activity (Hughes & Pilatasig, 2002; Vallejo, 2007; Vallejo et al., 2009). The age for this formation is dated from intercalated andesites in the marine sequence that have an $^{40}Ar/^{39}Ar$ age of 34.81±1.35 Ma (Vallejo, 2007; Vallejo et al., 2009). The Pilaló Fm is a sequence with a sedimentary discordance at the base due to a collision event (Vallejo et al., 2019). The occurrence of Pilaló Fm is along the

Pilaló-Angamarca road, at the east of Pilaló village in Cotopaxi province (Boland et al., 2000; Vallejo, 2007).

2.1.3.2. Saguangal Formation

This formation is composed of volcanic breccia with clasts of andesitic composition, that progressively changes to black mudstone, intercalations of siltstones, and sandstones rich in muscovite and plagioclase (Almagor, 2019; Vallejo, 2007). This sequence is mainly dominated by mudstones (Almagor, 2019; Vallejo, 2007). The environment interpreted is a shallow marine environment or a lacustrine environment due to the high presence of mudstones (Hughes & Pilatasig, 2002; Vallejo, 2007; Vallejo et al., 2009). This formation has been dated to 58.8±8.9 Ma (2σ) using the U/Pb method on detrital zircons (Vallejo, 2007; Vallejo et al., 2009). From this data, it was interpreted that the formation occurs during Maastrichtian to the earliest Paleocene (Almagor, 2019; Vallejo, 2007). Saguangal Fm occur in near the intersection of the el Chontal road and la Gualea road along the Guayllabamba river (Vallejo, 2007)

2.1.3.3. Saquisilí Formation.

The Saquisili Fm is composed of silty mudstones, siltstones, and micaceous sandstones, with conglomerates towards the top of the formation (Almagor, 2019; Vallejo, 2007). The Saquisili Fm was interpreted as the distal to medial part of a turbidite fan with evidence of marine regression (Hughes & Bermúdez, 1997¸ Vallejo, 2007). The age for these formations was established as Early Paleocene to Middle Eocene by foraminifera fauna Trochammina sp, Turrillina sp cf robertsi, Cibicides sp cf pseudoperlucidus, and Gyroidinoides planatus (Hughes & Bermúdez, 1997). The occurrences of this formation are better exposed in the central part of the WC, east of Guaranda in the Bolivar province (Vallejo, 2007).

2.1.3.4. Unacota Formation.

Unacota Fm. is composed of calcareous rocks with intercalations of micrites and bioclastic limestone, also mudstones interbedded with siltstones are at the top of the formation (Egüez, 1986; Vallejo, 2007). The age was interpreted as Middle to Late Eocene by alga and foraminifera fauna which are Nummulites sp, Globorotalia, Discocyclina marginata, Discocyclina barkeri, Sphaerogypsino, Amphistegina sp. (Egüez, 1986; Vallejo, 2007). The Unacota Fm has very good outcrops along the La Maná to Latacunga road, and the Rios Chilcas section in the west of the village of Apagua (Vallejo, 2007)

2.1.3.5. Apagua Formation

The Apagua Formation is composed of siliceous silty mudstones, mudstones, siltstones, and sandstones. Also, in this Formation sills and stocks of andesitic composition are observed (Egüez, 1986; Vallejo, 2007). The Apagua Fm is interpreted as medial to the proximal part for a submarine turbidite fan with inputs of volcanic materials (Vallejo, 2007). Egüez (1986) indicates that this formation corresponds to Middle Eocene age by foraminifera fauna. The occurrences of this formation are along the La Maná-Latacunga road and Guaranda-Riobamba road, there is also an isolated outcrop in the cone of the Quilotoa volcano in the Cotopaxi province (Vallejo, 2007)

2.1.3.6. Laurel Formation

The lithologies for this formation are fine-grained sandstones, black and gray mudstones, and limestones rich in bioclast material (Vallejo, 2007; Van Thournout et al., 1992). Some foraminifera fauna has been recovered from limestones which suggest Lower Oligocene age (Vallejo, 2007; Van Thournout et al., 1992). These lithologies have been interpreted as the distal part of a submarine fan (Vallejo, 2007; Van Thournout et al., 1992). This formation occurs along the Colombia-Ecuador border in the Laurel village and Tufiño village in Carchi province (Vallejo, 2007).

2.1.3.7. Rumi Cruz Formation

The Rumi Cruz Fm is a coarsening upward sequence composed of red mudstones and shales, sandstones, breccias, and matrix-supported conglomerates (Almagor, 2019; Vallejo, 2007). This formation is interpreted as a fan-delta environment with great inputs from metamorphic and volcanic sources rocks (Almagor, 2019; Vallejo, 2007). According to Vallejo (2007), this formation is assumed to be Late Eocene to Oligocene age, and many outcrops can be found northwest of Quito and along the Apagua – Angamarca road.

2.1.4 Zambagua Group

Zambagua Group are Oligocene continental arc deposits which overlie deformed Cretaceous-Paleogene deposits with a discordant contact. The Zambagua Group is mainly composed of conglomerate, sandstone, and siltstone rich in volcaniclastic material, principally deposited in fluvial, alluvial, and lacustrine settings in intramontane basins (Vallejo et al., 2019).

2.1.4.1. San Juan de Lachas Formation

The lithologies for the San Juan de Lachas Fm are breccias with intercalations of lavas and sandstones, and andesitic lavas rich in plagioclase and hornblende (Almagor, 2019; Vallejo, 2007; Van Thournout et al., 1992). The age has been determined from an andesite to be 32.9±1.2 Ma (2σ) with the $^{40}Ar/^{39}Ar$ method (Vallejo, 2007; Vallejo et al, 2009; Van Thournout et al., 1992). This formation is overlaying the El Laurel Fm. and Rumi Cruz Fm with an unconformable contact (Vallejo, 2007; Vallejo et al, 2009; Van Thournout et al., 1992). The San Juan de Lachas Fm outcrops along the Salinas –Lita road, and Guayllabamaba river (Vallejo, 2007; Van Thournout et al., 1992).

2.1.5 Macuchi Block

The Macuchi Block is an Eocene submarine volcanic arc associated with volcaniclastic deposits (Vallejo et al. 2019). Some authors have proposed that it was an allochthonous body that collided against the continental margin in the late Eocene (Egüez, 1986; Hughes and Bermúdez, 1997; Kerr et al., 2002; Van Thournout et al., 1992), while others propose that it was formed *in-situ* (Vallejo et al. 2019). The Macuchi Block is composed of Macuchi Unit.

2.1.5.1. Macuchi Unit

Macuchi unit is composed of volcanic rocks like pillow lavas, andesites, volcanic breccia, dolerites, and also turbidite sandstones (Almagor, 2019; Egüez, 1986; Vallejo, 2007). The mafic rocks show a low grade of metamorphism evidenced by the occurrences of epidote, zeolite, and prehnite-pumpellyite (Almagor, 2019; Egüez, 1986; Vallejo, 2007). Many ages have been proposed for this unit: Egüez (1986) proposed 35.8±1.8 Ma usingK/Ar method in basalt, and 41.6±2.1 using K/Ar method in basaltic andesite; Spikings et al. (2005) proposed 68±11 Ma using U/Pb method on zircons from an Andesite; finally, Vallejo (2007) using $^{40}Ar/^{39}Ar$ method proposed ages of 42.62±1.3 Ma and 35.12±1.66 Ma. According to Vallejo (2007), very well defined outcrops are located in the Aloag-Santo Domingo road between La Union del Toachi and El Paraiso, there are also outcrops along the Pilalo- La Mana road in the small town of Alluiquin, and in the village of Lita in the Imbabura province.

2.1.6 Silante Formation

The Silante Fm is composed of red mudstone, volcanic conglomerate, matrix-supported conglomerates, poorly sorted massive sandstones, red breccias, crystal-rich tuffs, andesites, dacites and volcanic breccia (Boland et al., 2000; Egüez, 1986; Hughes & Bermúdez,1997; Vallejo 2007). The lithologies for this formation have been interpreted as sedimentary red-bed continental sequences, with inputs from volcanic arc activity (Almagor, 2019; Boland et al., 2000; Egüez, 1986; Hughes & Bermúdez,1997; Vallejo 2007). The Silante Fm extends from the north beginning with the small town of Naranjal, near the Salinas-Lita road, and appears intermittently to the south, outcropping along the roads Calacalí-Nanegalito, Alog-Santo Domingo, Quito-Chiriboga, Nono-Tandayapa, Otavalo-Selva Alegre, and finally disappears north of the Illinizas volcano (Almagor, 2019; Boland et al., 2000; Egüez, 1986; Hughes & Bermúdez,1997; Vallejo 2007).

2.2. Silante Formation Previous Works

From the time of the discovery of the Silante Fm to the present day, it has been a topic of discussion in relation to its stratigraphic relationships and age of deposition. This controversy arises from the different age ranges attributed by different authors, and the different chronostratigraphic positions attributed to it.

Savoyat et al. (1970) proposed Paleocene ages based on foraminifera fauna Gaudryina aff, laevigata Franke, Globotruncana sp. that were found in Silante Fm, but there is no evidence that these foraminifera are found in situ. In 1977, Bristow and Hoffstetter described the Silante Fm on the Nono-Nanegalito road, and interpreted it as a transitional stratigraphic sequence that formed below to the Yunguilla Fm. The stratigraphic top of the Silante Fm was described by Henderson (1979) as made up of lavas, he also mentioned that the Yunguilla Fm is overlapping the Silante.

Egüez (1986) describes the Silante Fm along the Chisinche river with presences of andesitic intrusions of porphyry texture, and some thin sills that are in contact with the lavas and breccias of the Tandapi Unit. Egüez (1986) proposed that the Silante Fm was deposited in the Paleocene -Eocene between marine deposits. Egüez proposes that the presence of the foraminifera comes from the erosion of the Yunguilla Fm. Egüez found that the Silante Fm is covering the Tandapi Unit. Van Thournout (1991) refuted Eguez's interpretation, with the idea of the Tandapi Unit as a sequence of Upper Oligocene age.

Hughes and Bermúdez (1997) propose that the Silante Fm had a post-Maastrichtian age since they report in their investigation a depositional contact in the base with the Yunguilla Fm on the Calacalí-Nanegalito highway. In addition, Steinmann (1997) carried out fission track analysis in zircons for the Silante Fm and reported ages of 16.8 ± 0.8 Ma. However, these data were interpreted that Silante Fm had a sedimentation age range from 53 Ma to 16.8 ± 0.8 Ma (Almagor, 2019; Hughes & Bermúdez,1997; Vallejo, 2007).

Boland et al. (2000) propose ages from the late Eocene to the early Oligocene based on Foraminifera fauna Bulimina scenes, Globigerina angiporoides, Globorotalia munda that were found in samples from mudstones. However, this sampling is controversial since the samples were taken from a faulted contact between Silante Fm and Angamarca Fm (Herrera, 2019).

According to Vallejo (2007), the Silante Fm was deposited in the Paleocene based on dating of four volcanic rocks from the Tandapi Facies in the Silante Fm using the ^{40}Ar / ^{39}Ar method. Vallejo reports ages of 58.1 ± 3.9 Ma, 61.0 ± 1.1 Ma, and 63.96 ± 10.7 Ma for the samples taken from the Calacalí-Nanegalíto highway, and the age of 65.68 ± 4.36 Ma from the samples taken on the Nono-Tandayapa highway. In addition, Vallejo (2007) presents summaries of the stratigraphic columns raised in the Nono-Calacalí, and Salinas-Lita areas (Figure 4).

Recent works by Almagor (2019) and Herrera (2018) propose that the Silante Fm was deposited during the middle Oligocene-Miocene based on the result of 45 dates obtained using U-Pb method on detrital zircons, which he reports an age of 16.51±0.105 Ma 2σ, and interpreted as a result of the erosion of San Juan de Lachas

Fm. As a result, the sedimentary facies and the volcanic Tandapi Facies, in which Vallejo (2007) dated, are not a single unit. Almagor (2019) also presents a lithologies description table and the stratigraphic column of the Silante Fm of the Calacalí-Nanegalito section (Figure 3), where he shows a summary of the facies found in Silante Fm.

In the Ministerio de Energía y Minas, et al. (1998) Geological Map of the Western Cordillera of Ecuador between 0 ° -1 ° N (scale of 1: 200000), the Silante Fm is delimited by faults on its east-west flanks. To the south, it borders the skirts of the Iliniza Norte volcano, and to the north on the Salinas-Lita road, but they only mark a small outcrop near the bridge to the community El Naranjal. This map proposes an age from the middle Eocene to the Oligocene based on Boland, et al. (1970). This geological mapping for the Silante Fm of the Salinas-Lita road coincides with that of some papers presented, and to date is still accepted, in which most of the continental strata exposed along the Salinas-Lita road is assigned to the occurrence of the Chota Fm.

Lithofacie code		Description	Interpretation
A	Gmm2	Granules, pebbles and blocks, supported matrix, sandy matrix, poorly sorted. Inverse gradation appears at the base of the strata.	Deposits formed by debris flows.
B	Fl	Red shales with occasional parallel lamination.	Represents flood deposits in alluvial plains.
	Fsm	Very fine red siltstones and sandstones, without sedimentary structures, with a tabular geometry.	The Fl and Fsm litho facies represent distal positions in an alluvial fan deposited only in occasional flood events.
C	Smp	Coarse to very coarse-grained sandstones with the presence of clasts whose size varies between granules and pebbles.	Lithofacies deposited by debris flows. Deposits can be found in alluvial fan systems.

D	Sh	Reddish cream sandstones, coarse to very coarse grain size with parallel lamination.	Sandstones with parallel lamination of medium to coarse grain size are interpreted as the result of reworking of debris flows.
E	Sm	Fine to coarse-grained purple and cream sandstones without sedimentary structures.	Massive sandstones interpreted as a result of rapid deposition of heavily laden sediment flows during less intense floods.
F	Gmm1	Granules and pebbles, supported matrix, sandy matrix, moderately drawn.	Matrix conglomerates supported by a sandy matrix are interpreted as deposits products of debris flows.
G	Gcm1	Conglomerates clast supported, moderately drawn, clasts rounded between granules - pebbles, clay matrix.	Classical conglomerates supported by a clay matrix are interpreted as deposits placed by debris flows where the collision of the clasts was hampered by the fine-grained matrix, which has a highly viscous behavior.
H	Gcm2	Conglomerates supported, poorly sorted, clasts between pebble-gravel granules, rounded with high sphericity, sandy matrix.	A product of non-cohesion debris flows, the parallel alignment of the clasts to the base of the strata suggests a frictional interaction between the clasts in the deposit.

Figure 3. Summary by Almagor (2019) of the lithofacies of Silante Fm in the Nono-Tandayapa and Calacalí-Nanegalito roads.

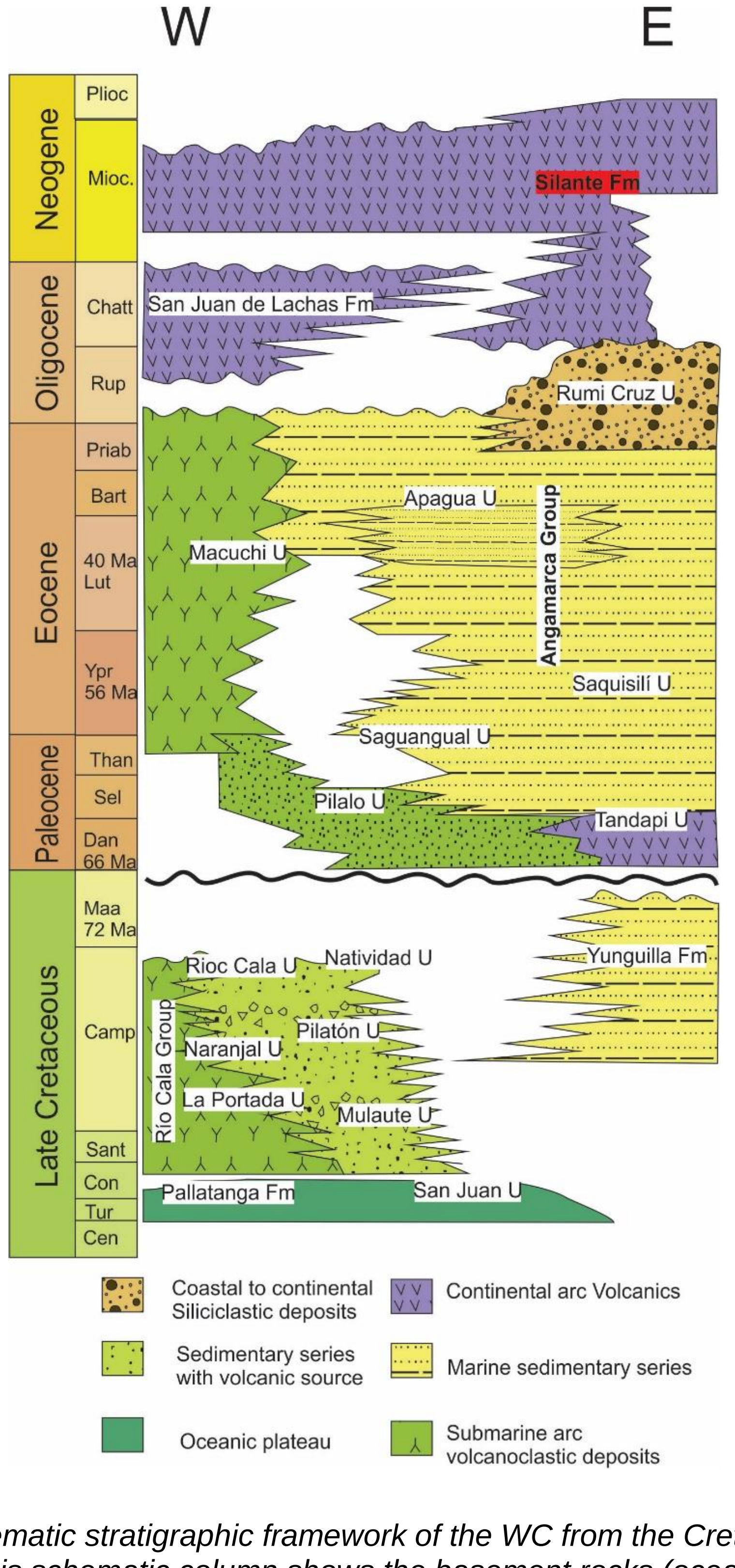

Figure 4. Schematic stratigraphic framework of the WC from the Cretaceous to the Neogene. This schematic column shows the basement rocks (oceanic plateau), volcanic rocks and sedimentary rocks. The Silante Fm. is highlighted with a red box. Modified image of Vallejo et al. (2019).

III. METHODS

This study consisted mostly of field surveys. These were conducted along the Salinas-Lita road, as well as secondary paths. The fieldwork was carried out over approximately 6 weeks. During this time the stratigraphy and structural features were measured, and samples were collected for petrographic analysis.

In order to characterize the Silante Fm in the Salinas-Lita transect, three stratigraphic sections were analyzed (Figure 5). The graphic sediment log or stratigraphic column is the common method used by the geologist to present stratigraphical information of the rock succession, and compare strata between different study areas (Zervas et al., 2019). In order to do the stratigraphic column, we considered the following parameters: grain size, layer thickness, sedimentary structures, tectonic structures, clast composition (in the case of conglomerates), the roundness of clasts, color of the beds, contacts, and any other notable information. The process for making these stratigraphic columns begins with the recognition of well-exposed outcrops to collect stratigraphic information. Then there is a recognition of the lithologies that must be described in detail considering the previously mentioned parameters. Finally, for the graphic sediment log digital presentation, we used the program SedLog which is a multi-platform program for creating graphic sediment logs (Zervas et al., 2019). In the program, the graphic sediment log uses a vertical scale for layer thickness, lithology patterns, and structure symbology.

The use of stereographic projections is necessary to analyze the tectonic structures that we find in this small intramontane basin. The stereographic projection is an azimuthal projection that provides a simple way to represent the orientations of three-dimensional structures on a two-dimensional plane (Marshak & Mitra, 1988). The stereographic projection helps us to statistically analyze the structural features found in the Salinas-Lita transect. We used the equal-area net which is constructed of projections of great circles and the small circles (Marshak & Mitra, 1988). The great circles, which defines the longitudinal grids, are built by drawing all the possible great circles that pass from North to South and that are separated by 2° (Marshak & Mitra, 1988). The small circles, which define the latitudinal grids, are made up of the projections of straight circular cones, drawing a line that goes from east to west and decreases in diameter from the center of the sphere towards the poles (Marshak & Mitra, 1988). In the same way, small circles are separated by 2° (Marshak & Mitra, 1988). The orientation of a bed, fault, joint, or any other planar structure will be represented as a line in the stereographic projection. The orientation of slickensides, fold hinge, the axis of a drill hole, poles (lines perpendicular to a plane), or any linear geologic structure will be represented as a point in the stereographic projection (Marshak & Mitra, 1988). The stereograms were plotted with the Stereonet 11 program developed by Allmendinger, R. W., Cardozo, N., and Fisher, D.

Another tool that we used were rock thin sections. These are slabs of rocks that have a thickness of 30 microns. The thin sections are necessary for the description of the mineralogy and microstructure of the rocks of this basin. These thin sections were described with the use of the polarized petrographic microscope. The first step to start with the thin section preparation is to determine which lithologies are most relevant for the study of the project. In this study, we analyze ten from selected targets. The targets were chosen to identify rocks that are difficult to describe in hand specimen. These rock samples were taken to the laboratory of the Instituto de Investigación Geológico y Energético (IIGE), where the thin sections were prepared. The preparation of the thin sections has a custody document and a key for each sheet which was the following denomination **LB2020-#**, where the (#) will be replaced by the corresponding number from 01 to 10.

The IIGE has its own methodology for making thin sheets which will be explained below:

1. Identification: a chain of custody or a document that serves as a guide must be made with the ID number (**LB2020-#**).
2. Primary cut: The samples that have dimensions beyond 15cm x 15cm should be selected to make the first cut with a large cutter.
3. Secondary cut: samples are cut to the final size of the chips. The chips must have the dimensions near to 8cm x 3cm, it does not matter that it is exactly the same.
4. The chips obtained are placed to dry on a hot plate.

5. Hardening: after drying, the samples are hardened with epoxy resin to act as a cement between the pores and fissures. This is especially important for friable samples.
6. On the front face of the chip, we add 5 drops of transparent resin.
7. Immediately add 2 drops of catalyst.
8. We mix with a small trowel, and expand the resin, over the entire surface of the chip.
9. Dry on the heat plate.
10. We polish a surface of the chip with a diamond inlay disc and silicon carbide as abrasive. This step is important because the surface to which the glass is stuck to the rock must be completely flat.
11. The polishing process is carried out on discs of varying size of grit (120, 240,360, 650, 1000), from the coarsest to the finest, to gradually improve the polish and remove all the resin.
12. The surface where we will glue the glass sheet must be very well polished and to give the final touch, we finish it on a thick glass plate with silicon carbide with a grit size of 1000.
13. We put the samples with the polished face to dry on the hot plate and the glass sheets that will be glued.
14. We place thermogenic resin on the glass while it heats up on the hotplate.
15. We place the glass sheet on the sample very carefully and avoid leaving air bubbles. For this, we will move the glass sheet circularly until we observe that the bubbles have disappeared.
16. Wait at least 1 hour for the resin to dry completely
17. Precision cut: for this step you need the precision cutter with the metallic arm connected to the vacuum pump to hold the glass sheet. At this point the sample thickness is reduced to about 1 to 0.5 cm thick.
18. The sample is reduced to the final thickness (around 30 µm) by polishing it with very fine abrasive.
19. The final surface is polished with the glass plate and a very fine abrasive.
20. The thickness is verified on the microscope by finding a mineral that is known (such as quartz) and confirming that the interference color is correct. The interference colors of quartz, under polarized light, serve as indicators of the thickness of the thin section. If the quartz or some other guide mineral has

interference colors different from those expected, repeat the process from step 18.

21. Dry the thin section on the hot plate.
22. Add 5 drops of clear resin and 2 drops of catalyst.
23. Quickly and carefully place the coverslip.
24. Remove bubbles.
25. Remove excess resin.
26. Let stand for 8 hours.
27. Soak 10 minutes in alcohol.
28. Clean the sheet and excess dried resin with a scalpel.
29. Label with the corresponding code.
30. Develop the petrographic description.

IV. GEOLOGICAL FEATURES OF THE STUDY AREA

Results based on field observations are presented in the next chapter. This chapter is composed of a geological map resulting from this work, the stratigraphy of the study area, and the structural characteristics.

4.1. Stratigraphy

In the following section we present the summary of the stratigraphic columns, and the descriptions of the lithologies found in the work area.

4.1.1. Stratigraphic Column

The following graphic logs in the Figure 6, show the majority of the lithologies found in the work area. The first column (Column A) was started on the Salinas-Lita highway in the southernmost part of the work area at the coordinate UTM 17N 818182/66927 (Figure 6), and spans 840 m of the road, ending at 17N 818423/67565. The second column (Column B) starts at coordinate UTM 17N 815065/71304 (Figure 5), and spans 560 m of the road ending at coordinate 17N 814898/70902. The third column (Column C) describes the strata at the bridge of the El Naranjal site at the coordinate UTM 17N 814442/73515 (Figure 5), it spans 430 m of the road and ends at coordinates 17N 814795/73391.

One of the most important characteristics of the studied strata is that there are conglomerates with different color. Green, red and gray conglomerates beds were observed. The other notable feature in the conglomerates is diversity in clast composition. The green conglomerates are composed by shales, cherts, quartzites, sandstones, and rarely diorites. The red conglomerates are formed by basalts, shales, cherts, sandstones, and diorites, and finally, the gray conglomerates present only diorites and andesites clasts. Thus, based on composition and color in conglomerates, the Silante Fm have been divided in two members: the lower Green Silante member and the upper Red Silante member. These two members show a widespread tilting. On the other hand, the gray conglomerates are a unit mapped as volcanic cover, which are formed by horizontal beds. These characteristics will be described in more detail in the following section (4.1.2).

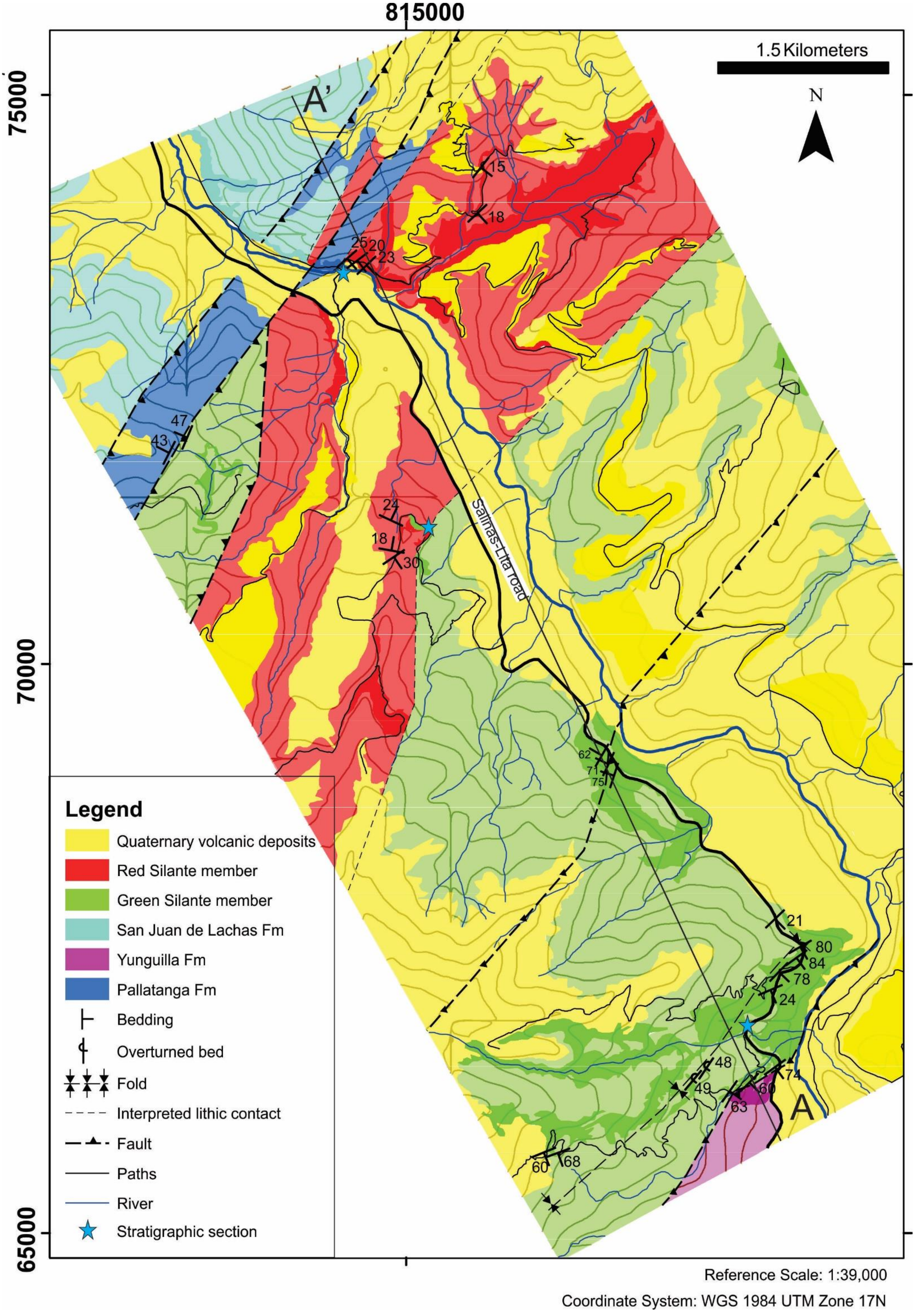
815000
75000
70000
65000
1.5 Kilometers
N
A'
A
Salinas-Lita road
15
18
25
20
23
47
43
24
18
30
62
71
75
21
80
84
78
24
48
49
74
60
63
60
68
Legend
Quaternary volcanic deposits
Red Silante member
Green Silante member
San Juan de Lachas Fm
Yunguilla Fm
Pallatanga Fm
Bedding
Overturned bed
Fold
Interpreted lithic contact
Fault
Paths
River
Stratigraphic section
Reference Scale: 1:39,000
Coordinate System: WGS 1984 UTM Zone 17N

Figure 5. Geological map from our work area. The blue stars on the map show the location of the stratigraphic columns, there are three columns in total. The blue polygons represent Pallatanga Fm.

We summarize the columns in the following stratigraphic profile (Figure 6), where we can see that Column A (Figure 22) is composed of the Green Silante member and Volcanic Cover which are separated by an erosive contact. Column C (Figure 24) is composed of the Red Silante member and Volcanic Cover, and they are separated by a discordant angular contact. Finally, column B (Figure 23) we find the Green Silante and Red Silante members and Volcanic Cover. The transition between these members is gradational, that is to say that we find intercalations of the members over a span of 13.2 m.

4.1.2. Lithofacies

In this section we will describe the lithofacies of the Silante Fm, but we will also mention the descriptions of other units that we have found in our study area as the rocks of the Pallatanga Fm, and Yunguilla Fm.

4.1.2.1. Pallatanga Formation

The Pallatanga Fm in the Salinas-Lita transect is composed of basalts that have a black color with an aphanitic texture with some phenocrysts of plagioclase. These rocks are concentric or pillow-shaped. The spaces between the pillows are filled with fine-grained material and oxides. These rocks present veins filled with calcite and quartz. Some fault planes and many fractures are observed. The occurrence of these rocks is on the railroad bridge at the entrance to the El Naranjal site that is accessed from the Salina-Lita highway, as well as along the road, east of our study area.

4.1.2.2. Yunguilla Formation

The rocks of the Yunguilla Fm in the Salinas-Lita transect are characterized by fine-grained, dark gray and black rocks. In general, two lithologies are observed for the Yunguilla Fm, but these rocks are very deformed and altered.

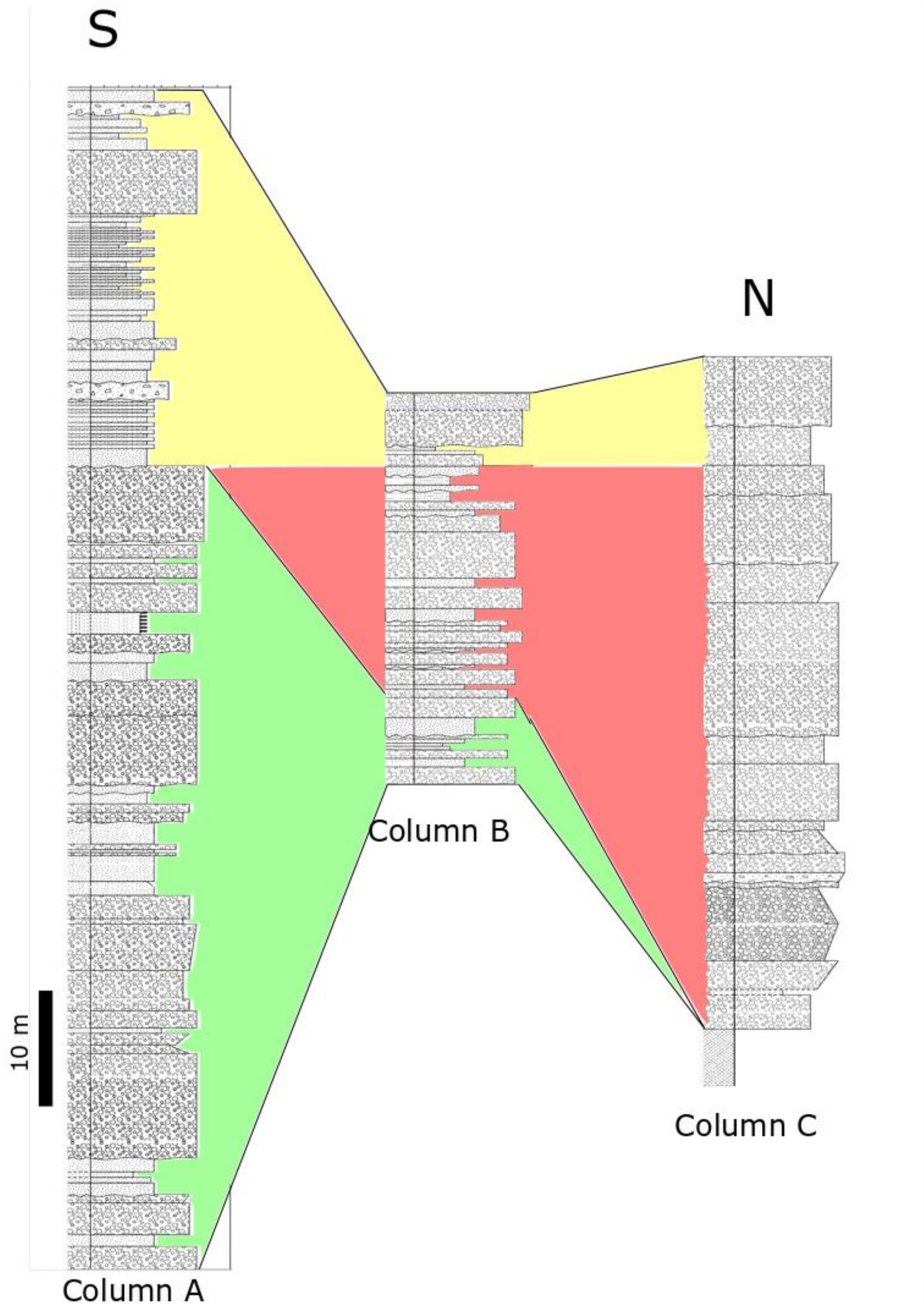

Figure 6. Stratigraphic section across study area. The green color represents the Green Silante member, the red color represents the Red Silante member. The yellow color represents the volcanic cover deposits.

4.1.2.2.1. Black Shales and Clayey Siltstone

The first lithofacies is formed by black shales with horizontal planar lamination, many fractures, and a low degree of metamorphism. The second lithofacies is composed of siltstone of light gray colors, and silt to clay-silt grain size, and presents cleavages (Figure 7). Due to the fact that the description in a hand sample was difficult, samples were taken to make thin sections.

The thin section (LB202-02) was taken at UTM coordinate 17N 818063/66290 (Figure 8). In this thin section, we observe the black shale rock which has fractures perpendicular to the laminations (Figure 7. A, B). The black shales mineralogy is composed of clays, very fine grains of muscovite parallel to the planar lamination as evidence of low degree of metamorphism, quartz and feldspars in veins, and the quartz was recrystallized that is the result of the silicification of the rock. In addition, this rock has a folded vein in the thin section (Figure 7. C, D).

The thin section (LB202-01) was taken at UTM coordinate 17N 817875/66238. In this thin section, we observe a part of the clayey siltstone which has some fragments of quartz and fractures perpendicular to the laminations (Figure 7. E, F).

The clayey siltstone mineralogy is composed of quartz, clay minerals difficult to identify, even with the microscope, and iron oxides cements.

The Yunguilla Fm in the study area is in tectonic contact with layers of conglomerates and sandstones. In addition, the rocks that are closer to fault contact are very fractured and altered by hydrothermal fluids, which gives them a tan to orange appearance, and almost completely obscuring its sedimentary layering. On the other hand, we observe how the two lithologies described are found in intercalations, and nodules of cherts of greenish to reddish colors are observed. These nodules are truncated by a poorly developed cleavage. These nodules of metamorphosed, fractured and deformed chets were an important key to identifying these rocks as Yunguilla Fm (Figure 8).

1.1.2.1. Silante Formation

In order to describe the Silante Fm, field work campaigns were carried out, going through secondary roads and drainages. Some of these places are easily accessible while others are difficult to reach.

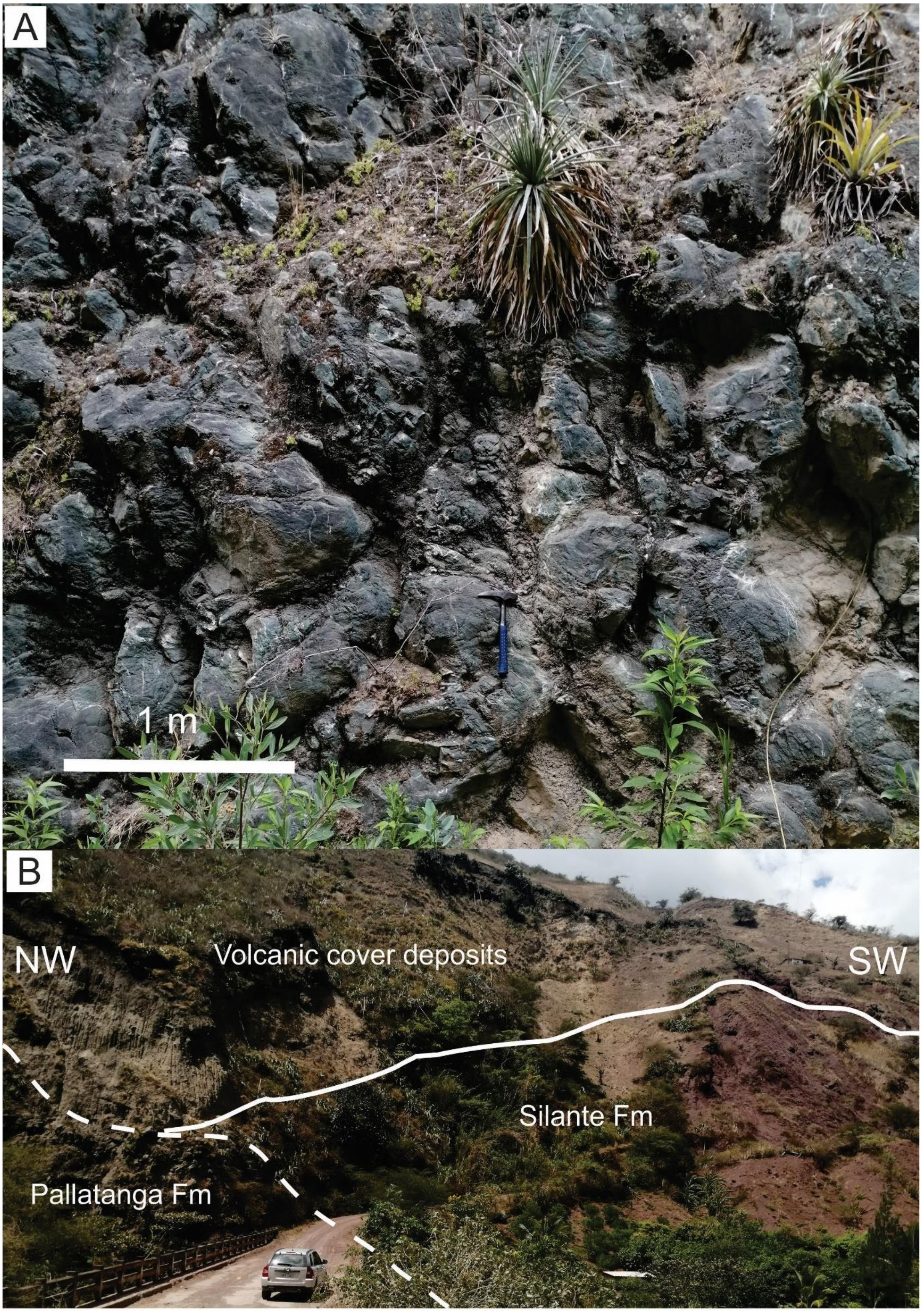

Figure 7.. A) Pillow basalts that have a black color B) Outcrop of the contact between Pallatanga Fm, and Silante Fm. Over the continuous line we have volcanic cover deposits. This outcrop is north of the map in UTM coordinate 17N 815065/71304.

The thickness of this formation cannot be defined since the stratigraphic base and top were not observed in our work area. Moreover, the Silante Fm has been divided in two members: the lower Green Silante member and the upper Red Silante member.

4.1.2.3.1. Green Silante member

The Green Silante member is composed of principally conglomerate with green colors, and massive sandstones. It differs from the Red Silante member by the composition of clasts, and the relationships of conglomerates versus sandstones.

Lithofacies 1: Matrix-supported Conglomerate (Gmm1)

The facies is massive, has rounded to sub-rounded clasts, light brown, very poorly sorted, matrix supported, clast size range from granule to cobble, has a low maturity, and it has a few meter with planar lamination but is rare. Most of the layer-to-layer contacts of these conglomerates are sharp contacts, on occasions it has sandstone intercalations.

Approximately 6m of this conglomerate presents grading, normal and inverse grading. These layers of conglomerates have a thickness range from 0.5 m to 20 m.

The sandstones that are interbedded between the conglomerates are massive, light brown, and have high quartz and feldspar content. These sandstones come in sizes from fine to coarse sand. Sometimes intervals with different grain size are stacked vertically with diffuse boundaries, but do not form graded beds. They can show planar lamination, but is rare. These layers of sandstones have a thickness range from 1m to 6m. The contacts between the conglomerates and the sands are generally erosive contacts and the geometry of the sandstone layers are tabular.

The clast composition of conglomerates is variable with the following lithologies presented from the one that occurs most frequently to the least:

- Andesites with light gray color, with a holocrystalline texture, massive, very small crystal size. It has very few differentiable crystals, among them some hornblende, plagioclase, and very rare one or another quartz.
- Black shales, clay grain size, foliation defined by planar lamination, very well-rounded, and low degree of metamorphism.

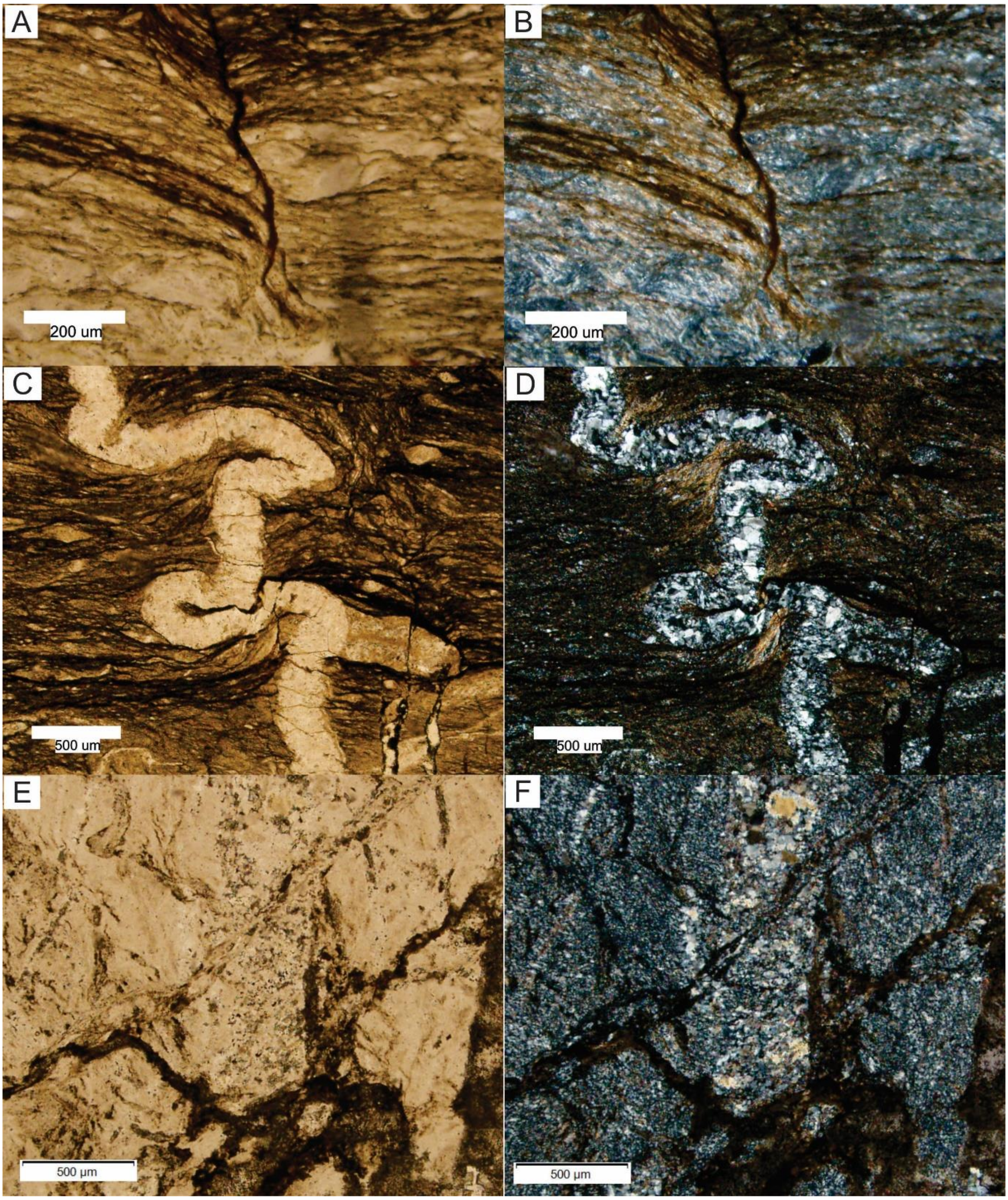

Figure 8.. A, B, C, and D, are the images of the thin section LB2020-02, and the E and F are de images of the thin section LB2020-01. the left column of tan images in plane polarized light and the column on the right in cross polarized light part. A and B show the black shale rock which has fractures perpendicular to the laminations are folded. C and D show the folded vein which is filled with recrystallized quartz and feldspar. E and F show the fragments of the chetrs, in this image we can see the massive packets of quartz result of the silicification of the rock.

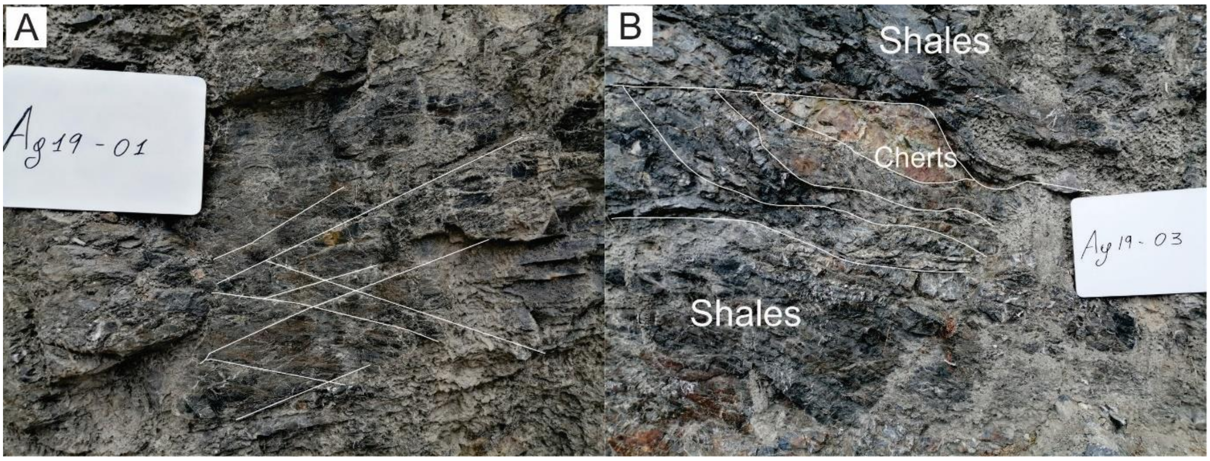

Figure 9. Yunguilla Fm outcrop showing shale rocks and cherts. In part A, the shales rocks are shown and fractures that were measured are marked. In part B black shales and cherts are observed. The cherts are in nodules and this nodule are truncated by a poorly developed cleavage. A was taken from coordinate Utm 17N 818174/66248, and B from coordinate Utm 17N 818172/66246

- Quartzite clasts with milky white color, well-rounded, presents conchoidal fracture and a hardness of 7, and clastic texture.
- Chert clast with dark bluish colors, conchoidal fracture, a hardness of 7, and it is translucent. Within this rock fragments of lithics are observed.
- Sandstone clasts with a clastic texture, rounded, the grains size within the clast is coarse sand and there is a high content of feldspar. This clast is well consolidated and comes from a previously formed sedimentary rock.

Lithofacies 2: Greenish Matrix-supported Conglomerate (Gmm2)

The facies is massive, has rounded to sub-rounded clasts, green color, very poorly sorted, matrix supported, clast size range from granular to cobble, has a low maturity, it has planar lamination but is rare. Most of the layer-to-layer contacts of these conglomerates are sharp contacts, and it has some sandstone intercalations. These layers of conglomerates have a thickness range from 1 m to 22 m.

The clast composition of conglomerates is variable with the following lithologies presented from the one that occurs most frequently to the least:

- Black shales, clay grain size, foliation defined by planar lamination, very well-rounded, and low degree of metamorphism.
- Quartzite clasts with milky white color, well-rounded, presents conchoidal fracture and a hardness of 7, and clastic texture.
- Chert clast with dark bluish colors, conchoidal fracture, a hardness of 7, and it is translucent. Within this rock fragments of lithics are observed.
- Sandstone clasts with a clastic texture, rounded, the grains size within the clast is coarse sand and there is a high content of feldspar. This clast is well consolidated and comes from a previously formed sedimentary rock.
- Andesite clasts with light gray color, holocrystalline texture, massive, very small crystal size. It is a volcanic rock with very few differentiable crystals, among them some hornblende, plagioclase, a few quartz.

Lithofacies 3: Greenish Massive Sandstone (Sm1)

The sandstones that are interbedded with green conglomerates are massive, light green, clastic texture, the shape of particles is sub-rounded, and have high feldspar content. These sandstones come in sizes from medium to coarse sand, and show planar lamination but is rare. These layers of sandstones have a thickness range from 0.5m to 5m, and the contacts between the conglomerates and the sands are generally sharp, but also has erosive contacts. The geometry of the sandstone layers has lateral continuity despite being very thin layers and the change of colors may be generated of a hydrothermal alteration.

4.1.2.3.2. Red Silante member

The green Silante member is composed of principally conglomerate with red-purple colors, massive sandstones, and some layers of mudstones.

Lithofacies 4: Reddish Matrix-supported Conglomerate (Gmm3)

The facies is massive, has rounded to sub-rounded clasts, red-purple in color, poorly sorted, matrix supported, clast size range from granular to cobble, has a between low and medium maturity, and this facies does not show sedimentary structure. Most of the layer-to-layer contacts of these conglomerates are sharp contacts. This conglomerate presents some meters with normal grading but is rare. These layers of conglomerates have a thickness range from 0.5 m to 20 m.

The clast composition of conglomerates is variable with the following lithologies presented from the one that occurs most frequently to the least:

- Basalt clasts with black color, holocrystalline texture, massive, very small crystal size. It is a volcanic rock with very few differentiable crystals, among them some plagioclase, and few hornblende.
- Red shales, clay grain size, foliation defined by planar lamination, very well-rounded, and low degree of metamorphism.
- Chert clast with dark bluish colors, conchoidal fracture, a hardness of 7, and it is translucent. Within this rock fragments of lithics are observed.
- Sandstone clasts with a clastic texture, rounded, the grains size within the clast is coarse sand and there is a high content of feldspar. This clast is well consolidated and comes from a previously formed sedimentary rock.

Lithofacies 5: Reddish Matrix-supported Conglomerate (Gcg1)

The facies is massive, has rounded to sub-angular clasts, red in color, very poorly sorted, clast-supported, clast size range from granule/pebble to pebble/cobble, has a between low maturity, and this lithofacie does not show stratigraphic structure. Most of the layer-to-layer contacts of these conglomerates are sharp contacts. This conglomerate presents normal and inverse grading. These layers of conglomerates have a thickness range from 0.2 m to 13 m.

The clast composition of conglomerates is variable with the following lithologies presented from the one that occurs most frequently to the least.

- Basalt clasts with black color, holocrystalline texture, massive, very small crystal size. It is a volcanic rock with very few differentiable crystals, among them some plagioclase, and few hornblende.
- Chert clast with dark bluish colors, conchoidal fracture, a hardness of 7, and it is translucent. Within this rock fragments of lithics are observed.
- Sandstone clasts with a clastic texture, rounded, the grains size within the clast is coarse sand and there is a high content of feldspar. This clast is well consolidated and comes from a previously formed sedimentary rock.

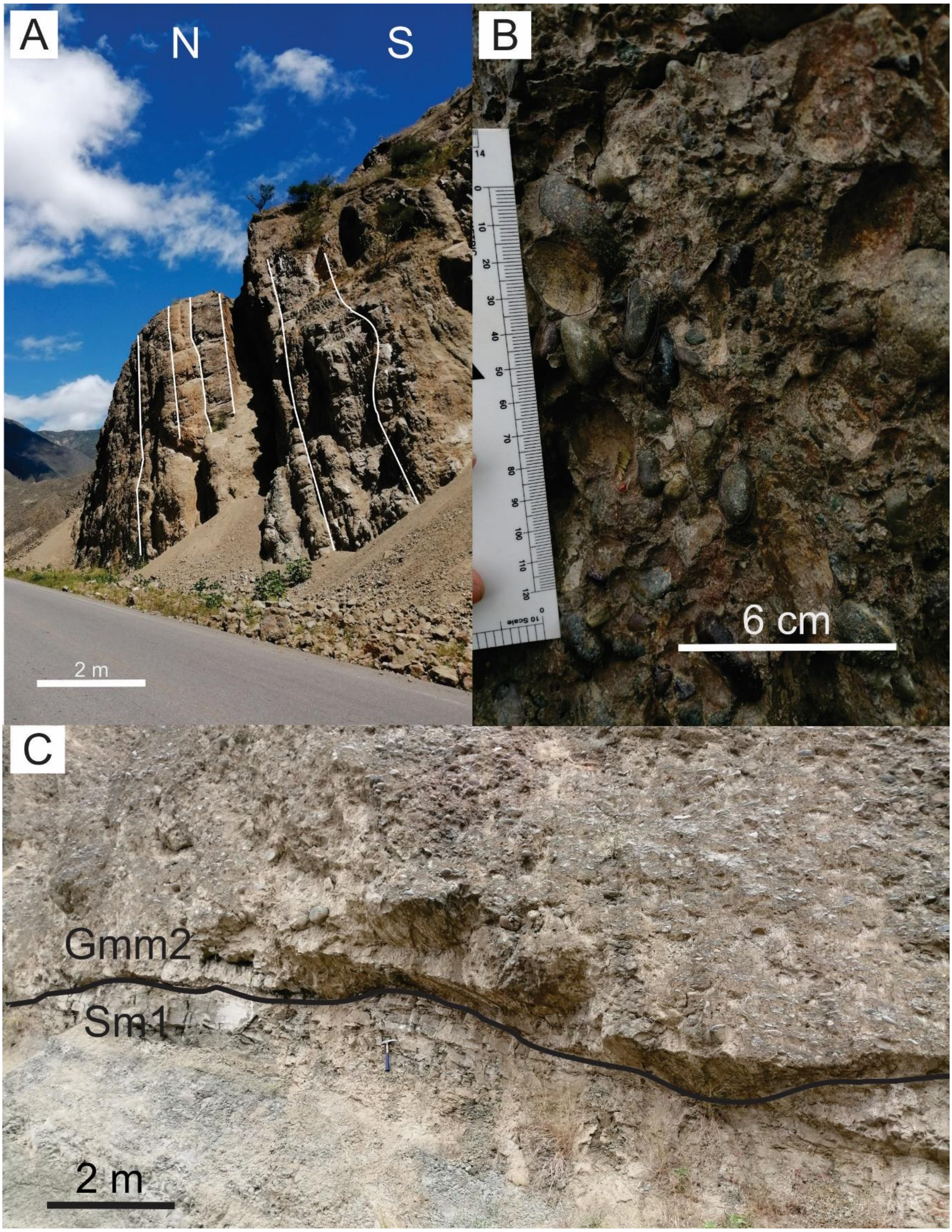

Figure 10.. A) Outcrop of the Green Silante member conglomerate layers on the Salinas -Lita road, 17N 818484/67503. B) Clasts that make up the green conglomerates of lithology of Green SIlante member. C) Erosive contact frequently observed between conglomerates and sandstone.

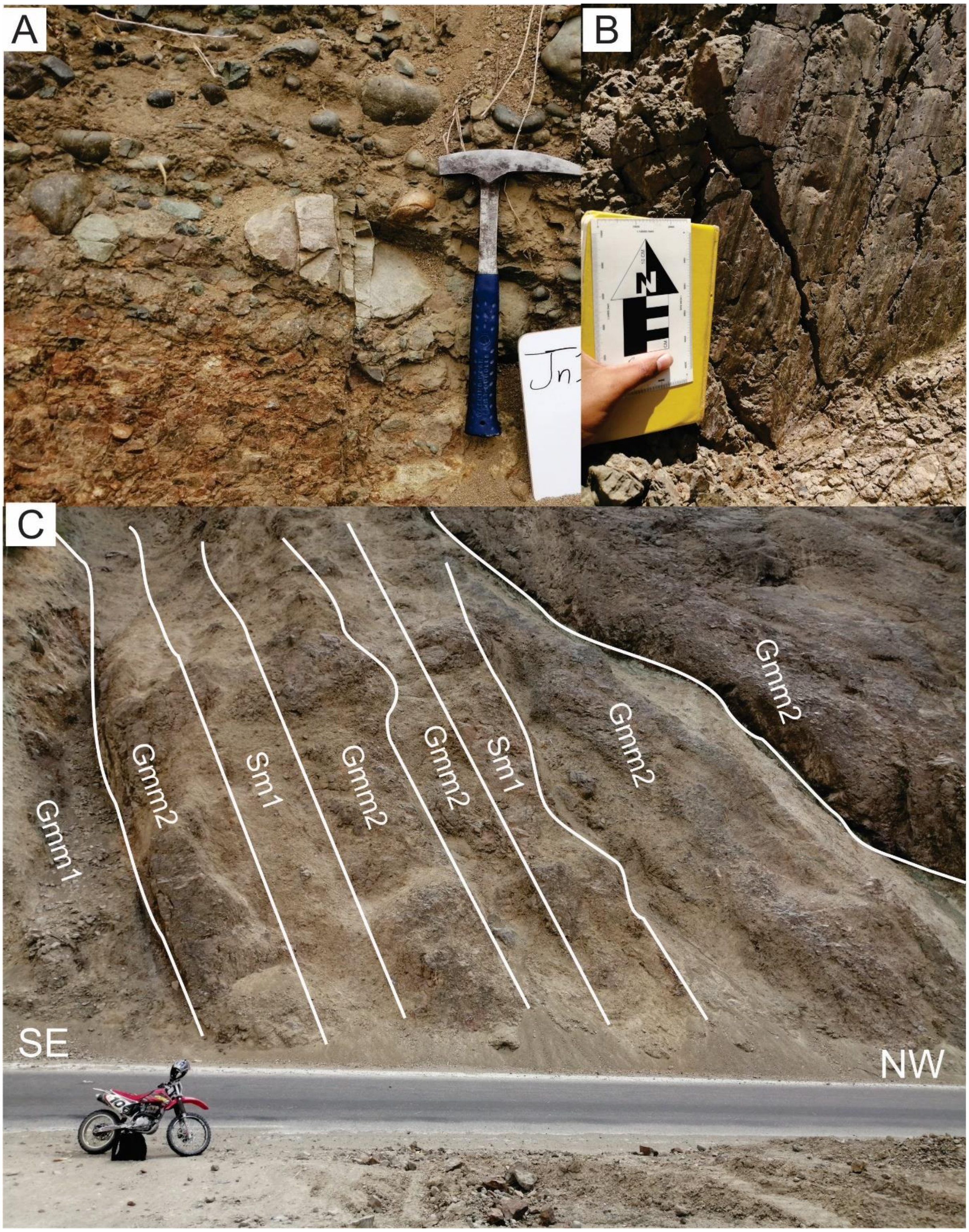

Figure 11. A) fractures with displacement on conglomerates of the Green Silante member resulting from post-deposition tectonism. B) fault plane over conglomerates with slickensides, this fault is represented in the stereonets below. C) outcrop of the Green Silante member that indicates the occurrence of the lithofacies Gmm1, Gmm2, and Sm1 on the Salinas-Lita road, 17N 816870/ 69068.

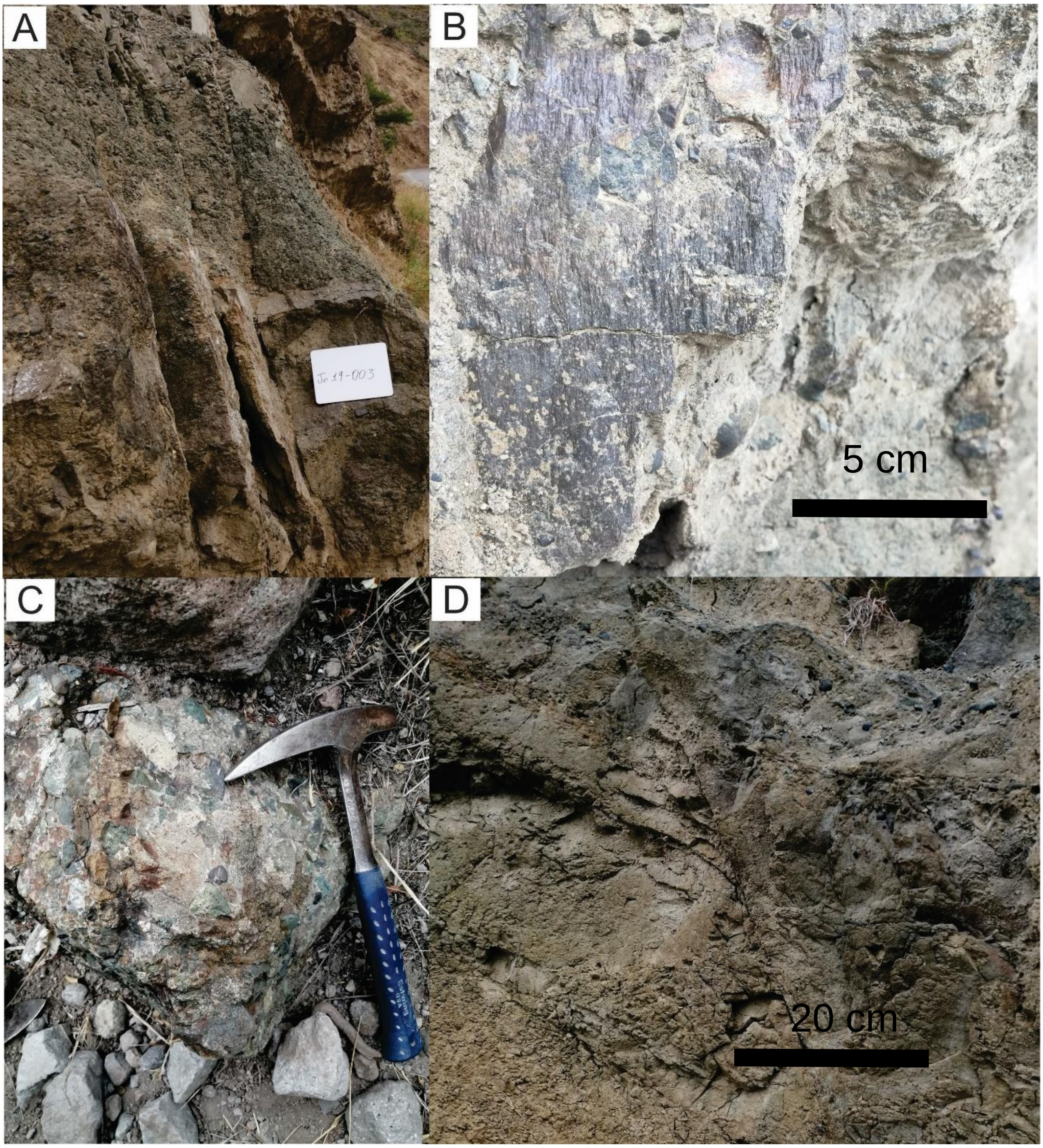

Figure 12. A) Gmm2 conglomerates with fractures, where the white board measures 20cm wide by 10cm long. B) Some of the mentioned fractures show displacement, this photo is one of them, and was taken at point 17N 818207/6703. C) In this image we can see the clasts that make up the conglomerates of the Green Silante member. D) Green Sandsotnes of the Sm1, massive and with the presence of fractures

Lithofacies 6: Reddish Massive Sandstone (Sm2)

The sandstones are massive, light red-purple, clastic texture. The grains are sub-rounded and the matrix is rich in iron oxide. These sandstones come in sizes from medium to coarse sand, and do not show stratigraphic structures. These layers of sandstones have a thickness range from 0.5m to 2m, and the contacts between the conglomerates and the sands are generally sharp, but also has erosive contacts. The sandstone layers have lateral continuity.

Lithofacies 7: Reddish Mudstone (Fl)

This lithology has reddish and light brown colors, planar lamination, and presents cleavage defined by fractures parallel to the bedding. The grain size is clay, and it does not show fossils or bioturbation. The contacts whit the other beds is always sharp at the base, and sometimes has erosive contact at the top with sandstones of the (Sm2).

4.1.2.4. Quaternary Volcanic Deposits

Below we describe the facies of the volcanic units, which are overlaying Silante Fm, in order to differentiate between volcanic units and Silante Fm.

Lithofacies 1: Gray Matrix-supported Conglomerate (Gmm4)

The facies is massive, has rounded to sub-angular clasts, gray color, very poorly sorted, matrix supported, clast size range from pebble to cobble, has a low maturity, it does not have sedimentary structure. The layer-to-layer contacts of these conglomerates are erosive contacts, and sometimes is sharp. These layers of conglomerates have a thickness range from 5 m to 12 m. There are three layers with approximate thicknesses of 2, 4 and 6 meters that the shape of the clasts of the conglomerate only has a sub-angular to angular shape but they maintain the same composition. The clasts are composed by diorites with porphyritic in texture, and do not have a fabric. These diorites are formed by alkali feldspar and a large portion of plagioclase.

Lithofacies 2: Gray Siltstone (Fm1)

This lithology has gray and light brown colors, is massive. The grain size ranges from clay/silt to silt, and it does not show fossils or bioturbation. The contacts with the other beds is always sharp at the base. These layers of siltstones have a thickness range from 1 m to 32 m.

Lithofacies 3: Yellow Sandstone (Sm3)

The sandstones are massive, light yellow, clastic texture, and the grains are sub-rounded. These sandstones come in sizes from medium to coarse sand, and do not show sedimentary structures. In general, these sands are largely composed of lithics, followed by feldspar and few quartz. These layers of sandstones have a thickness range from 0.5m to 2m, and the contacts between the conglomerates and the sands are generally sharp, but also has erosive contacts. The sandstone layers have lateral continuity.

4.2. Structural Features

4.2.1. Faults

Within the study area, there are two main faults, both of which are thrust faults. The first of these is a tectonic contact where the older Yunguilla Fm. overrides the Green member of Silante Fm. The rocks are very fractured showing a cleavage defined by fractures. In Figure 9, we see with red lines marking the fractures which display different orientations. The fractures have measurements of N61W / 29S, N58W / 26S, N51W / 21S, N80E / 19N, N62E / 12N, N75E / 5N. (Figure 8)

The second main fault occurs to the north of the study area between the Red Member of the Silante Fm and the pillow basalts of Pallatanga Fm. There, we find a tectonic sliver of Red member Silante Fm that has been metamorphosed between the pillow lavas (Figure 13). These rocks are all adjacent to a porphyritic intrusion (which likely caused the metamorphism of the Silante Fm strata) (Figure 5).

Besides these main faults, various structural measurements of faults were taken throughout the field campaigns that are not large enough to represent on the map. The faults found are characterized by gouge zones, as well as an increased fracture density near them.

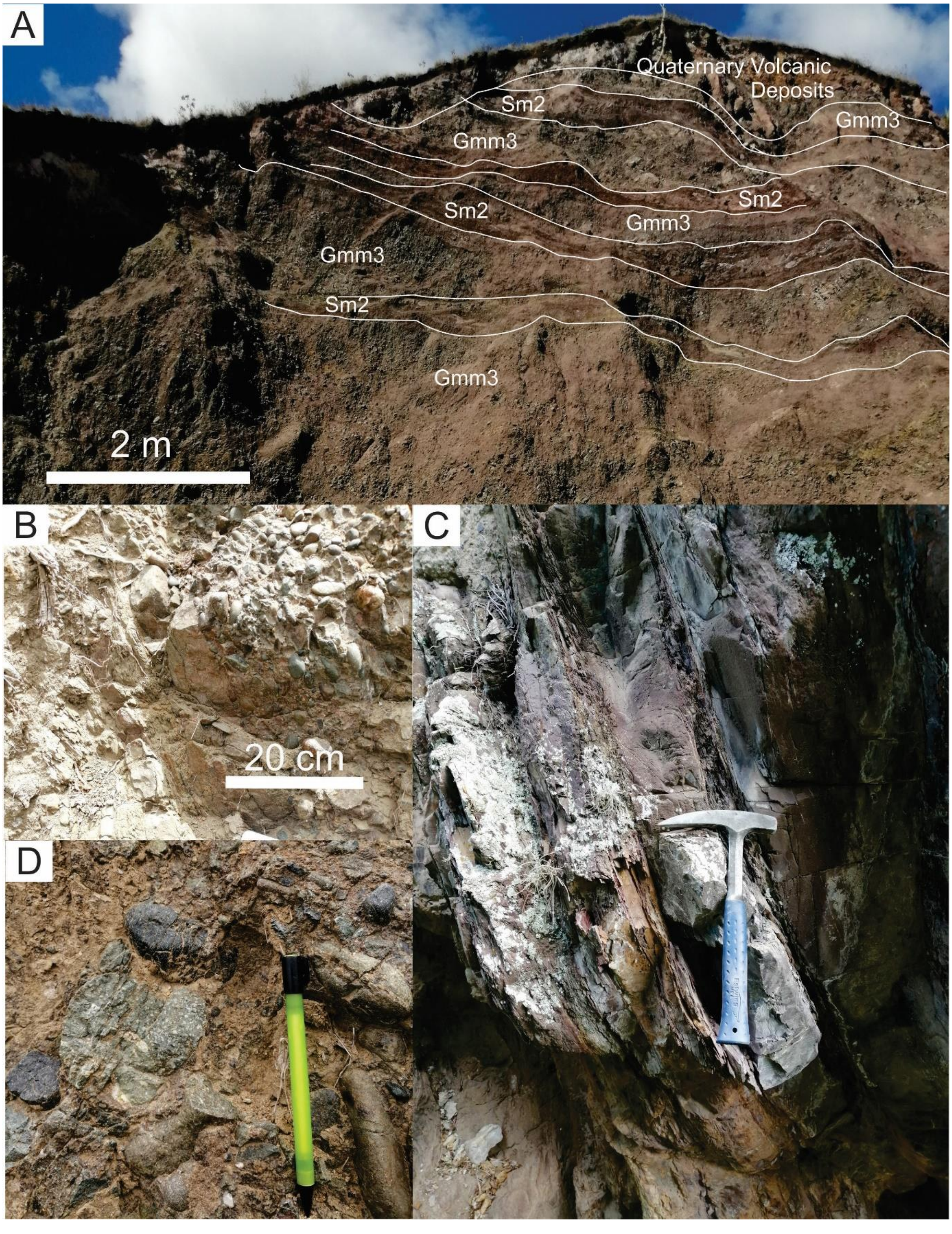

Figure 13. A) Outcrop of Red SIlante member with layers of the Gmm3 conglomerates interbedded with the Sm2 sandstones. We can see that they are characterized by reddish colors. B and D are the images of the conglomerates of Red Silante member. C) Shales of the Red Silante member, that are in tectonic

contact with the Pallatanga Fm at the coordinate 17N 814288.92 / 73486.82. These shales have a low degree of metamorphism which was interpreted as a contact metamorphism due to a nearby intrusive body

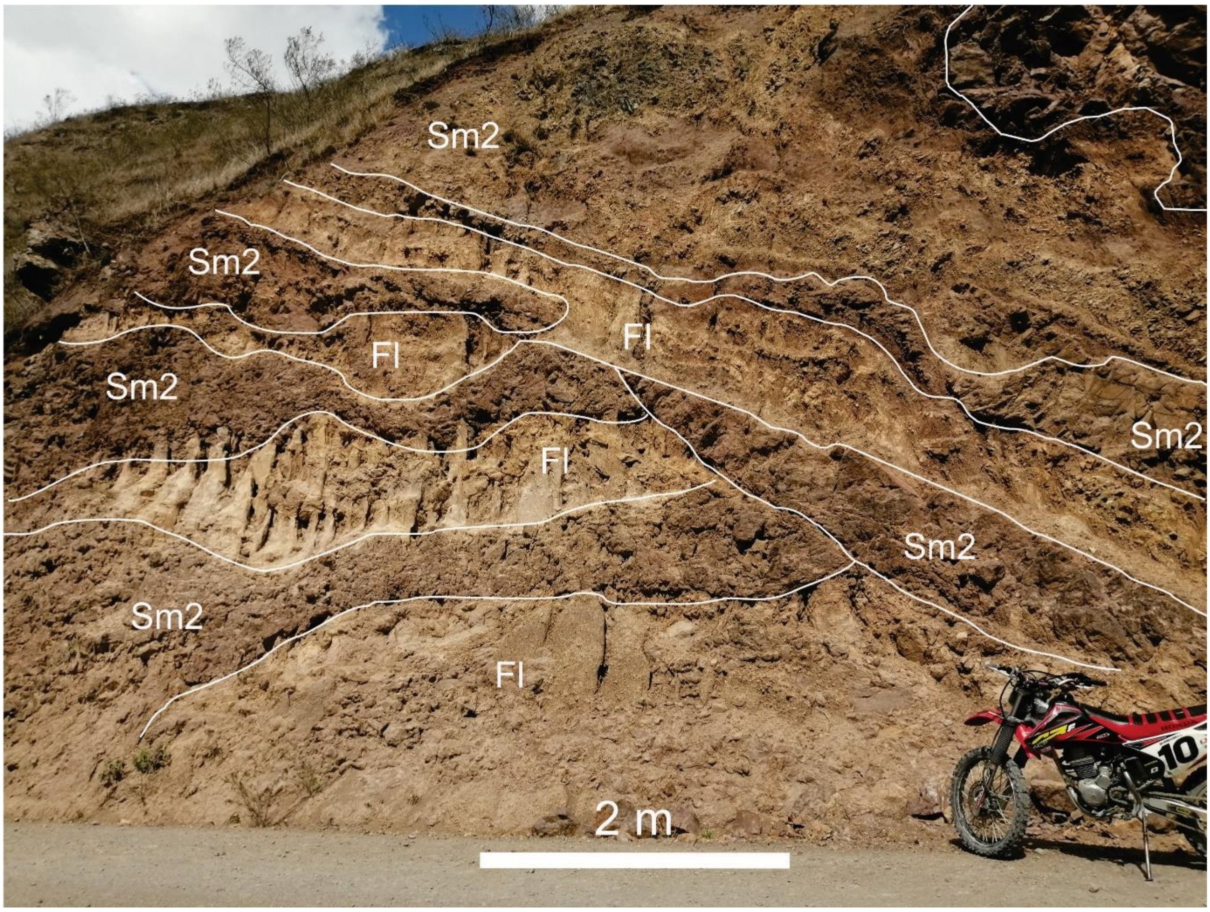

Figure 14. Stratigraphic relationship between the lithofacies Sm2 and Fl of Red Silante member. The sandstones of this outcrop present a high degree of consolidation and irregular geometries whit truncations of the beds that were interpreted as unconformity.

In Figure 16, we show that the fault orientations are consistent, suggesting that they formed under the same structural conditions. In the Figure 16, the green great circle represents the contact between Yunguilla Fm and the Green member of Silante, the red great circles represent the faults planes measured between the Red member of the Silante Fm, and the Pallatanga Fm pillow basalts, and the black great circles represent the fault planes of the small faults in different outcrops. The resulting plane of the mean vector (T,P, 316.7°, 42.3°) obtained from the fault poles is marked in blue which has measurements of N46.7E/47.7S.

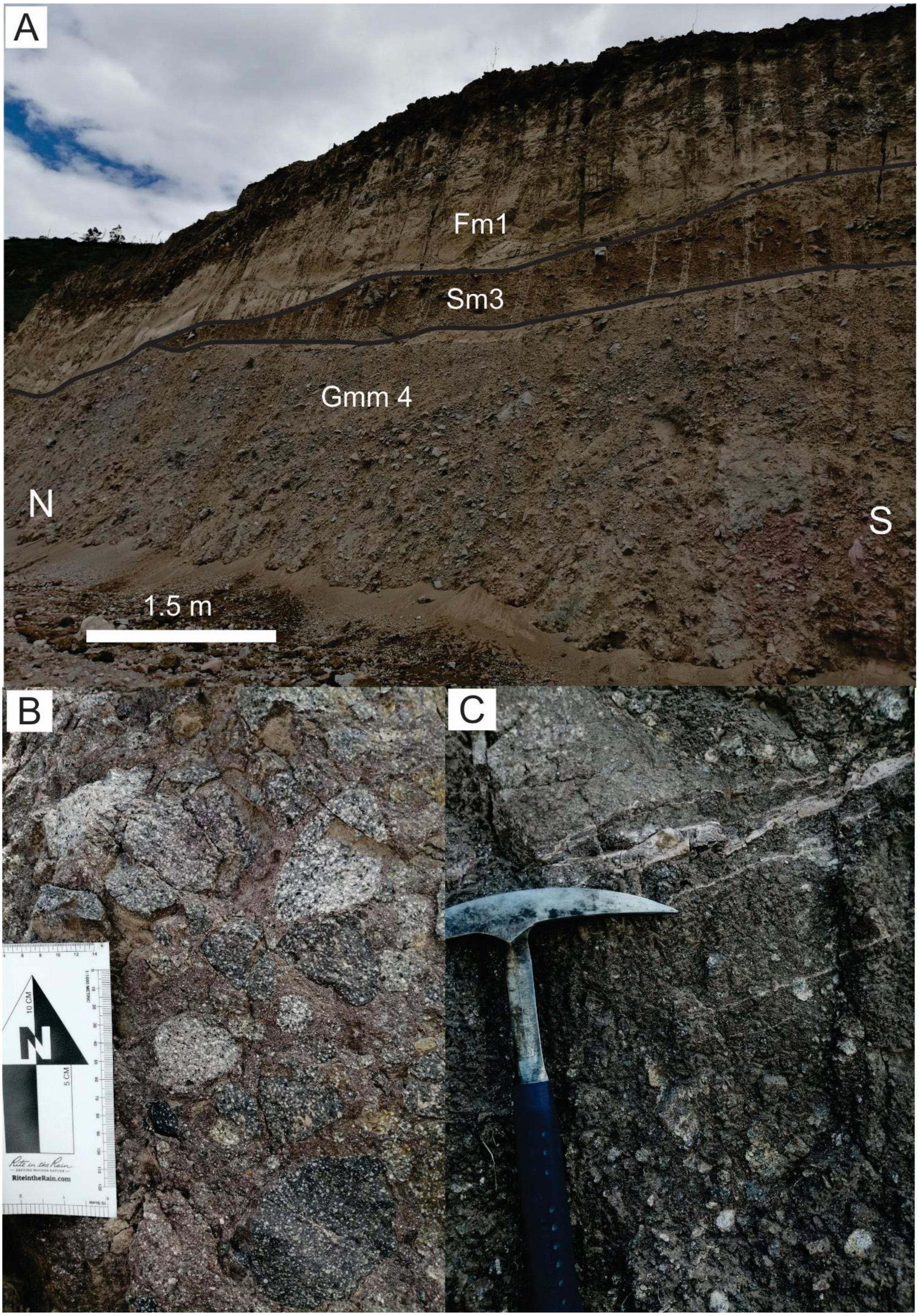

Figure 15. A) Volcanic cover outcrop where we observe the Gmm4, Sm3 and Fm1 lithologies. B and C, we observe the clasts of the Gmm4 lithology, as mentioned in the description, these conglomerates are monolithic

4.2.2. Folds

The bedding measurements taken define several folds. The most prominent one occurs to the south of the study area and adjacent to the fault that separates Yunguilla and Silante Fm. The fold is a tight syncline with a slightly overturned southern limb that is truncated by the fault. Figure 17 shows all the bedding measurements.

4.2.3. Fractures

Structural measurements were also taken of joints. In the conglomerates of the Green member, we found fractures that are cutting clasts, and small displacements (Figure 12). These fractures; however, do not show a preferential orientation.

4.2.4. Structural Cross Section

We summarize our field observations in a structural cross-section (location shown in Figure 5) where we can better understand the deformation of the Silante Fm. In Figure 19 we show a NW-SE cross-section of the work area with no vertical exaggeration. The thicknesses of the units were constrained by surface observations, however there is still some uncertainty which required certain assumptions which we will explain. The Red member of the Silante Fm is inferred to be 900-700 m, which is a minimum thickness, because we do not observe the stratigraphic top.

The thickness of the Silante Green member is inferred to be a minimum of 1200-1300 meters, based on field observations. However, we do not know the total thickness of this member because the base of it does not outcrop. The marine sequences found on top of the Pallatanga Fm are made up of the Portada, Mulaute, Pilaton, Natividad, and Yunguilla formations of the Rio Cala Group. In previous works the thicknesses of these units are well-defined due to their deformation, therefore we will infer their total thickness to be able to represent them in the cross-section.

On the Salinas-Lita road, before arriving at our work area, these marine sedimentary sequences outcrop over ~ 5km, however they are isoclinaly folded, and faulted so it is very difficult to determine their true thickness. For these reasons we assign a thickness of 1800- 2000 m to these strata. Within our cross-section we observe several thrust faults which we interpret to sole into a decollement below the pillow basalts (layer 2a of oceanic crust) of the Pallatanga Fm. This is because nowhere does we observe the sheeted dike complex that would correspond to layer 2b the accreted oceanic crust. In normal oceanic crust, layer 2a can be 600-800 m in thickness, but in an oceanic plateau that is considerably thicker than regular oceanic crust (15- 20 km instead of 6-7 km), layer 2a can reach thicknesses of over 1 km (Mutter and Mutter, 1993). Therefore, we place the decollement level at 2 km below the top of the Pallatanga Fm.

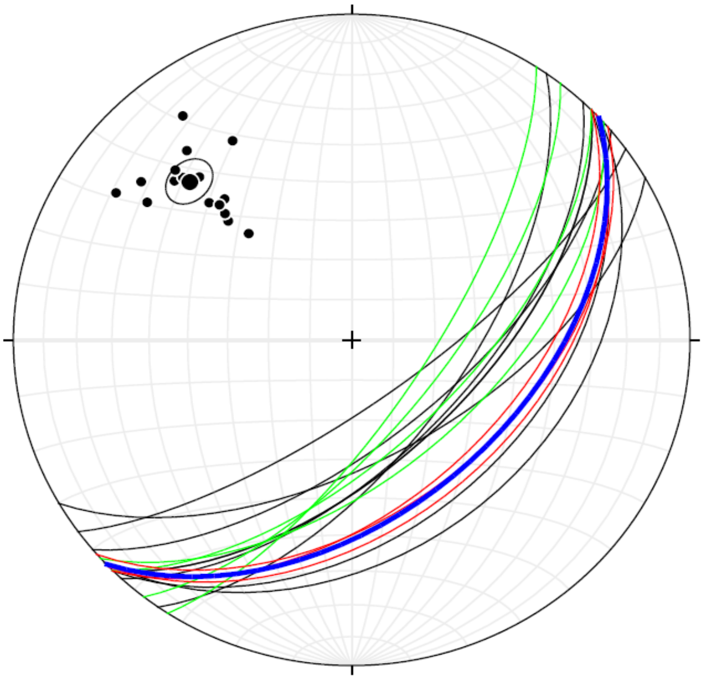

Figure 16. Stereonet showing measured fault planes and their poles. Green: contact between Yunguilla Fm and green Silante; Red: contact between red Silante and Pallatanaga Fm; Black: small faults; Blue: mean vector mean vector (T,P, 316.7°, 42.3°) plane from all faults.

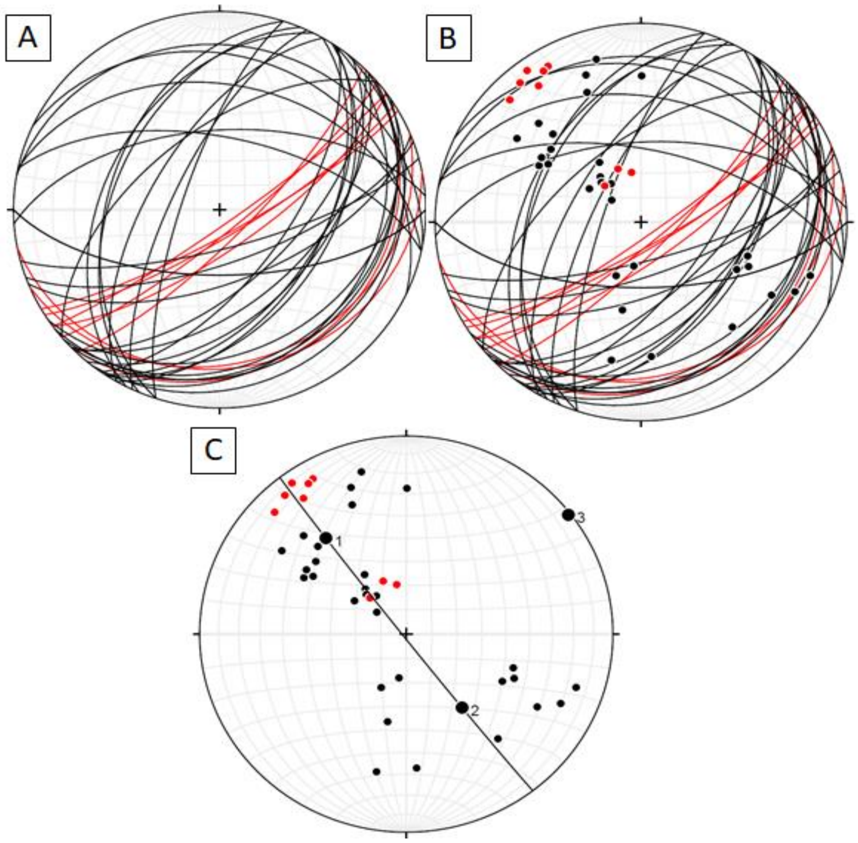

Figure 17. Stereonets showing measured bed planes and their poles. Red: color for synclinal fold. A) Represents the bedding planes, B) shows the planes and poles of the same planes, C) shows only the poles with the cylindrical best fit of the data Bedding calculated poles showing the cylindrical best fit of the data: 1) T, P, 321.2°, 37.5°; 2) T, P, 144.0°, 52.5°; 3) T, P, 052.3°, 01.3°.

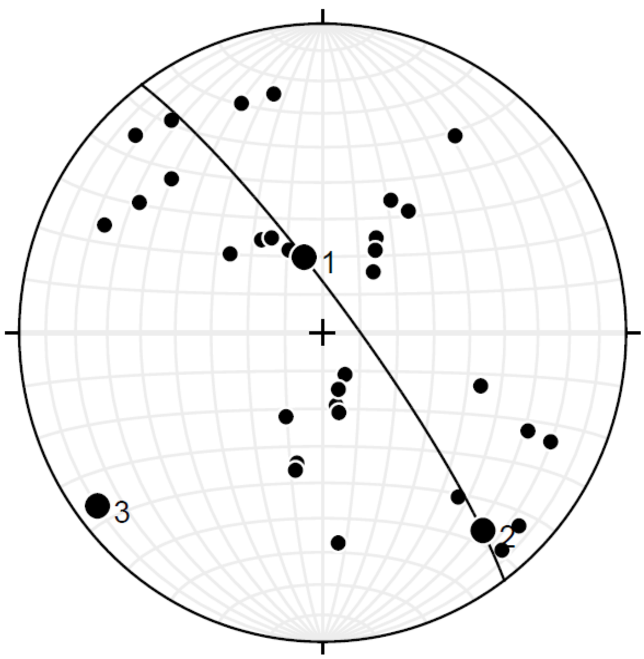

Figure 18. Stereonets showing measured bed poles of the fractures plane. The cylindrical best fit of the data results in the following values: 1) T, P, 342.2°, 68°; 2) T, P, 142.3°, 20.1°; 3) T, P, 223.7°, 08.3°.

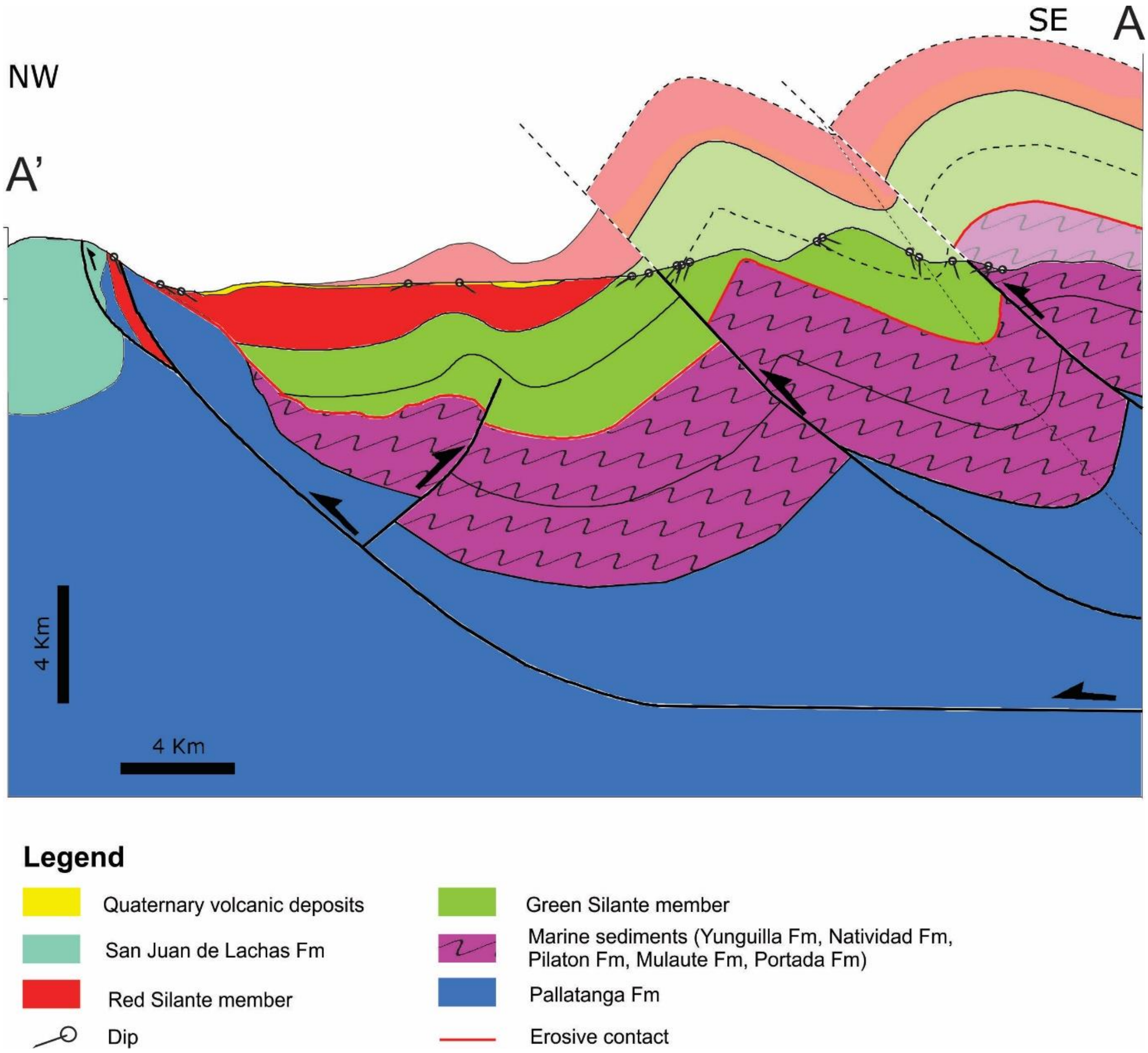

Figure 19. Structural cross-section of study area. Location shown in Figure 5.

V. DISCUSSION

5.1. Stratigraphy of the Silante Fm in the intramontane basin of Salina-Lita transect

To figure out the facies association that characterizes the Silante Fm deposits is important to classify the lithofacies encountered. The lithofacies are summarized in Gmm, Gmg, Gmi, Gcg, Gci, Sm, Sh, Fl. According to Miall (1978) and James & Dalrymple (2010), the interpretation of these lithofacies are as follows:

- Gmm lithofacies are deposits formed by high-strength and viscous plastic debris flow.
- The lithofacies Gmg and Cmi are interpreted as deposits of pseudoplastic debris flow with low-strength and low-viscosity.
- Gcg and Gci lithofacies are interpreted as clast-rich debris flow with high strength.
- Sm lithofacies are interpreted as sediment gravity-flow deposits.
- Sh lithofacies are interpreted as plane-bed flow deposits.
- Fl lithofacies are interpreted as waning flood deposits.

The Silante Fm in the Salinas Lita transect is interpreted to be composed of two members, the basal Green member and the upper Red member.

The Green member is composed of the lithofacies Gmm1, Gmm2, Sm1. This member is characterized by thick layers of conglomerates of green color with clasts of the Yunguilla Fm. The black shales and greenish cherts that we can find in the composition of the clasts of these conglomerates give us an indication that the marine sequences, specifically the Yunguilla Fm, were already outcropping in a paleo relief during the deposition of the Silante Fm. We interpret that Silante Green member was deposited in the proximal part of an alluvial fan (Collinson, 1996) characterized of many beds of conglomerate and few layers of massive sandstone.

The Red member is composed of the lithofacies Gmm3, Gcg1, Fl, Sm2. This member is characterized by layers of red conglomerates with clasts of basalts. The shales that we find in this formation in some lithofacies are black, others reddish. The presence of basalt clasts in the conglomerates leads us to interpret that the rocks of the Pallatanga Fm and San Juan de Lachas Fm were also outcropping when the Silante Fm was being deposited. This is consistent with the stratigraphic contact of onlap that we find between Silante and Pallatanga Fms. to the north of our work area. Sandstones and siltstones are observed with more frequency in the stratigraphic top of the Silante Fm. According to Collinson (1996), these observations indicate that the red member of Silante could be interpreted a mid-fan, with the influence of a fluvial depositional environment.

In general, the occurrence of the conglomerates is higher compared to the massive sandstones. In the same way, the occurrence of massive sandstones is higher than the sandstones and siltstones with sedimentary structures. According to James, & Dalrymple, (2010), if the principal facies assemblage is Gmm, Gci, Gcm, it will be related to sediment gravity flows. These observations indicate that the deposits described for Silante Fm in this work area are part of a semi-arid alluvial fan that is dominated by processes of intermediate water flows (Colombo, 1996).

5.2. Structural geology of the Silante strata

To the south, we find the green member Silante Fm in tectonic contact with fine-grained rocks, which have tightly folded quartz-filled veins, which suggest that they were deformed at temperature > 300 C (when quartz crystal plasticity becomes activated) (Figure 8). These fine-grained rocks are interbedded with cherts which allowed us to identify them as part of the Yunguilla Fm. These rocks were pervasively faulted and folded, having undergone a more protracted deformation history than the rocks of Silante Fm, evidenced by the cherts which now form ribbons. The Yunguilla Fm strata are overriding the conglomerates of green Silante Fm. The thrust fault that places Yunguilla Fm over Silante Fm is interpreted to have caused a fault-propagation fold that was cut by the fault, and resulted in the syncline that we interpret as a footwall syncline of a thrust.

On the other hand, the fault between the Red member of the Silante Fm and Pallatanga Fm is interpreted as a tectonic slice that formed as a horse between two backward-breaking thrust faults. This sequence of thrusting (also referred to as out of sequence thrusting) is uncommon, but not unheard off (Morley, 1988). In this same location though, we also have Red member of the Silante Fm in depositional contact with the Pallatanga Fm. This implies that prior to the deposition of Silante Fm, there was uplift and erosion of the marine sequence overlying Pallatanga Fm.

Our results also show that the faults measured in the area have a preferred orientation, with a mean pole orientation of N047E / 48S. This allows us to interpret that the deformation of the Silante Fm was caused by SE-NW compression with a maximum horizontal stress azimuth of 136° (assuming plane strain). This is also consistent with the folds observed in the study area.

5.3. Basin Evolution

Based on the field observations, we have come up with a tentative model for the evolution of the Silante intermontane basin.

1) The deposition of the marine sequences occurs over the oceanic plateau that would become accreted to the South American margin followed by the accretion event around 90-95 Ma recorded by previous works (Vallejo et al., 2019). This accretion and burial by subsequent deposits allowed these rocks to undergo low-grade metamorphism as well as intense deformation.
2) The transect only preserves rocks of the Rio Cala Gp, so there may have been an exhumation event that led to the erosion of the Sanguagal, Saquisilí, Apagua, Larurel and Rumi Cruz formations. These erosive events allowed the Yunguilla formation to emerge near our Intramonane basin and contribute clasts to the basin fill.
3) Part of the erosion was likely due to deformation that created a preexisting topography in which Silante Fm was deposited. The first period of deposition resulted in the Green Member of the Silante Fm. Although we do not see the basal contact of this unit, we speculate that it is deposited over Yunguilla Fm, based on the clasts of cherts and shales found in the conglomerates. The deposits were accumulated in an alluvial fan environment, with no preserved evidence of fluvial systems.
4) After this, we have a transitional contact to the Red Member of Silante Fm, which is preserved in outcrops. The sedimentary environment is interpreted to

still be alluvial fans, but with more fluvial reworking of sediments (possibly streams forming on the fan in a wetter environment). The Red Member strata are found in depositional contact with the Pallatanga Fm, implying that the latter was outcropping then. This also allows us to infer that the deformation events that uplifted Yunguilla Fm towards the eastern side of the basin, resulted in more uplift, and thus more unroofing on the western side of the basin, removing all the marine sedimentary sequence and exposing the Pallatanga Fm.

5) We cannot know the original width of the Silante basin because the original basin margins are not preserved, and instead at present there are faulted contacts. This means that after the deposition of Silante Fm, there were more compressional tectonic events. These are recorded in the folding and faulting of the Silante Fm, resulting in an approximate shortening of -50% (lf= 24km, lo= 48km).

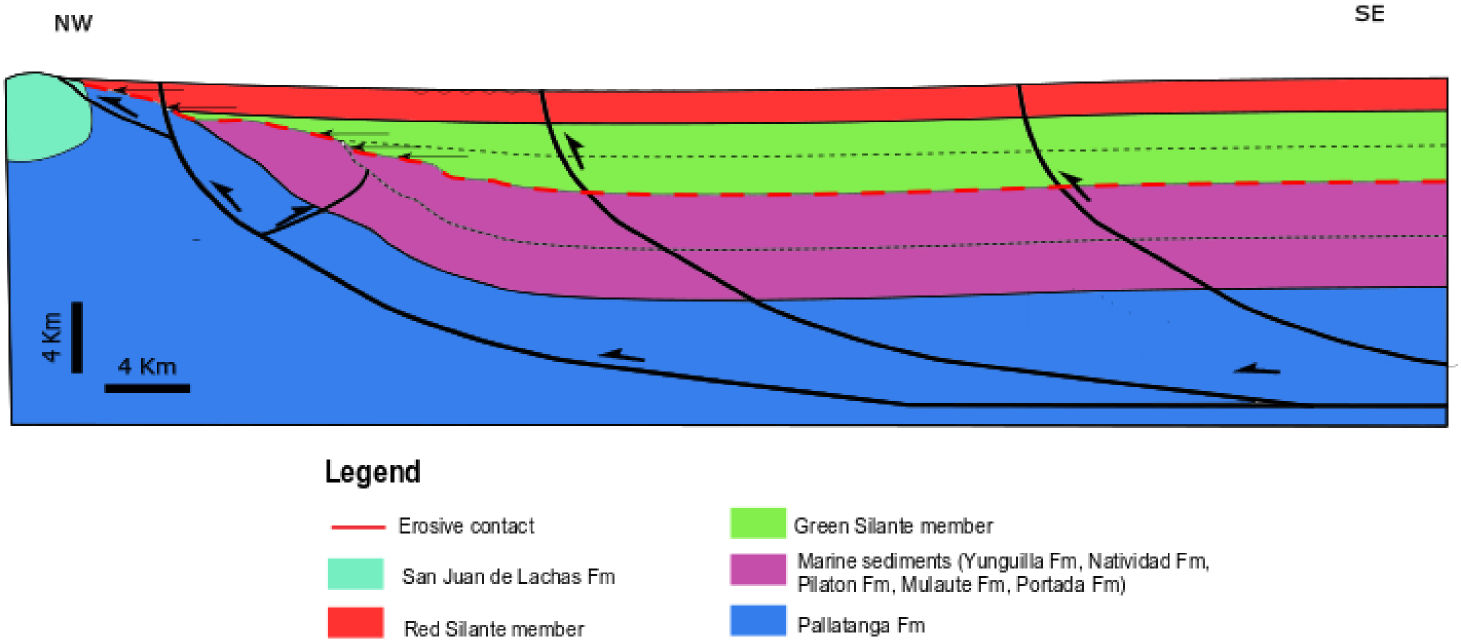

Figure 20. Pre-deformation schematic diagram of the basin were Silante Fm where Silante fm was deposited

If we assume that the age of the Silante Fm in our transect is equal to that determined by Almagor (2019), ~16 Ma, then the deformation of this basin must be younger than this. Spikings et al. (2005) reports an episode of cooling in the WC based on thermochronology data (interpolating of the apatite partial annealing zone, zircon partial annealing zone and Ar retention zones) between approximately 13 to 9 Ma, interpreted to be due to an increase in the rate of convergence between the South America and Nazca plates. Our results are consistent with the deformation that we observe in our work area corresponding to this cooling event.

5.4. Comparison with previous studies

One of the objectives of this work was to compare the sedimentary model that we obtain in our study, with those from strata of other parts of the WC that have been identified as Silante Fm. We compare our results to those of Almagor (2019) who presents the description of the lithofacies of the Silante Fm west of Quito. There are similarities in seven of the nine lithofacies described there compared to those in this study:

- Almagor's Fl lithofacies coincide with Lithofacies 13: Reddish Shales (Fl).
- The lithofacie Sm coincides with the Lithofacies 11: Reddish Massive Sandstone (Sm3); the lithofacie Sh coincides with the Lithofacies 6: Brownish Laminated Sandstone (Sh1).
- The Smp lithology coincides with Lithofacies 8: Greenish Massive Sandstone (Sm2).
- The lithofacie Gmm1 matches Lithofacies 9: Reddish Matrix-supported Conglomerate (Gmm4), Lithofacies 10: Reddish Matrix-supported Conglomerate (Gmm5), and Lithofacies 9: Reddish Matrix-supported Conglomerate (Gmg2).
- The Gcm1 lithofacie matches Lithofacies 12: Reddish Matrix-supported Conglomerate (Gcg1), and Lithofacies 13: Reddish Matrix-supported Conglomerate (Gci1.
- The Gmm2 lithofacie matches Lithofacies 7: Greenish Matrix-supported Conglomerate (Gmm3).

In both works, the interpretation is reached that Silante is characterized by rocks with an alluvial fan depositional environment. However, sandstone associations are less frequent in the Salinas-Lita transect, compared to Almagor (2019), which has stratigraphic associations with a higher frequency of sands and shales. Another difference is that Almagor (2019) describes crossbedding and other stratigraphic structures more frequently in its sand layers. These crossbedding structures are indicators that the strata represent distal parts of the fan, in addition to having greater influence from fluvial deposits such as flood plains, and channel migration.

Based on this we interpret the deposits west of Quito as deposited in a more central part of the basin where there was an interaction of distal fans and fluvial systems, while the strata analyzed in our study represents the more proximal facies, suggesting that it was much closer to the basin margin.

5.5. Correlation with Chota Basin

In the Ministry of Energy and Mines, et al. (1998) Geological Map of the Western Cordillera of Ecuador between 0 ° -1 ° N (scale of 1: 200000) the continental strata exposed along the Salinas-Lita road are assigned to the Chota Formation. The Chota Formation is described in that map as follows: "The Chota Formation comprises massive gray sandstones and conglomerates supported by the matrix, containing clasts of shales, cherts, and weakly foliated granitoids". However, our initial hypothesis is that the deformed strata that outcropped in the Salinas Lita highway was part of the Silante Fm.

In order to assess which of these correlations was correct, we carried out a brief survey of the rocks that outcrop around the towns of Chota and Ambuquí, which correspond to the Chota Formation. In Figure 21-B, C and D, show black, dark brown, and light brown,shales and siltstones. These rocks are characterized by having organic matter and in some cases fossils of leaves as we observed in Figure 21-D. These strata have been interpreted to have been deposited in a lacustrine setting (Barragan et al., 1996). The sandstone sequences that are found in the town of Ambuquí and are characterized by being yellow and having a high content of micas. In Figure 21- A, we observe sequences of red conglomerates, which correspond to the Peñas Colaradas Fm (Barragan et al., 1996). These red conglomerates are composed of clasts of chert, shales, granitoids, and quartzites, but there are no clasts of basalts. Furthermore, there are abundant sedimentary structures and channel geometries that suggest a fluvial depositional setting.

After comparing these rocks to the lithofacies we found in the Salinas Lita Road work area, we conclude that these belong to the Silante Fm. While the Chota Fm also likely formed in an intermontane basin, reported ages are much younger (6 Ma Barragan et al., 1996), and so the basin was spatially and temporally distinct from the Silante basin.

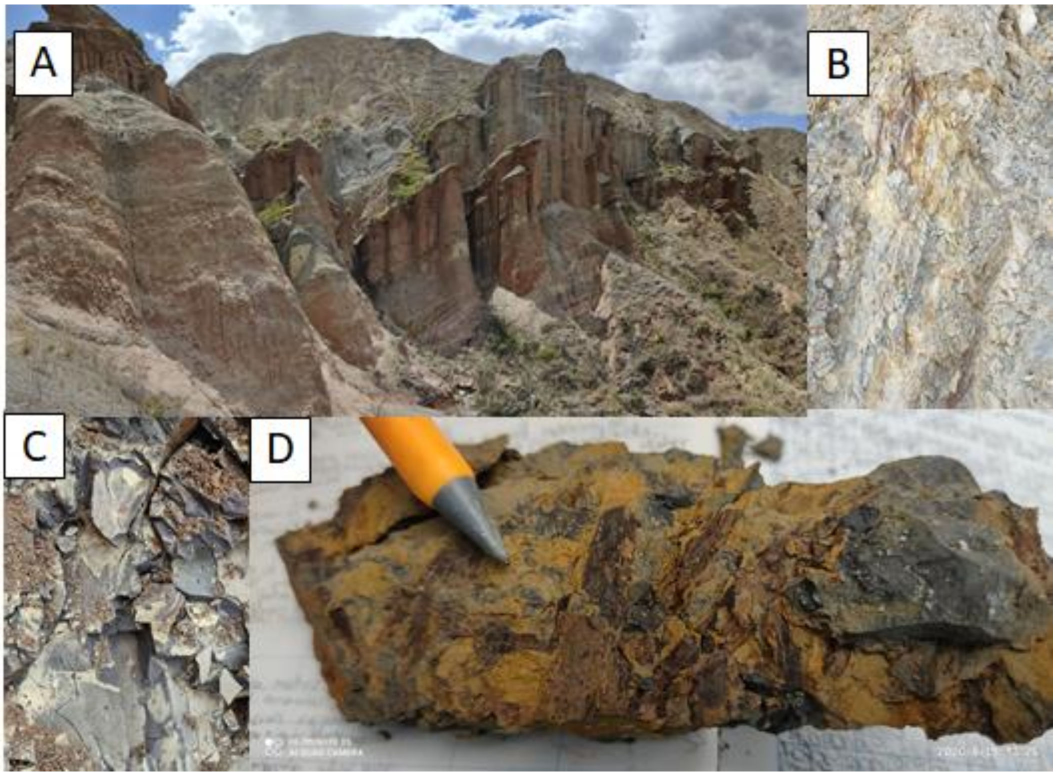

Figure 21. Rocks of the Chota Fm. A) Panoramic image of the conglomerates of the Peñas Coloradas Unit. B) Light brown, siltstones, C) and D) black, dark brown, shales with organic content (leaves) that can be seen in part D.

VI. CONCLUSIONS

- Stratigraphic columns were raised and the lithofacies of Silante Fm in our work area were classified. The Silante Fm in the Salinas Lita transect is interpreted to be composed of two members, the basal Green member and the upper Red member which differ by their composition of clasts and their relationship of occurrence of conglomerates versus sandstones. The deposits described for Silante Fm in this work area are interpreted to have formed in a semi-arid alluvial fan that is dominated by processes of intermediate water flows.

- One of our objectives was to determine why there were subvertical layers outcropping on the Salinas-Lita highway. After determining the contacts of the different rocks, it was possible to identify that rock outcrops from the Yunguilla Fm on Silante Fm in tectonic contact at the south of the work area. North of our work area, the Silante Fm is in onlap contact with the WC basement. After performing the cross section of our work area and analyzing the steronet of the measured faults, it is concluded that the intermontane basin in the Salinas-Lita transect is dominated by SE-NW compression of fault-propagation fold with a maximum horizontal stress azimuth of 136 ° (assuming plane strain). In addition, the Pallatanga Fm and the marine sequances that were deposited on the basement of WC emerged forming a relief on which the Silante Fm was deposited.
- One of the counter arguments that were presented in previous works on Silante Fm on the Salinas-Lita highway was that they were interpreted as Chota Fm. A description was made of the rocks that emerge in Ambuqui and Chota and it was compared with the rocks that emerged in the Salinas-Lita highway trying to find similarities. However, we conclude that rocks of Salinas-Lita road belong to the Silante Fm. While the Chota Fm also likely formed in an intermontane basin, reported ages are much younger (6 Ma Barragan et al., 1996), and so the basin was spatially and temporally distinct from the Silante basin.

VII. Bibliography

Almagor, E. (2019). *Identificación y Caracterización de las Facies Sedimentarias de la Formación Silante en las Secciones Nono-Tandayapa y Calacalí-Nanegalito.* (Escuela Politécnica Nacional del Ecuador). Retrieved from https://bibdigital.epn.edu.ec/handle/15000/20270

Allmendinger, R. W., Cardozo, N., and Fisher, D., 2012, Structural geology algorithms: Vectors and tensors in structural geology: Cambridge University Press (book to be published in early 2012).

Cardozo, N., and Allmendinger, R.W., 2013, Spherical projections with OSXStereonet: Computers & Geosciences, v. 51, p. 193 – 205, doi:10.1016/j.cageo.2012.07.021.

Collinson, J.D. (1996). Alluvial sediments. In: Sedimentary Environments: processes, facies and stratigraphy (Ed. H.G. Reading). 3rd ed, Blackwell Publishing, pag. 37-82

Colombo, F. (1992): Abanicos aluviales. In: Sedimentología (ed. A. Arche). Vol. 1, Consejo Superior de Investigaciones Científicas, pag. 143-218

Hughes, R. A., & Pilatasig, L. F. (2002). Cretaceous and tertiary terrane accretion in the Cordillera Occidental of the Andes of Ecuador. *Tectonophysics*, *345*(1–4), 29–48. https://doi.org/10.1016/S0040-1951(01)00205-0

Jaillard, E., Ordoñez, M., Suárez, J., Toro, J., Iza, D., & Lugo, W. (2004). Stratigraphy of the late Cretaceous-Paleogene deposits of the cordillera occidental of central ecuador: Geodynamic implications. *Journal of South American Earth Sciences*, *17*(1), 49–58. https://doi.org/10.1016/j.jsames.2004.05.003

James, N. P., & Dalrymple, R. W. (Eds.). (2010). Fácies models 4. Canada: Geological association of Canada.

Kerr, A. C., Aspden, J. A., Tarney, J., & Pilatasig, L. F. (2002). The nature and provenance of accreted oceanic terranes in western Ecuador: Geochemical and tectonic constraints. *Journal of the Geological Society*, *159*(5), 577–594. https://doi.org/10.1144/0016-764901-151

Kerr, A. C., White, R. V., Thompson, P. M. E., Tarney, J., & Saunders, A. D. (2003). No Oceanic plateau - No caribbean plate? The seminal role of an oceanic plateau in Caribbean plate evolution. *AAPG Memoir*, (79), 23–26. Retrieved from http://archives.datapages.com/data/specpubs/memoir79/Chapter6/CHAPTER6.HTM

Lapierre, H., Dupuis, V., Le, B. M. De, Bosch, D., Monie, P., Tardy, M., … Cotten, J. (1999). Late Jurassic Oceanic Crust and Upper Cretaceous Caribbean Plateau Picritic Basalts Exposed in the Duarte Igneous Complex , Hispaniola. *Journal of Geology*, *107*, 193–207.

Mccann, T., Saintot, A., & Bonn, U. (2003). Tracing tectonic deformation using the sedimentary record : an overview. *Geological Society*, *208*(Special Publication), 1–28. Retrieved from https://sp.lyellcollection.org/content/208/1/1.short

Marocco, R. (1994). Las cuencas sedimentarias, un aporte al conocimiento de una cadena montanosa.

Montgomery S.L., Selley R.C., and Morrill D.C., (1984) Exploration for nonmarine sandstone reservoirs: IHRDC Video

Pindell, J., Kennan, L., Maresch, W. V., Stanek, K. P., Draper, G., & Higgs, R. (2005). Plate-kinematics and crustal dynamics of circum-Caribbean arc-continent interactions: Tectonic controls on basin development in Proto-Caribbean margins. *Special Paper of the Geological Society of America*, *394*(September), 7–52. https://doi.org/10.1130/0-8137-2394-9.7

Rodríguez, J., Azor, A., & Azañón, J. (2012). The Betic intramontane basins (SE spain): stratigraphy , subsidence , and tectonic history. In C. Busby & A. Azor (Eds.), *Tectonics of sedimentary basisns: Recents advances* (First edit, pp. 461–479). Noida, India: Blackwell Publishing Ltd.

Spikings, R. A. Y., Winkler, W., Seward, D., & Handler, R. (2001). Along-strike variations in the thermal and tectonic response of the continental Ecuadorian Andes to the collision with heterogeneous oceanic crust. *Earth and Planetary Science Letters*, *186*, 57–73. Retrieved from https://www.sciencedirect.com/science/article/pii/S0012821X01002254

Toro, J., & Jaillard, E. (2005). Provenance of the Upper Cretaceous to upper Eocene clastic sediments of the Western Cordillera of Ecuador : Geodynamic implications. *Tectonophysics*, *399*, 279–292. https://doi.org/10.1016/j.tecto.2004.12.026

Vallejo, C. (2007). *Evolution of the western cordillera in the Andes of Ecuador (late*

Cretaceous-Paleogene). (ETH Zürich). https://doi.org/10.3929/ethz-a-010782581

Vallejo, C., Winkler, W., Spikings, R. A., Luzieux, L., Heller, F., & Bussy, F. (2009). Mode and timing of terrane accretion in the forearc of the Andes in Ecuador. *Memoir of the Geological Society of America*, *204*(09), 197–216. https://doi.org/10.1130/2009.1204(09)

Zervas, D., Nichols, G.J., Hall, R., Smyth, H.R., Lüthje, C., and Murtagh, F., 2009 Computers & Geosciences, 35, 2151-2159

ANNEXES

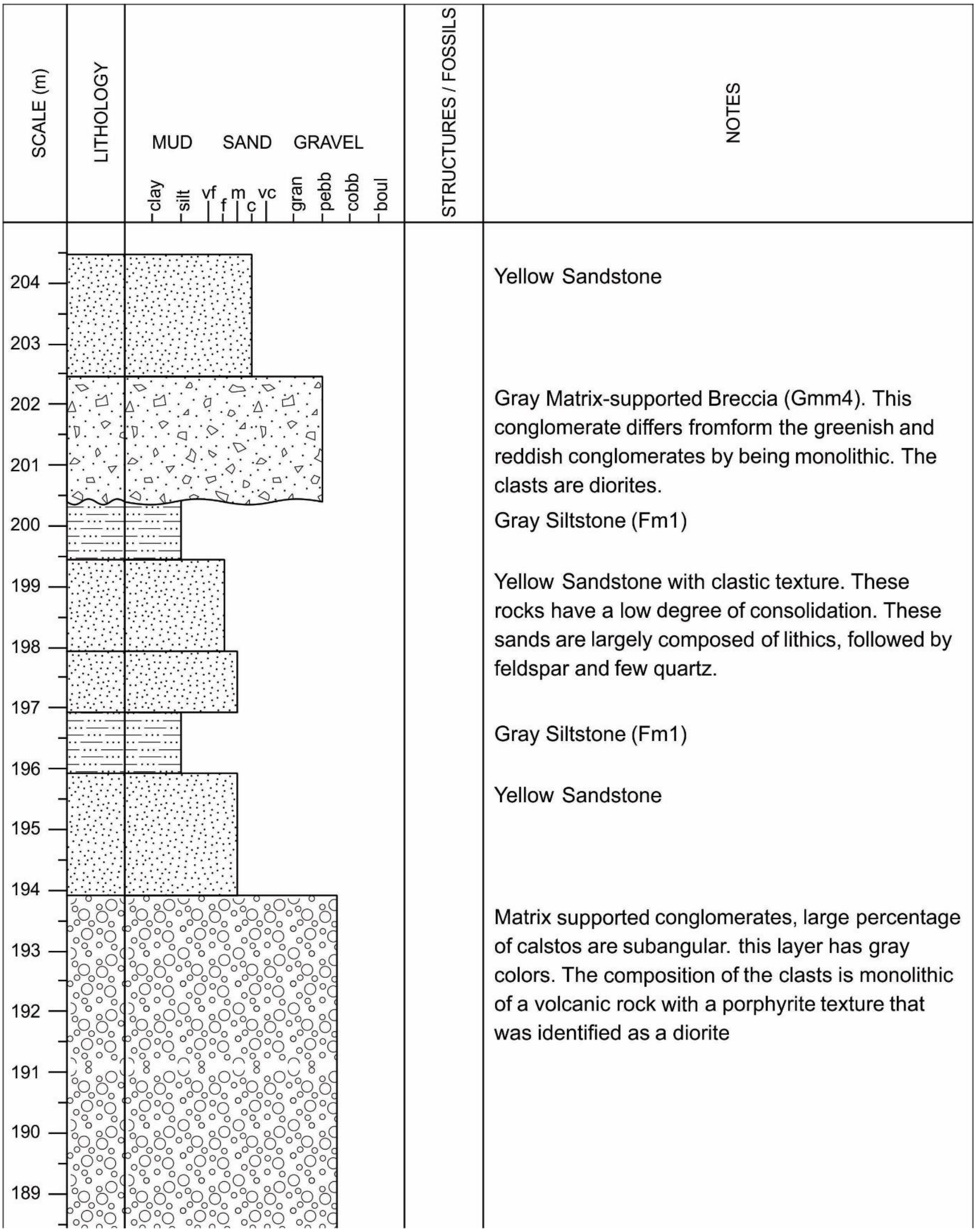
SCALE (m)
LITHOLOGY
MUD SAND GRAVEL
clay silt vf f m c vc gran pebb cobb boul
STRUCTURES / FOSSILS
NOTES
204
203
202
201
200
199
198
197
196
195
194
193
192
191
190
189
Yellow Sandstone
Gray Matrix-supported Breccia (Gmm4). This conglomerate differs fromform the greenish and reddish conglomerates by being monolithic. The clasts are diorites.
Gray Siltstone (Fm1)
Yellow Sandstone with clastic texture. These rocks have a low degree of consolidation. These sands are largely composed of lithics, followed by feldspar and few quartz.
Gray Siltstone (Fm1)
Yellow Sandstone
Matrix supported conglomerates, large percentage of calstos are subangular. this layer has gray colors. The composition of the clasts is monolithic of a volcanic rock with a porphyrite texture that was identified as a diorite

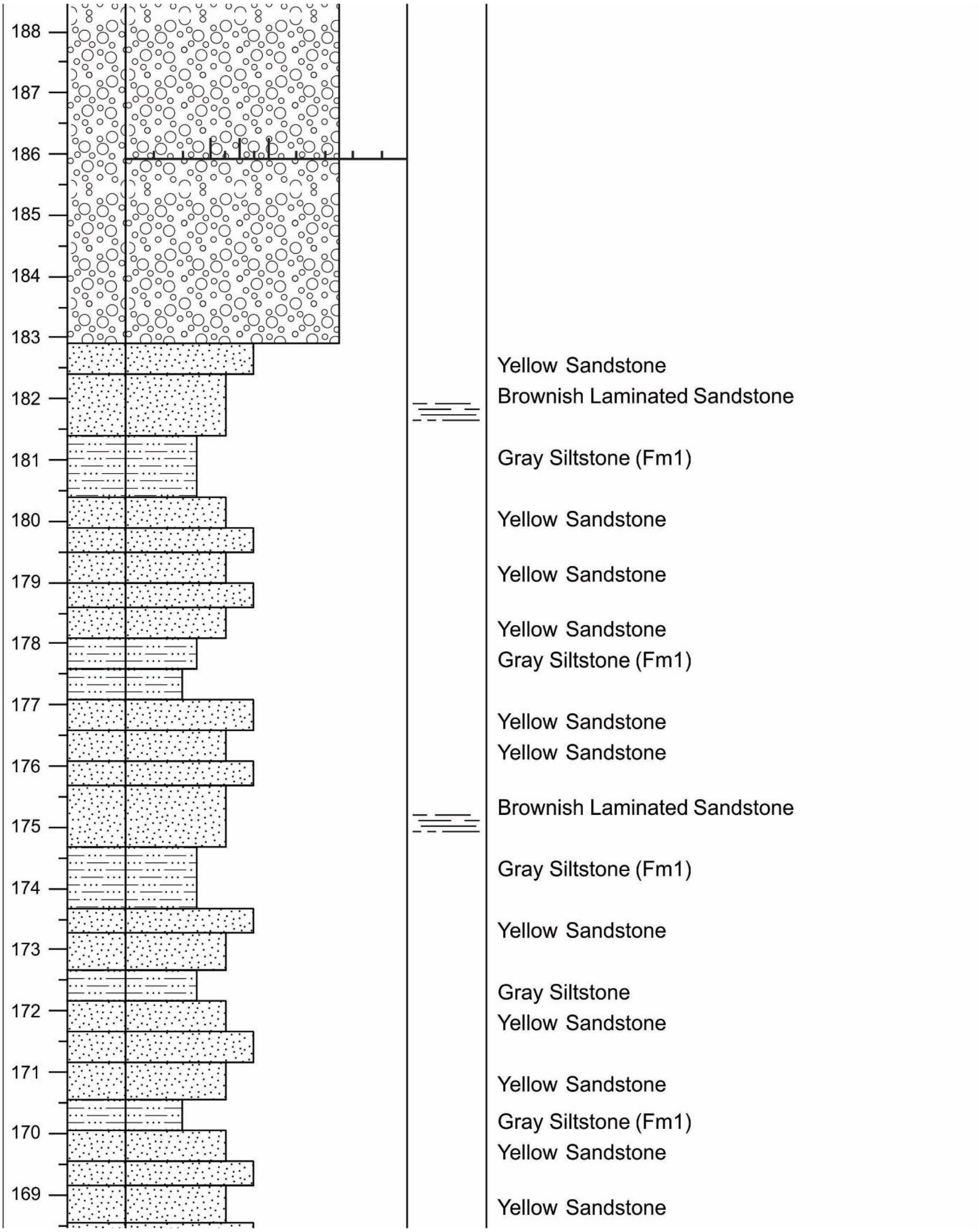
188
187
186
185
184
183
182
181
180
179
178
177
176
175
174
173
172
171
170
169
Yellow Sandstone
Brownish Laminated Sandstone
Gray Siltstone (Fm1)
Yellow Sandstone
Yellow Sandstone
Yellow Sandstone
Gray Siltstone (Fm1)
Yellow Sandstone
Yellow Sandstone
Brownish Laminated Sandstone
Gray Siltstone (Fm1)
Yellow Sandstone
Gray Siltstone
Yellow Sandstone
Yellow Sandstone
Gray Siltstone (Fm1)
Yellow Sandstone
Yellow Sandstone

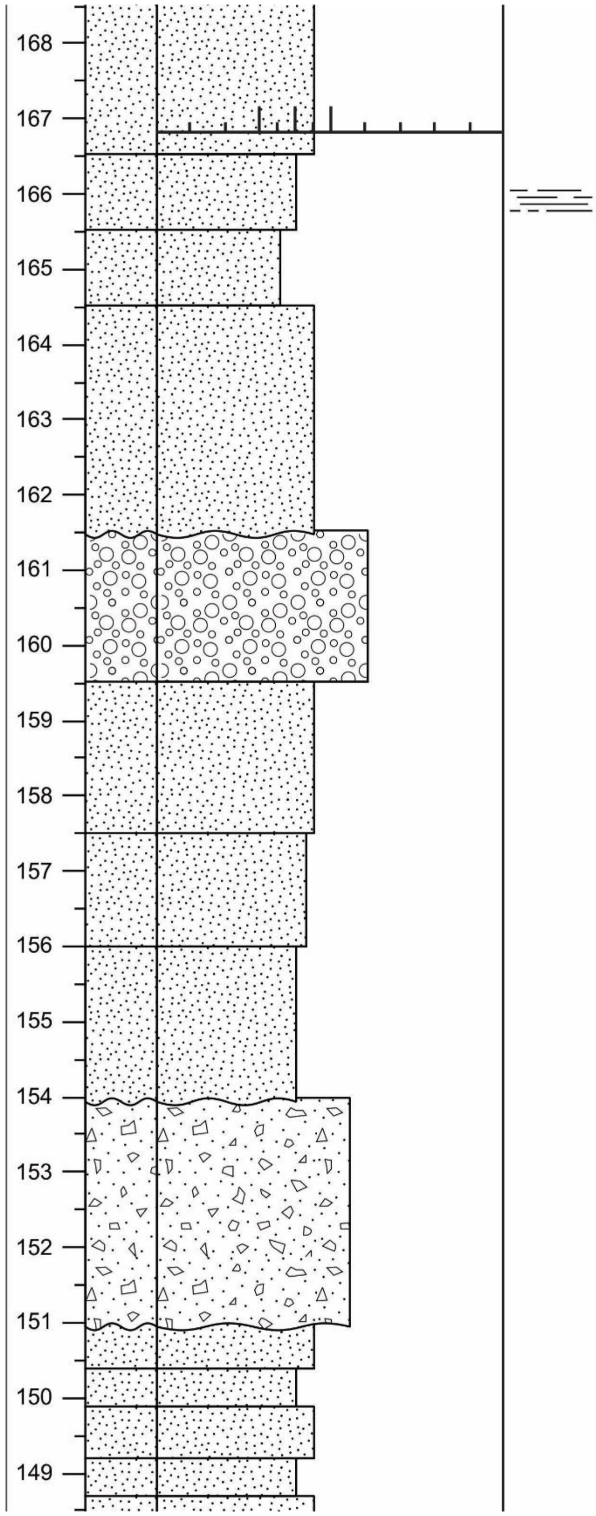

Yellow Sandstone

Brownish Laminated Sandstone.

Yellow Sandstone

Yellow Sandstone

Gray Matrix-supported Conglomerate (Gmm4) This conglomerate differs fromform the greenish and reddish conglomerates by being monolithic. The clasts are diorites

Yellow Sandstone

Yellow Sandstone

Yellow Sandstone

Gray Matrix-supported Breccia (Gmm7). This conglomerate differs fromform the greenish and reddish conglomerates by being monolithic. The clasts are diorites.

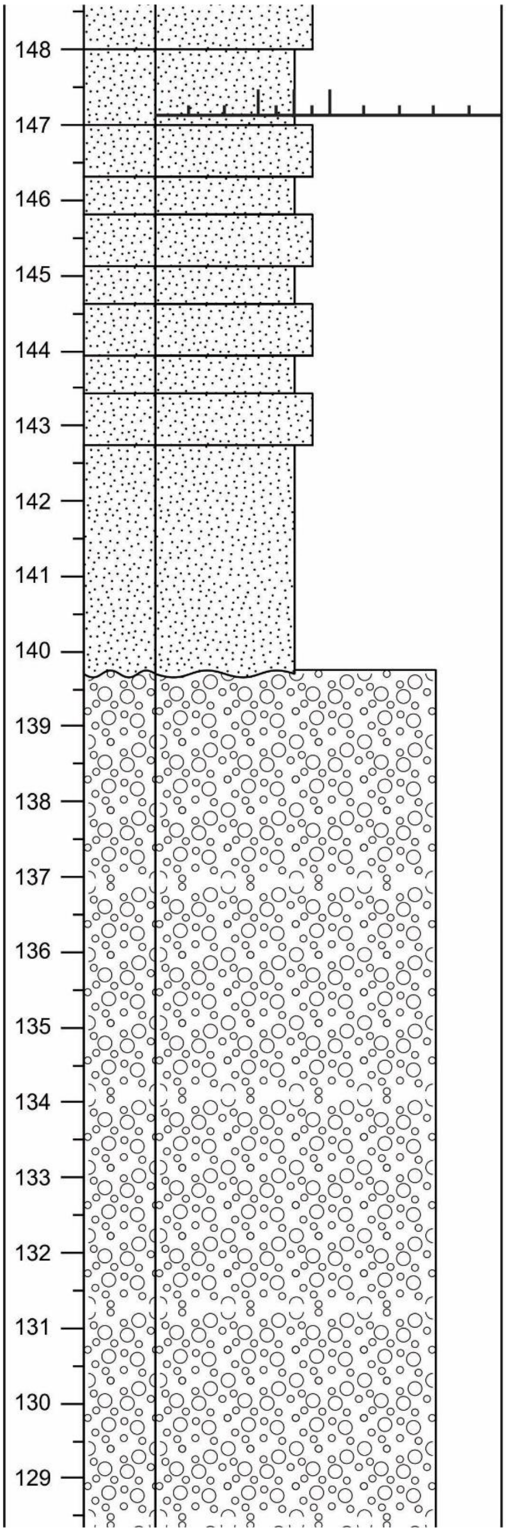

Interbeded sandstones with Yellow Sandstone and Greenish Massive Sandstone (Sm1)

Greenish Massive Sandstone (Sm1)

Greenish Matrix-supported Conglomerate (Gmm2). The composition are: Black shales; Quartzite clasts; Andesite clasts; Chert clast; Sandstone clasts

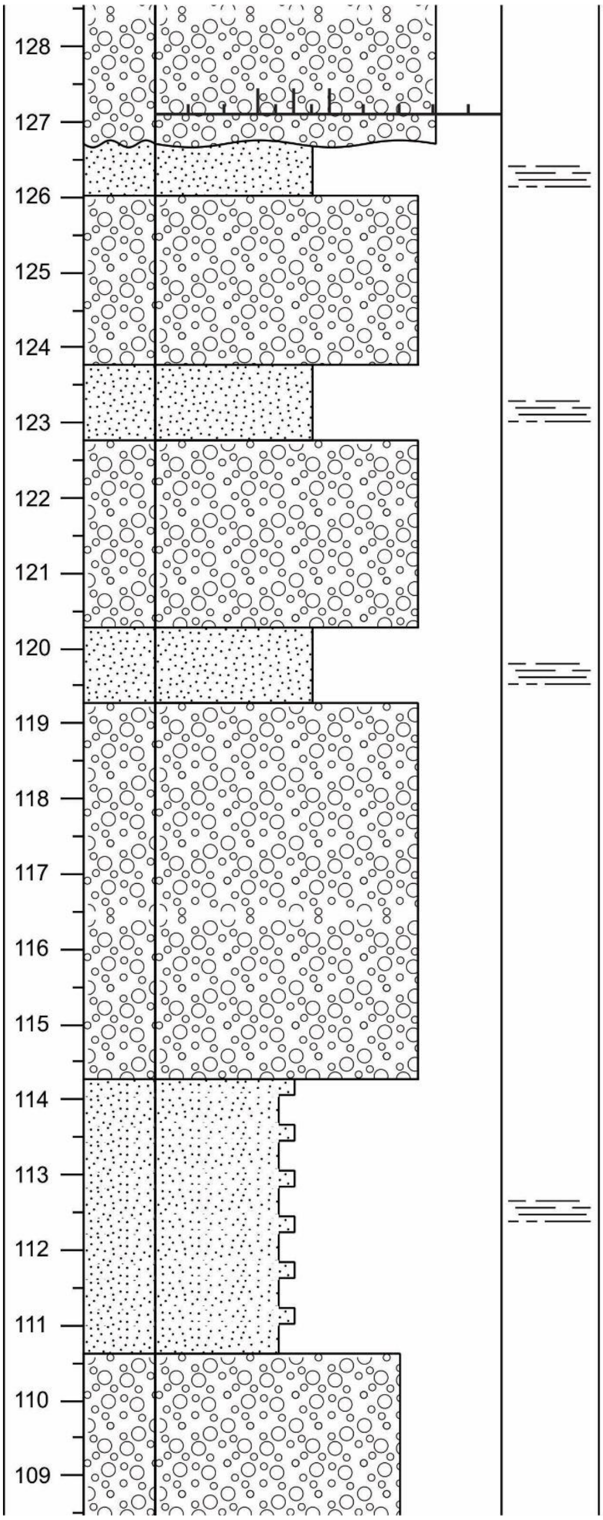

Brownish Laminated Sandstone..

Greenish Matrix-supported Conglomerate (Gmm2). The composition are: Black shales; Quartzite clasts; Andesite clasts; Chert clast; Sandstone clasts

Brownish Laminated Sandstone.

Greenish Matrix-supported Conglomerate (Gmm3). The composition are: Black shales; Quartzite clasts; Andesite clasts; Chert clast; Sandstone clasts

Brownish Laminated Sandstone (Sh1).

Greenish Matrix-supported Conglomerate (Gmm2). The composition are: Black shales; Quartzite clasts; Andesite clasts; Chert clast; Sandstone clasts

Intercalations of fine sand every 40 cm of Greenish Massive Sandstone (Sm1) with 10 cm thickness of Brownish Laminated Sandstone

Greenish Matrix-supported Conglomerate (Gmm2). The composition are: Black shales; Quartzite clasts; Andesite clasts; Chert clast; Sandstone clasts

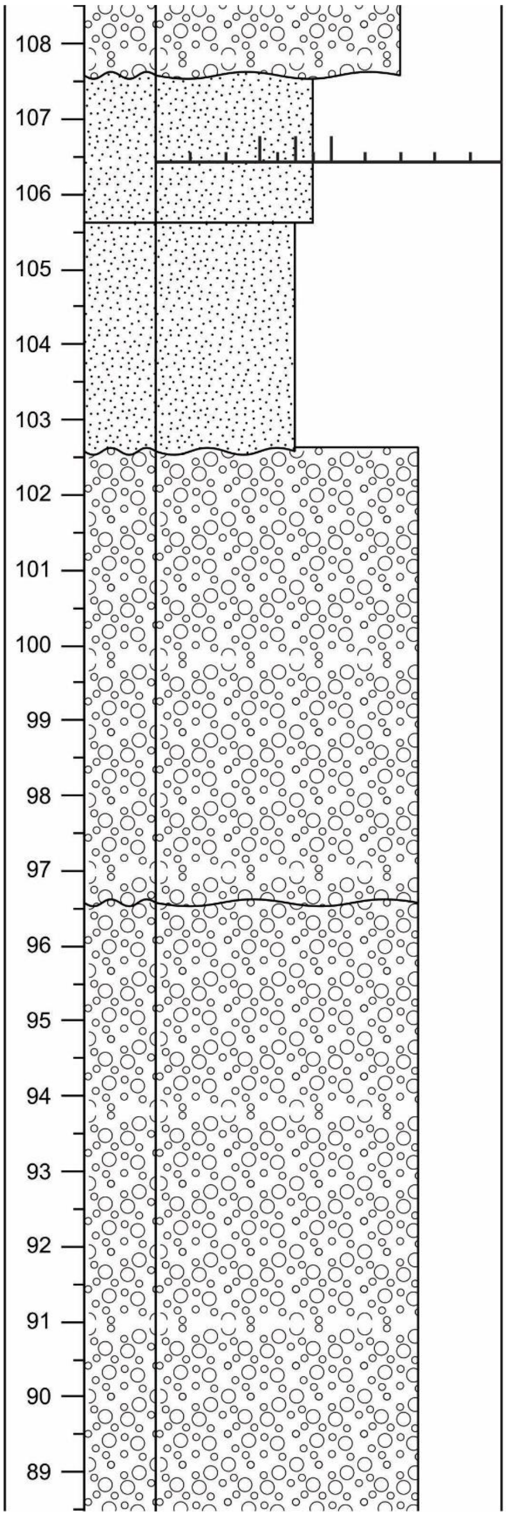

Greenish Massive Sandstone (Sm1) whit high content of feldspar

Greenish Massive Sandstone (Sm1)

Greenish Matrix-supported Conglomerate (Gmm2). The composition are: Black shales; Quartzite clasts; Andesite clasts; Chert clast; Sandstone clasts

Greenish Matrix-supported Conglomerate (Gmm2). The composition are: Black shales; Quartzite clasts; Andesite clasts; Chert clast; Sandstone clasts

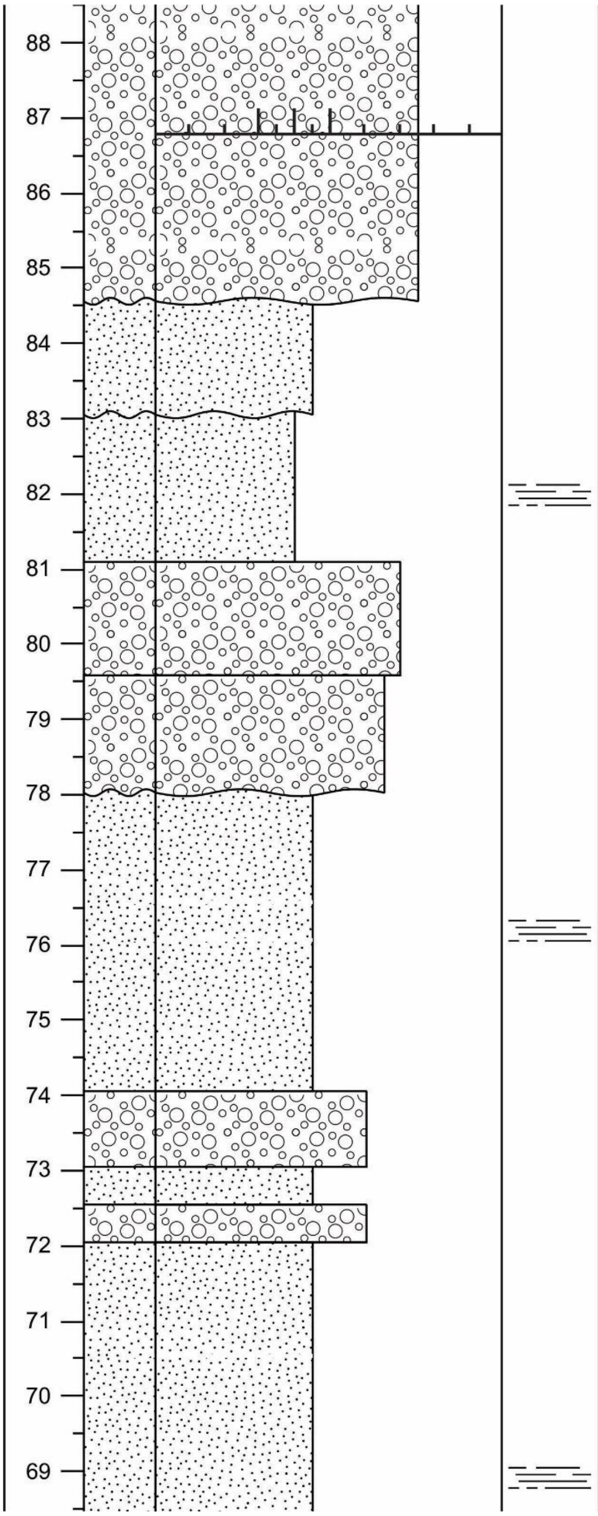

Greenish Massive Sandstone (Sm1) whit high content of feldspar

Brownish Laminated Sandstone whit high content of feldspar

Brownish Matrix-supported Conglomerate (Gmm1). The composition are: Black shales; Quartzite clasts; Andesite clasts; Chert clast; Sandstone clasts

Brownish Laminated Sandstone whit high content of feldspar

Brownish Matrix-supported Conglomerate (Gmm1).

Brownish Matrix-supported Conglomerate (Gmm1).

Brownish Laminated Sandstone whit high content of feldspar

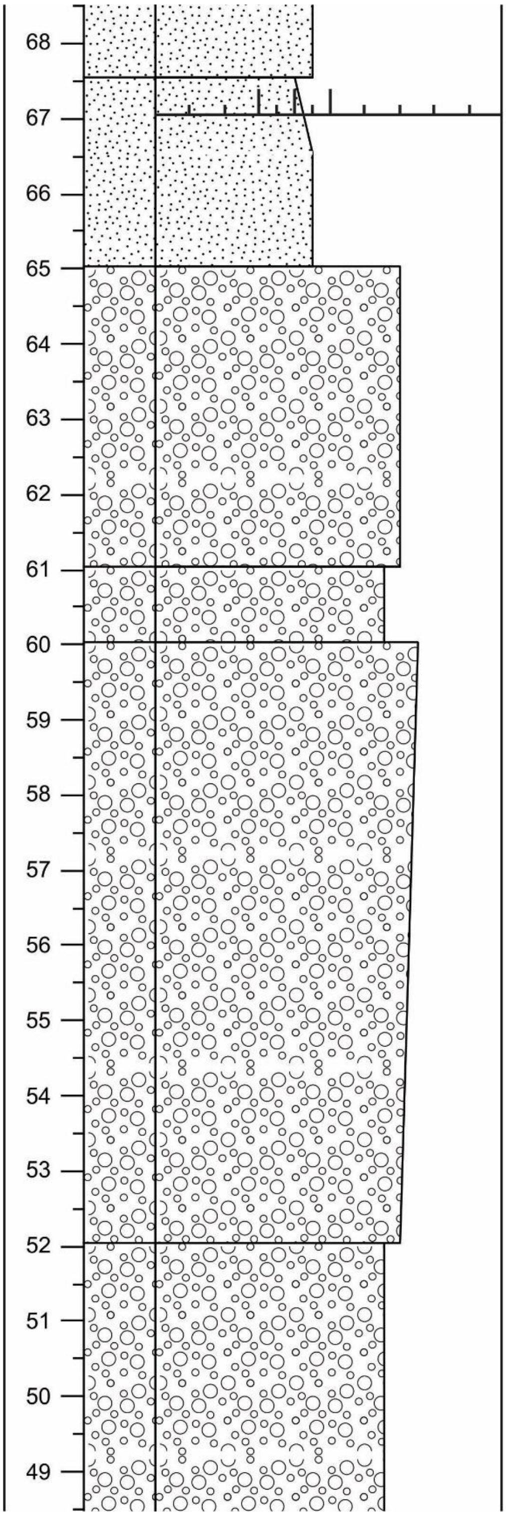

Brownish Massive Sandstone (Sm1)

Brownish Matrix-supported Conglomerate (Gmm1). The composition are: Black shales; Quartzite clasts; Andesite clasts; Chert clast; Sandstone clasts

Brownish Matrix-supported Conglomerate (Gmm1).

Brownish Matrix-supported Conglomerate (Gmm1). Black shales; Quartzite clasts; Andesite clasts; Chert clast; Sandstone clasts

Brownish Matrix-supported Conglomerate (Gmm1). The composition are: Black shales; Quartzite clasts; Andesite clasts; Chert clast; Sandstone clasts

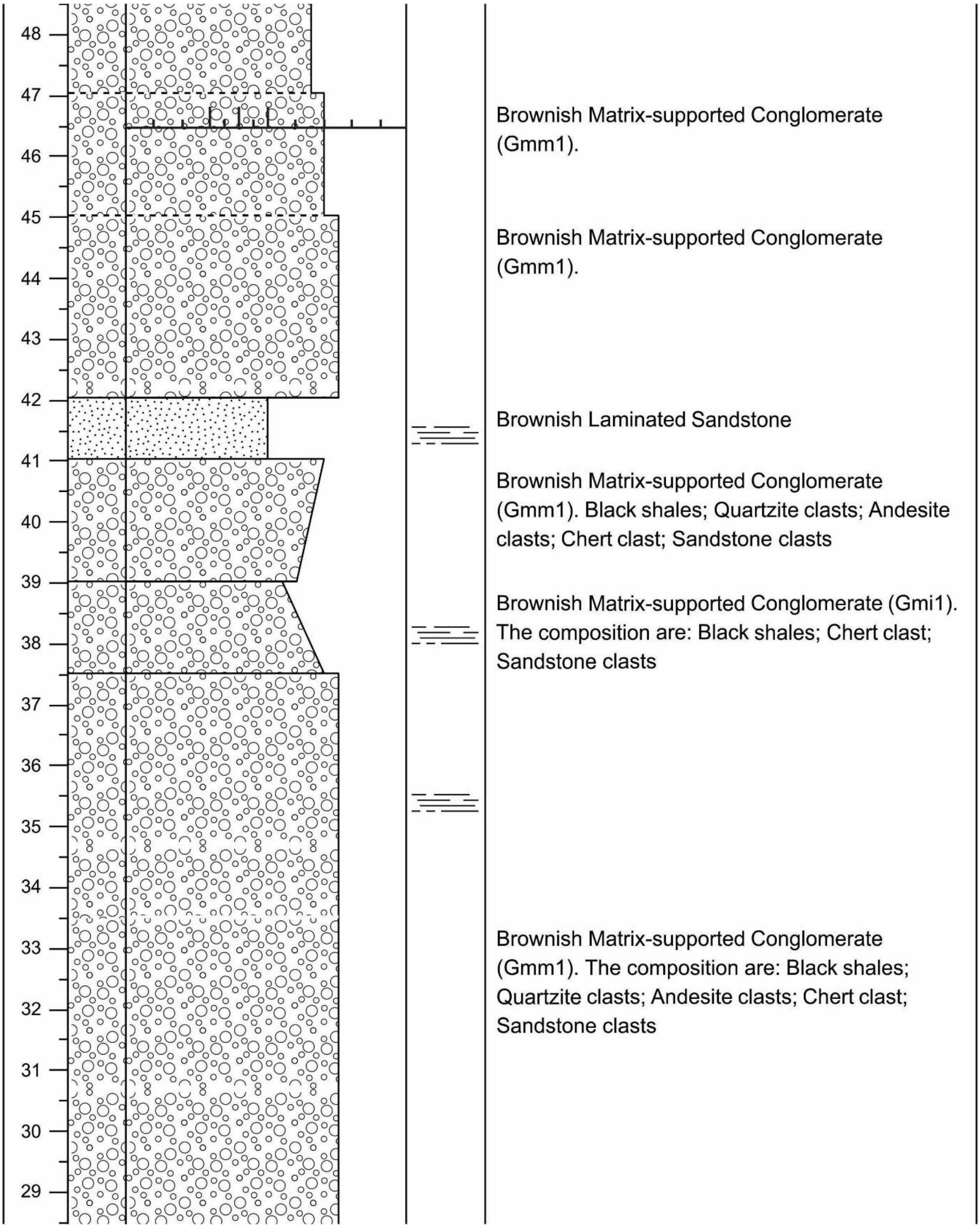
48
47
46
45
44
43
42
41
40
39
38
37
36
35
34
33
32
31
30
29
Brownish Matrix-supported Conglomerate (Gmm1).
Brownish Matrix-supported Conglomerate (Gmm1).
Brownish Laminated Sandstone
Brownish Matrix-supported Conglomerate (Gmm1). Black shales; Quartzite clasts; Andesite clasts; Chert clast; Sandstone clasts
Brownish Matrix-supported Conglomerate (Gmi1). The composition are: Black shales; Chert clast; Sandstone clasts
Brownish Matrix-supported Conglomerate (Gmm1). The composition are: Black shales; Quartzite clasts; Andesite clasts; Chert clast; Sandstone clasts

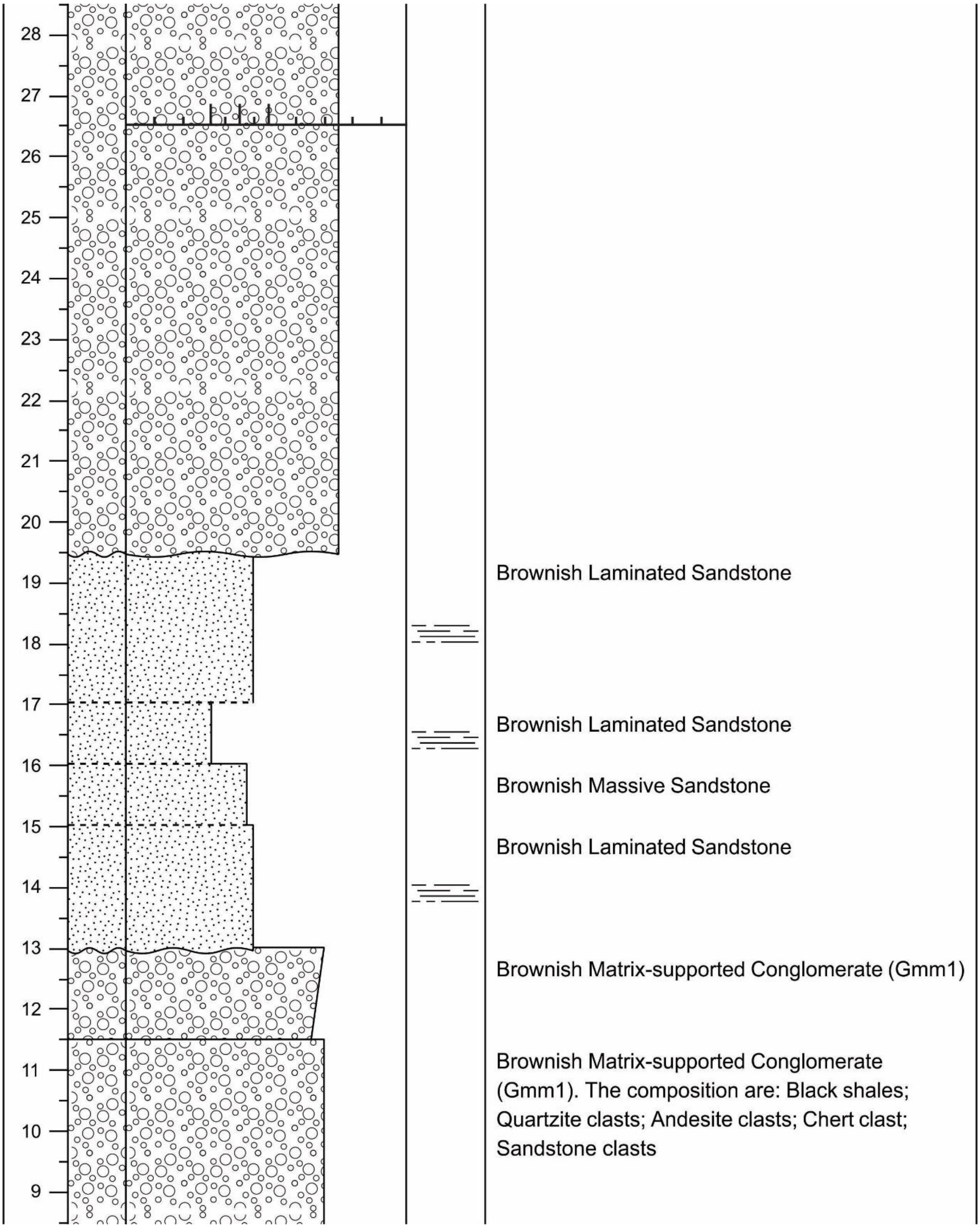

28
27
26
25
24
23
22
21
20
19
18
17
16
15
14
13
12
11
10
9
Brownish Laminated Sandstone
Brownish Laminated Sandstone
Brownish Massive Sandstone
Brownish Laminated Sandstone
Brownish Matrix-supported Conglomerate (Gmm1)
Brownish Matrix-supported Conglomerate (Gmm1). The composition are: Black shales; Quartzite clasts; Andesite clasts; Chert clast; Sandstone clasts

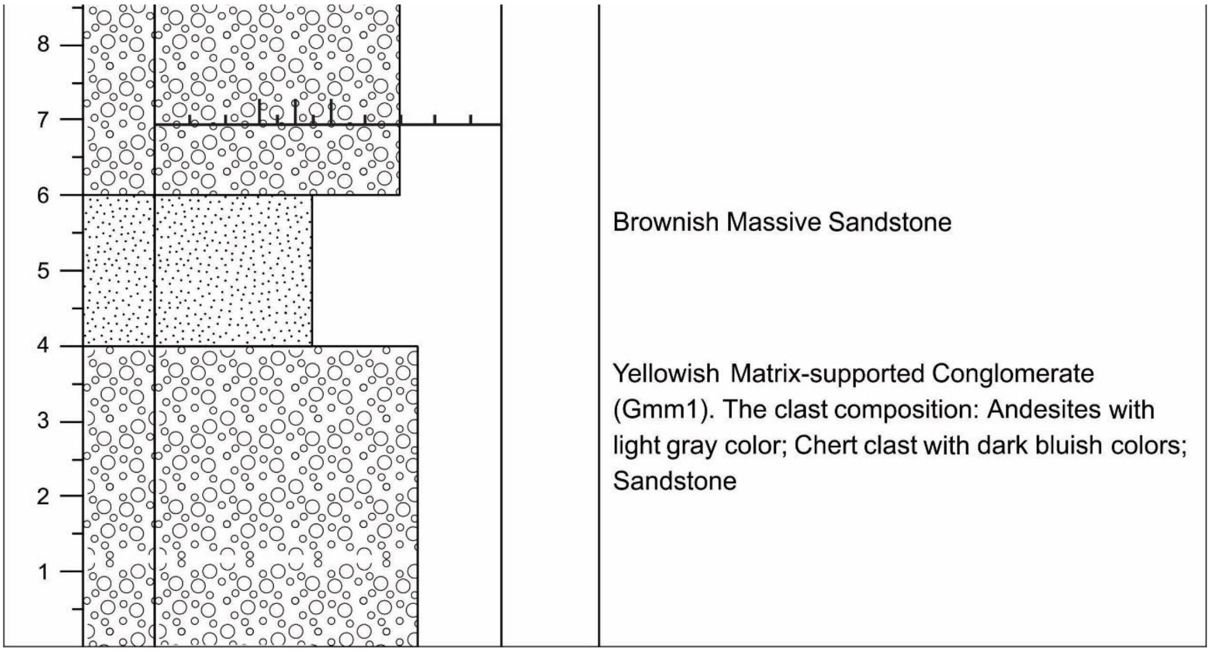

Figure 22. Column A

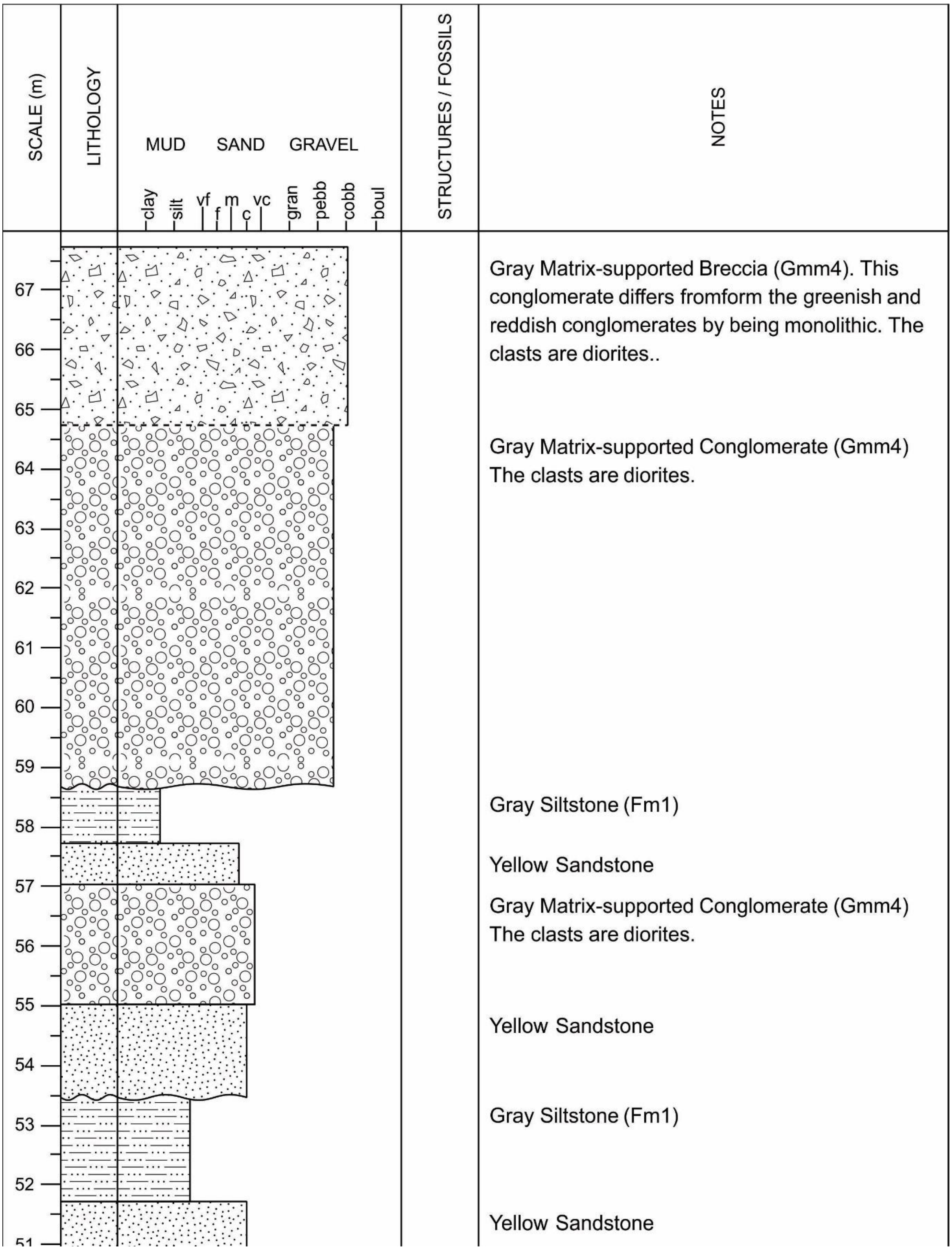
SCALE (m)
LITHOLOGY
MUD SAND GRAVEL
clay silt vf f m c vc gran pebb cobb boul
STRUCTURES / FOSSILS
NOTES
67
66
65
64
63
62
61
60
59
58
57
56
55
54
53
52
51
Gray Matrix-supported Breccia (Gmm4). This conglomerate differs fromform the greenish and reddish conglomerates by being monolithic. The clasts are diorites..
Gray Matrix-supported Conglomerate (Gmm4) The clasts are diorites.
Gray Siltstone (Fm1)
Yellow Sandstone
Gray Matrix-supported Conglomerate (Gmm4) The clasts are diorites.
Yellow Sandstone
Gray Siltstone (Fm1)
Yellow Sandstone

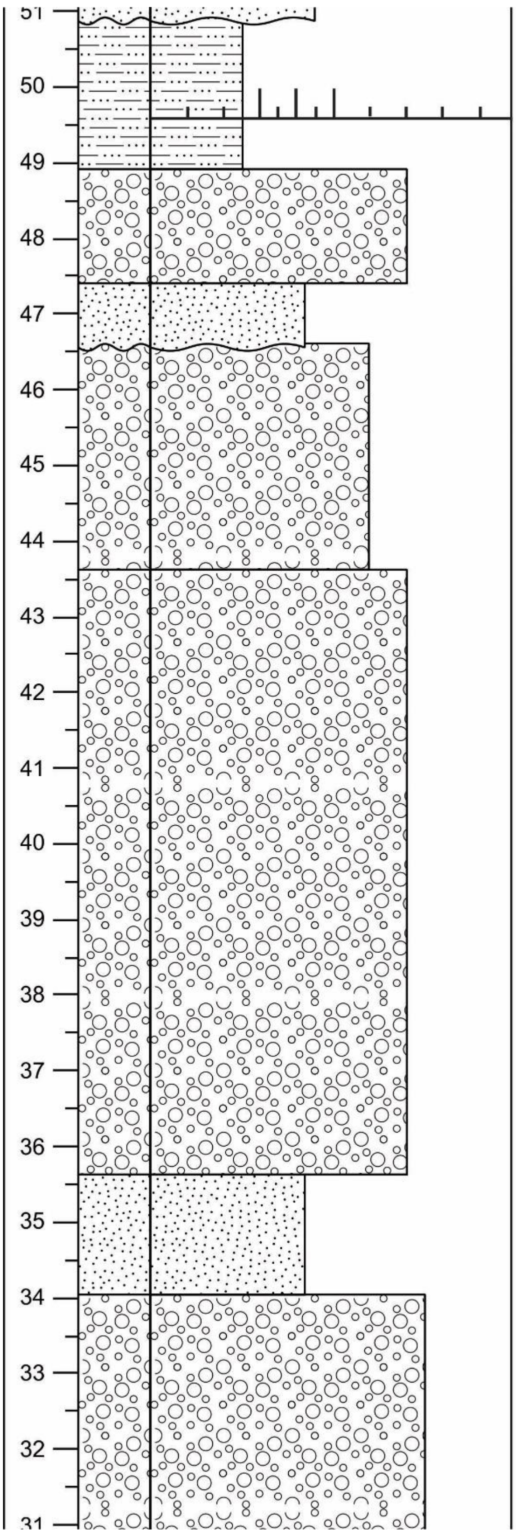

Gray Siltstone (Fm1)

Reddish Matrix-supported Conglomerate (Gmm3).

Reddish Matrix-supported Conglomerate (Gmm3). The composition of the different clasts are: Black shales; Sandstone clasts; Basalt clasts

Reddish Matrix-supported Conglomerate (Gmm3). The composition of the different clasts are: Black shales; Sandstone clasts; Basalt clasts

Reddish Massive Sandstone (Sm2)

Reddish Matrix-supported Conglomerate (Gmm4). The composition of the different clasts are: Black shales; Sandstone clasts; Basalt clasts

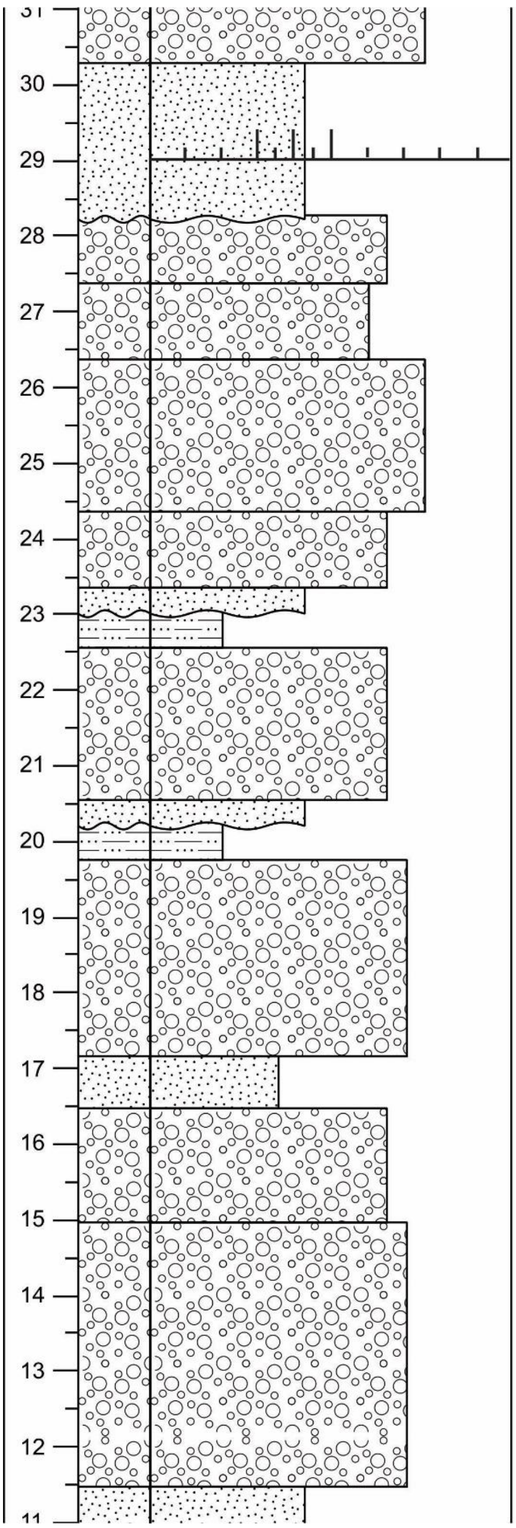

Reddish Massive Sandstone (Sm3)

Reddish Matrix-supported Conglomerate (Gmm4).

Green matrix-supported conglomerate with subrounded clasts

Reddish Matrix-supported Conglomerate (Gmm3).

Greenish Matrix-supported Conglomerate (Gmm2).

Reddish Shales (Fl)

Reddish Matrix-supported Conglomerate (Gmm3). The composition of the different clasts are: Black shales; Chert clast; Sandstone clasts; Basalt clasts

Reddish Shales (Fl)

Greenish Matrix-supported Conglomerate (Gmm2). The composition are: Black shales; Quartzite clasts; Andesite clasts; Chert clast; Sandstone clasts

Reddish Massive Sandstone (Sm2)

Reddish Matrix-supported Conglomerate (Gmm3).

Greenish Matrix-supported Conglomerate (Gmm2). The composition are: Black shales; Quartzite clasts; Andesite clasts; Chert clast; Sandstone clasts

Brownish Massive Sandstone

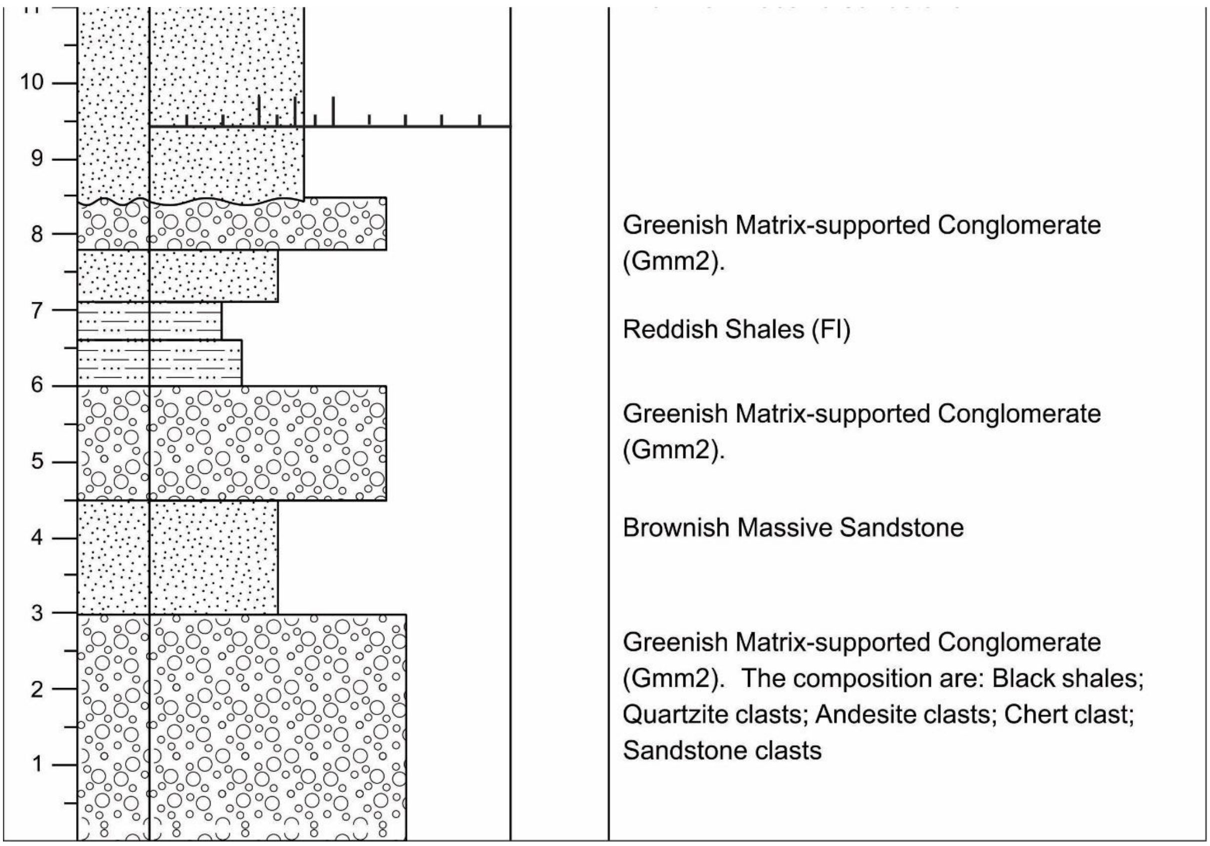

Figure 23. Column B.

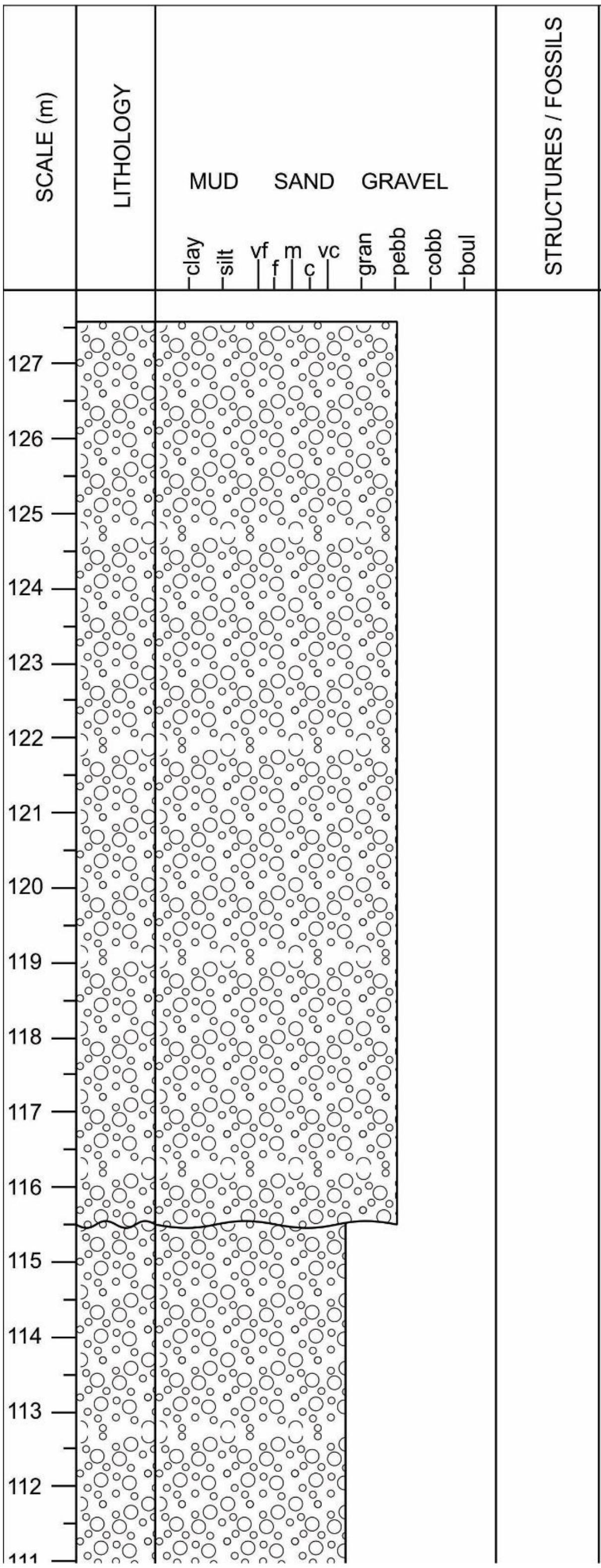

NOTES

Gray Matrix-supported Conglomerate (Gmm4)
This conglomerate differs fromform the greenish and reddish conglomerates by being monolithic. The clasts are diorites

Gray Matrix-supported Conglomerate (Gmm4)
The clasts are diorites. The basal contact is sharp and is an angular nonconformity.

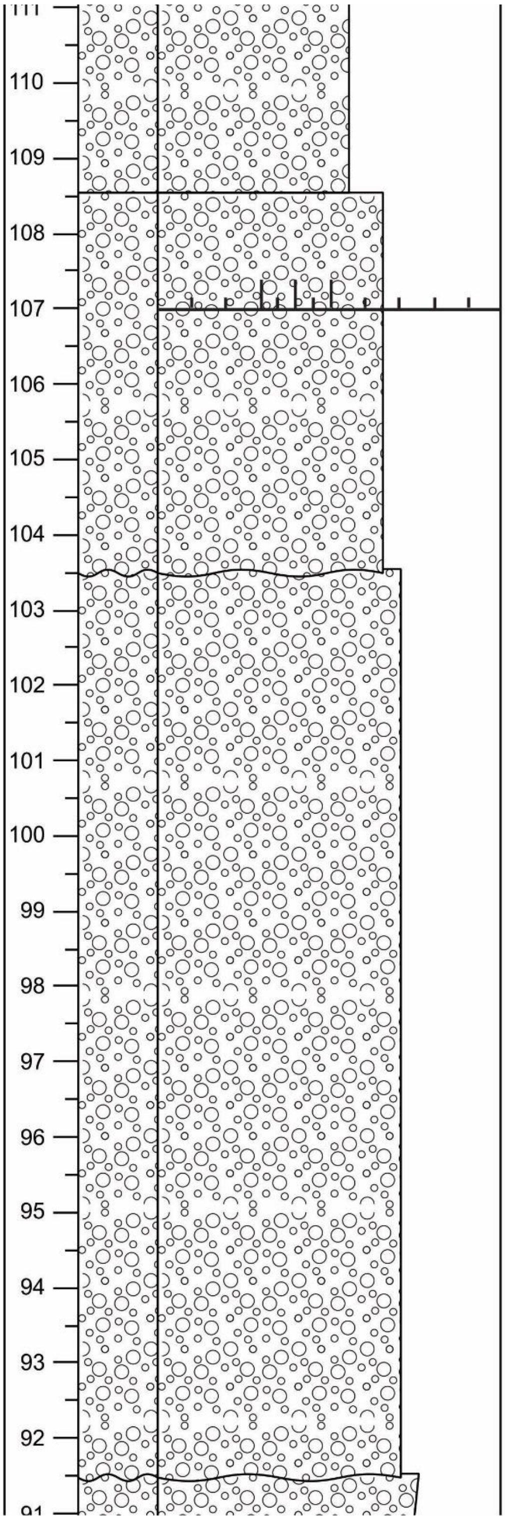

Reddish Matrix-supported Conglomerate (Gmm3). The composition of the different clasts are: Black shales; Chert clast; Sandstone clasts; Basalt clasts

Reddish Matrix-supported Conglomerate (Gmm3). The composition of the different clasts are: Black shales; Chert clast; Sandstone clasts; Basalt clasts

Matrix-supported conglomerate, subrounded

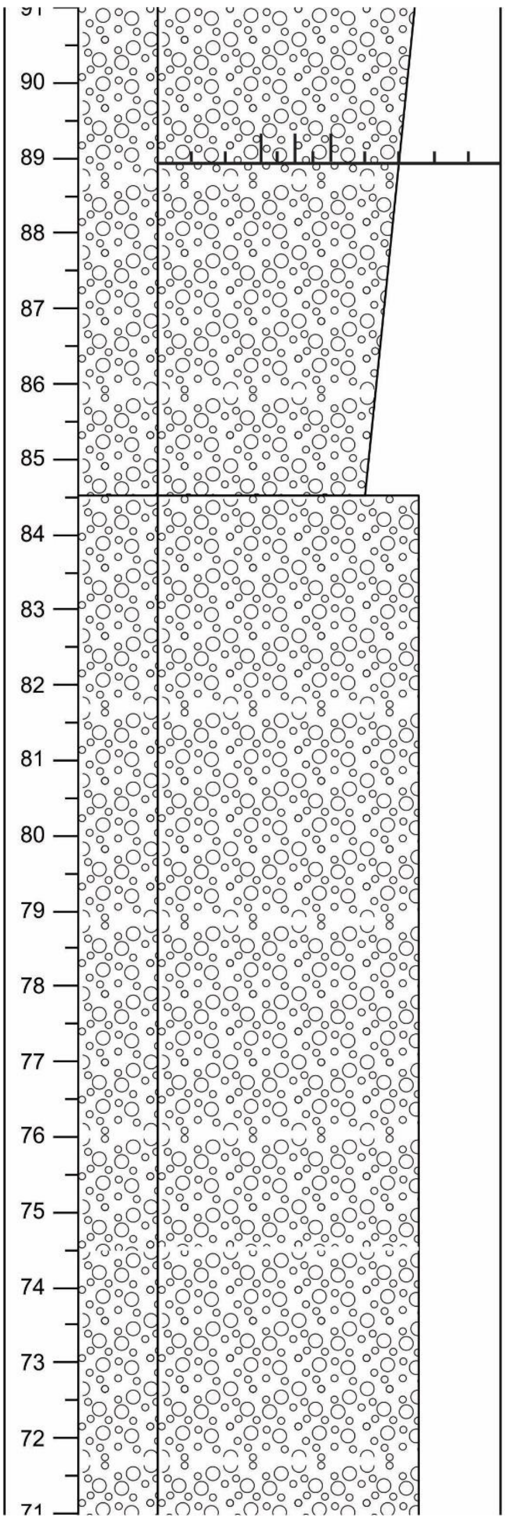

clasts, very poorly classified, red in color, and some intraclasts. The composition of the clasts: 1) Shelds; 2) Sandstone; 3) Basalt

Reddish Matrix-supported Conglomerate (Gmm3). The composition of the different clasts are: Black shales; Chert clast; Sandstone clasts; Basalt clasts

Reddish Matrix-supported Conglomerate (Gmm5). The composition of the different clasts are: Black shales; Chert clast; Sandstone clasts; Basalt clasts

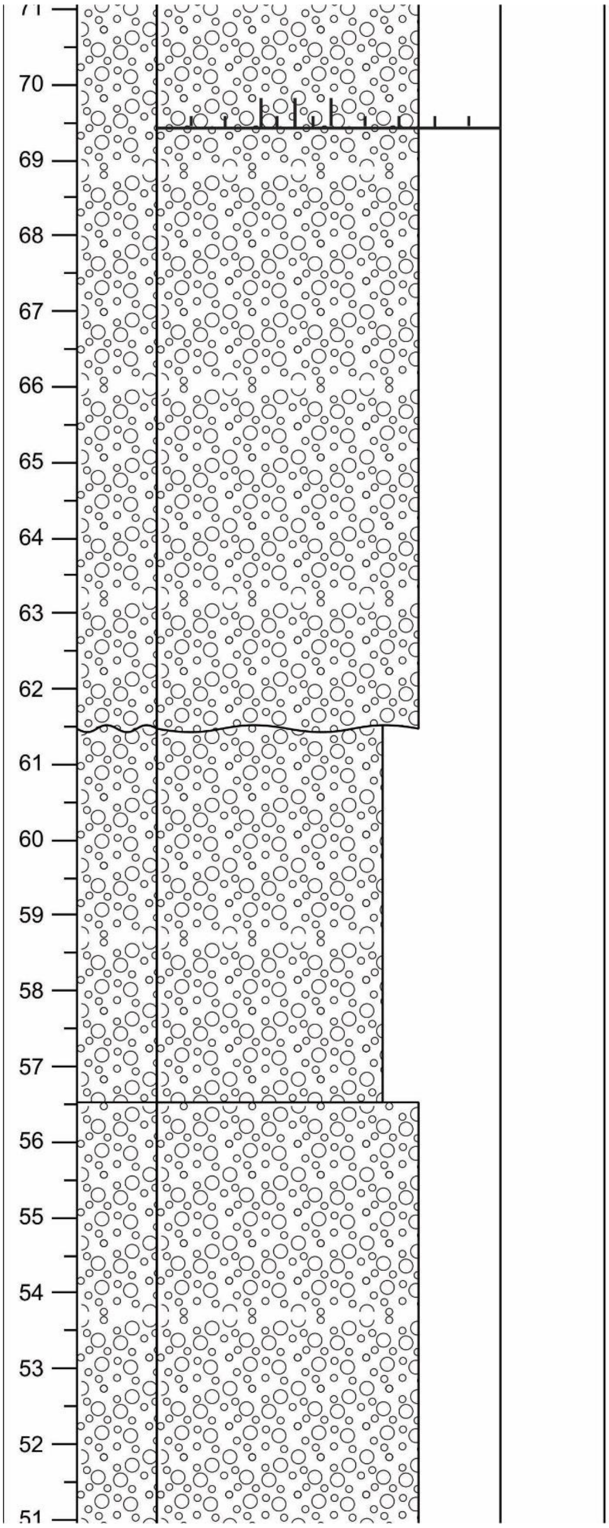

Matrix-supported conglomerate, rounded clasts, very poorly classified, and a red color is distinguished. The composition of the clasts: 1) Sandstone; 2) Basalt

Reddish Matrix-supported Conglomerate (Gmm3). The composition of the different clasts are: Black shales; Sandstone clasts; Basalt clasts

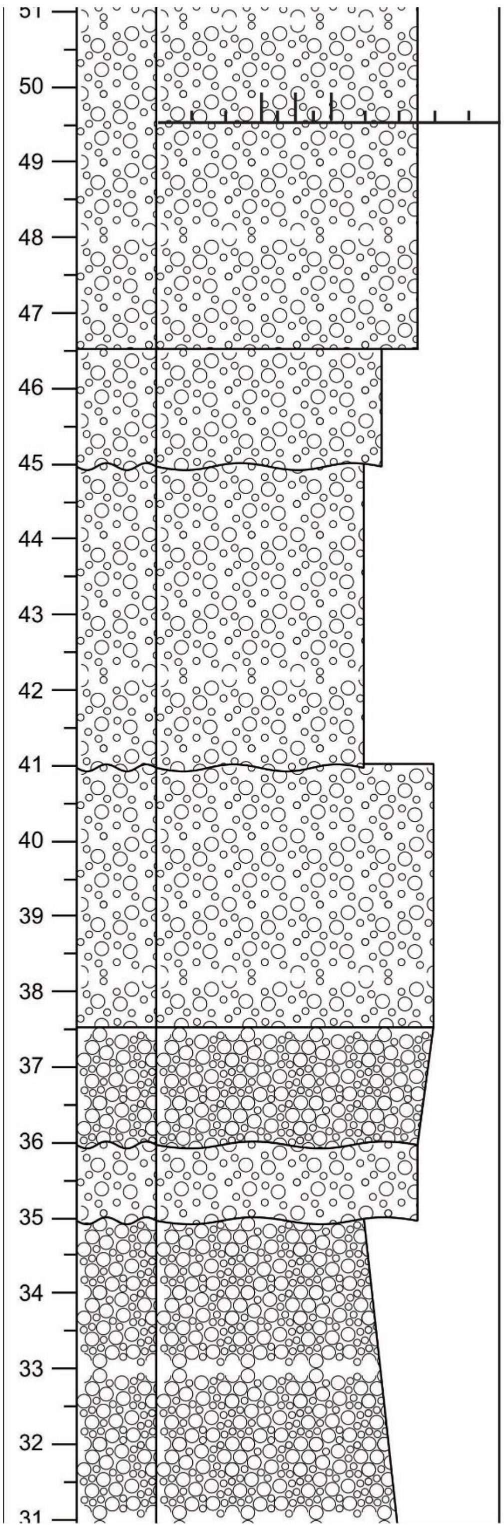

Reddish Matrix-supported Conglomerate (Gmm3).

Reddish Matrix-supported Conglomerate (Gmm3). The composition of the different clasts are: Black shalest; Sandstone clasts; Basalt clasts

Reddish Matrix-supported Conglomerate (Gmm3). The composition of the different clasts are: Black shales; Chert clast; Sandstone clasts; Basalt clasts

Reddish Matrix-supported Conglomerate (Gcg1).

Reddish Matrix-supported Conglomerate (Gmm3).

Reddish Matrix-supported Conglomerate (Gcg1). The composition of the different clasts are: Black shales; Chert clast; Sandstone clasts; Basalt clasts

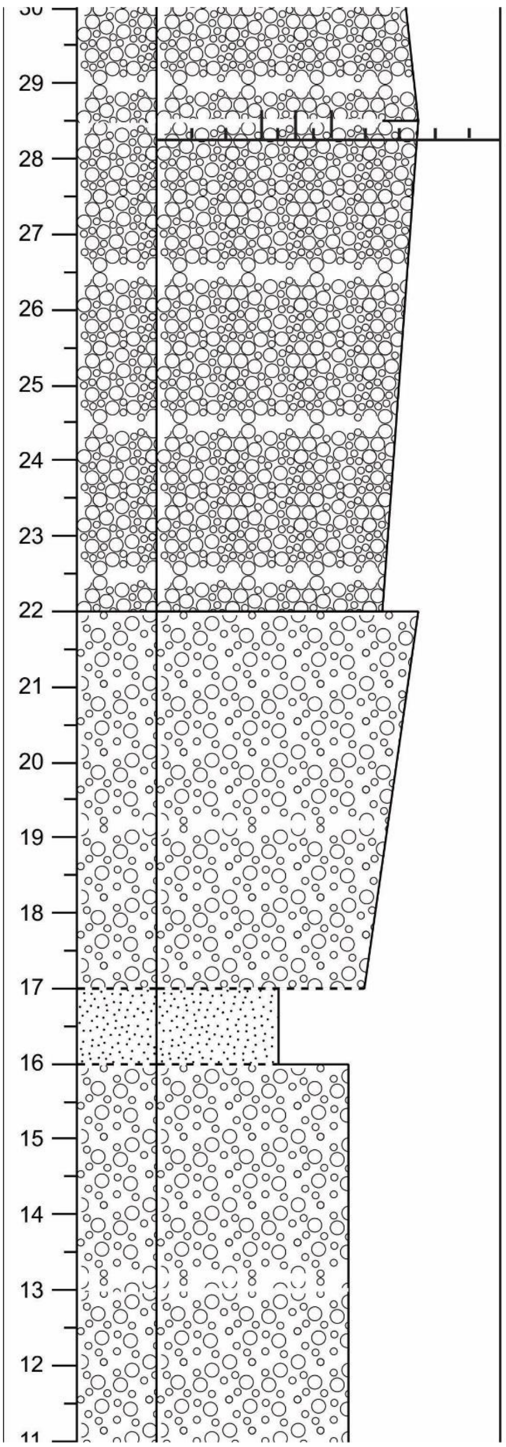

Reddish Matrix-supported Conglomerate (Gcg1). The composition of the different clasts are: Black shales; Chert clast; Sandstone clasts; Basalt clasts

Reddish Matrix-supported Conglomerate (Gmm3). The composition of the different clasts are: Black shales; Chert clast; Sandstone clasts; Basalt clasts

Reddish Massive Sandstone (Sm2)

Reddish Matrix-supported Conglomerate (Gmm3). The composition of the different clasts are: Black shales; Chert clast; Sandstone clasts; Basalt clasts

Reddish Matrix-supported Conglomerate (Gmm3). The composition of the different clasts are: Black shales; Sandstone clasts; Basalt clasts

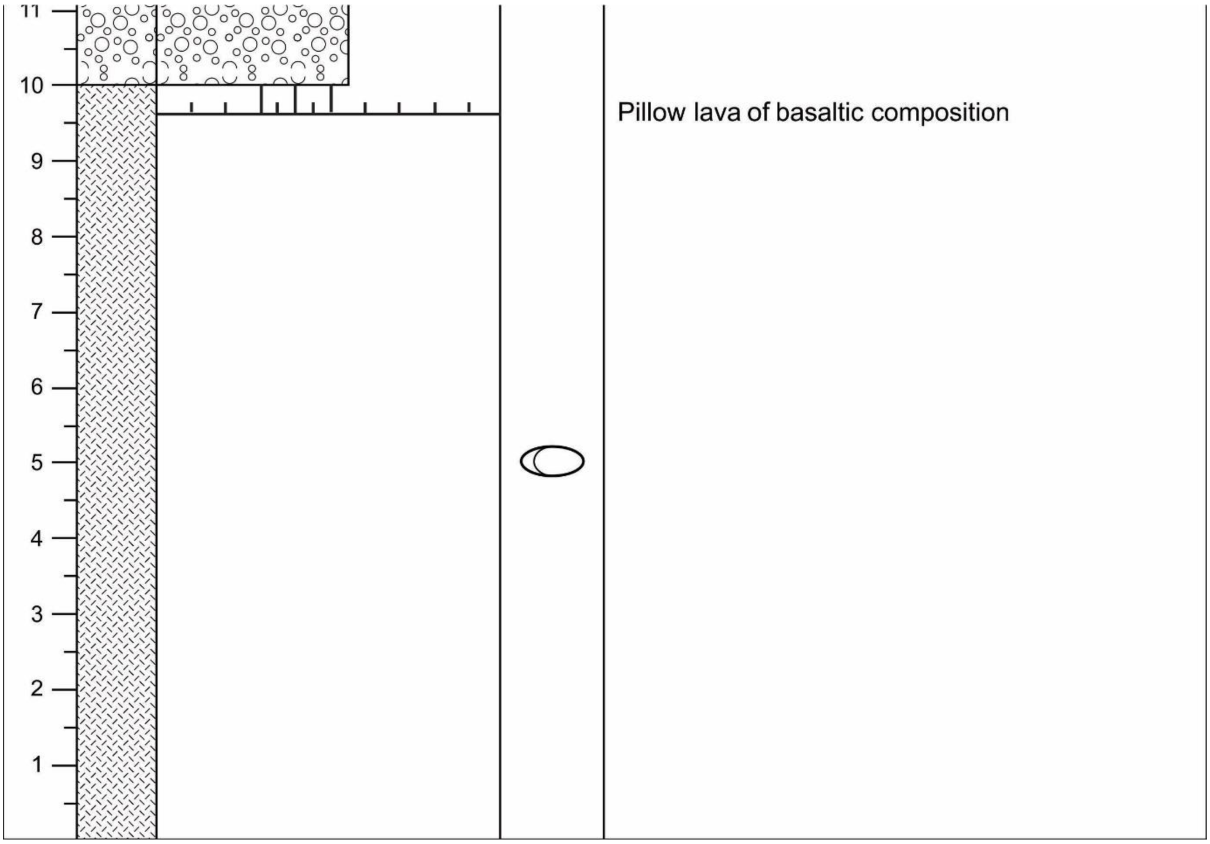

Figure 24. Column C